UNIVERSITA DEGLI STUDI DI MILANO
Department of Pharmacological and Biomolecular Sciences
PhD School in Integrative Biomedical Research

$GABA_A$ RECEPTOR AS A NOVEL REGULATOR OF PERIPHERAL PAIN SENSITIVITY AND LOCAL NEURON-GLIA INTERACTION

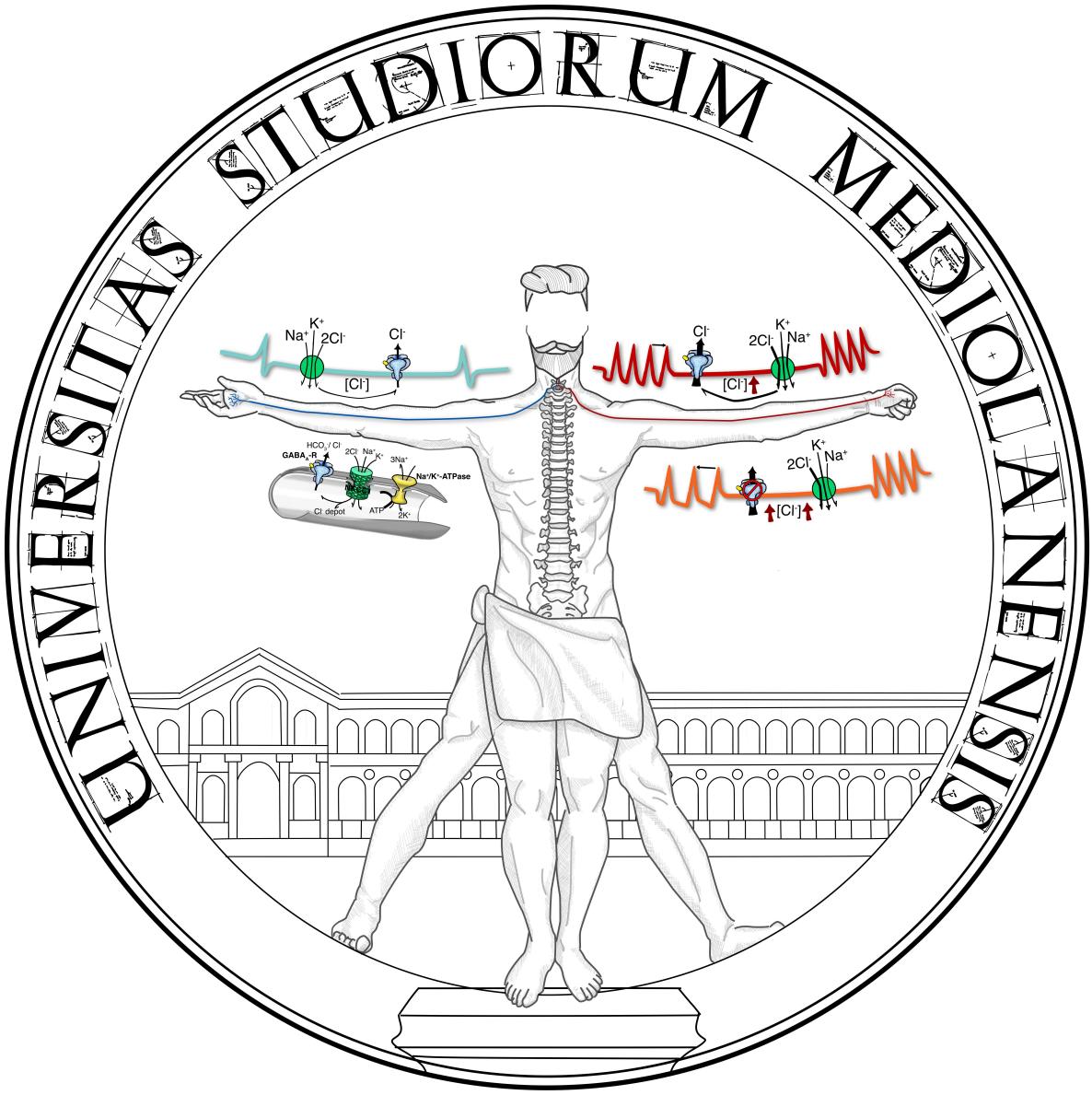

PhD Tutor: Prof. Valerio Magnaghi
PhD co-tutor: Prof. Richard Carr
PhD School coordinator: Prof Chiarella Sforza

Veronica Bonalume
R11647
Academic year 2015/2016

UNIVERSITÀ DEGLI STUDI DI MILANO

PhD School in Integrative Biomedical Research

Department of Pharmacological and Biomolecular Sciences

Curriculum: Neuroscience

$GABA_A$ receptor as a novel regulator of peripheral pain sensitivity and local neuron-glia interaction

SDD BIO/09 - Physiology

Veronica Bonalume

R11647

PhD Tutor: Prof. Valerio Magnaghi

PhD co-tutor: Prof. Richard Carr

PhD School Coordinator: Prof. Chiarella Sforza

Academic year 2015/2016

INDEX

ABSTRACT

The pathogenesis of neuropathic pain and its chronicization process are still not fully elucidated. For this reason, therapies currently ongoing in clinic are aimed to treat mostly the symptoms, considering poorly the target mechanisms causing those pathologies.

The approach that we choose to investigate new pharmacological targets for the therapy of chronic pain, was to firstly investigate the mechanisms of nociception in physiological condition, finding new molecular pathways responsible of nociception modulation. Secondly, we were aimed to study the contribution of these targets in pathological condition.

In particular, in this PhD thesis, I focused on the characterization of the GABAergic system, primarily the $GABA_A$ receptors ($GABA_AR$), along peripheral nociceptors axons (forming C-fibers), evaluating their putative role in the modulation of pain peripheral conduction, during different physio-pathological conditions. All these studies were performed relying on a combination of *in vitro*, *ex vivo* and *in vivo* models (i.e. transgenic conditional mice) and applying electrophysiological and biomolecular techniques.

$GABA_AR$ mediate fast synaptic inhibition in mature neurons of central nervous system. However, immature neurons as well as mature olfactory and somatosensory neurons are characterized by elevated intracellular chloride concentration, that originate depolarizing $GABA_AR$ currents. We demonstrated that peripheral nociceptors express functional $GABA_AR$ along their unmyelinated axons. $GABA_AR$ activation induce depolarizing currents mediated by efflux of Cl^- ions, regulated through the modulation of NKCC1 transporter activity. In peripheral axons, depolarizing responses to GABA (1μM-1mM) were mimicked by muscimol (>1μM) and THIP (>1μM) and blocked by bicuculline (50μM). Depolarizing axonal responses to GABA were absent in mice lacking β3 subunit in either all sensory neurons ($advillin^{CRE}$ conditional KO mice) or selectively in DRG neuronal subset expressing $Na_V1.8$ (Sns^{CRE}

conditional KO mice). Altogether, these outcomes demonstrated that GABA currents are selectively mediated by specific $GABA_AR$ activation, that need the β3 subunit. Thus, we showed that the prevalent form of $GABA_AR$ in nociceptors is the synaptic subtype composed by $\alpha2\beta3\gamma2$, characterized by low sensitivity, fast kinetic and specific pharmacology.

We showed that GABA currents were strongly modulated by electrical activity of C-fibers, going from nearly undetectable depolarizing currents to strong and fast depolarizations. $GABA_AR$ activation, indeed, resulted in strong currents after challenges of sustained activity (3min at 2.5Hz), secondary to a shift in E_{Cl^-} mediated by a NKCC1 activity increase. In addition, $GABA_AR$ was able to reduce the physiological phenomenon of activity-dependent slowing, occurring to unmyelinated fibers during firing. Altogether, these modulations indicated the axonal GABAAR possessed a physiological role in the modulation of C-fibers conductance and the presence of constitutive $GABA_AR$ activation, through endogenous ligands released within the peripheral nerves.

Established the capability of peripheral GABAergic currents to stabilize nociceptor conductance during sustained activity, we investigated the GABAergic modulation in pathological conditions characterized by hypersensitivity of nociceptors. In this regard, we studied *in vivo* model of inflammatory pain on sns^{CRE}:$\beta3^{-/-}$ mice. The outcomes indicated that $GABA_AR$ activity increment mechanical allodynia and prevent the insurgence of hyperalgesia. In addition, $GABA_AR$ activity prolonged the recovery time, maintaining the hypersensitive phenotype for a longer period of time (up to 4 weeks). This finding corroborated the hypothesis that GABAergic transmission within peripheral fibers is able to stabilize the physiological conduction of pain, although it appeared dangerous in pathological condition, promoting nociceptor hypersensitivity and chronicization.

Then we supposed that $GABA_AR$ is constitutively activated by endogenous ligands, which local source could be the peripheral glial Schwann cells (SCs). It is known that SCs synthetize both GABA and the neuroactive steroid ALLO (positive allosterical modulator of $GABA_AR$). Furthermore, the efforts were aimed at study the involvement of ALLO on the cross-talk between axons and SCs. We found that ALLO induces the release of the growth factor BDNF from SCs, which is able to target trkB receptors on axons, in turn inducing PKCε upregulation and activation. PKCε is a typical protein kinase known to be involved in the process of pain chronicization. Overall, these set of data suggested that $GABA_AR$ is involved in a complex paracrine mechanism mediated by SCs, which activate the $GABA_AR$ and subsequently modulate its hyperactivity by the BDNF release.

In conclusion, the results presented in this PhD thesis highlight the novel role of peripheral $GABA_AR$ in the modulation of nociceptor conduction in different physio-pathological conditions affecting the peripheral nervous system. Moreover, our findings stressed the role of local neuron-glia interaction in such mechanisms. $GABA_AR$ is able to dynamically stabilize nociceptor conduction of action potential during sustained activity, preventing excessive C-fiber slowing. On the other hand, $GABA_AR$ promotes pain hypersensitive state after neuronal inflammation and prolong the symptoms, likely leading to the pain chronicization. SCs play a fundamental role in the regulation of GABAergic signalling along C-fibers, although further studies are needed to unveil this process. in this direction might leads to the individuation of new pharmacological targets, exploiting endogenous pathways to obtain selective peripheral treatments. Hopefully, the complete comprehension of all the mechanisms would lay the basis for future identification of novel, possibly local, therapeutic strategies for the treatment of peripheral neuropathies and associated chronic pain.

INTRODUCTION

1. Neuronal excitability

Equilibrium potential of excitable cells

Neuronal cells and muscle cells are able to generate transient bioelectrical signal that can be transmitted by long distances. For this reason, those cells are classified as excitable cells capable to transmit signals as action potentials.

Charge distribution across the membrane leads to the establishment of a chemical gradient that raises in magnitude until it exactly balances the electrical gradient. Thus, ions are moving down their electrochemical gradient. For a given ion, when the chemical and electrical gradients are equal in magnitude, the ion is in electrochemical equilibrium, so that the generated membrane potential at equilibrium is defined as the equilibrium potential ($V_{eq.}$) for that ion. Consequently, the difference in charges across a membrane, under basal condition, is defined as the resting potential. In this case, the system is said to be at steady state. Although there are exceptions, in most mammalian cells, the major ions contributing to V_{eq} are K^+, Na^+, and Cl^-. In particular, resting potential is mainly maintained by outward K^+ efflux because the membrane is more permeable to K^+. In muscles cells also Ca^{++} flux is relevant in the modulation of membrane potential.

For most of neuronal cells, $V_{eq.}$, or resting potential is approximately -70mV and represent the difference between intracellular and extracellular charges, given by the constant flux of ions across the plasma membrane. In mature central nervous system (CNS) neurons, resting condition potassium equilibrium (E_{K+}) potential is E_{K+} =-84mV with a chemical gradient due to 5mM K^+ outside and 140mM inside, Na^+ equilibrium potential is E_{Na+} = +66mV with 12 mM sodium inside and 140mM sodium outside and chloride equilibrium potential E_{Cl-} = -64mV with 10mM chloride inside and 110mM chloride outside. At equilibrium, intracellular and

extracellular ion concentrations are maintained because of the constant energy consumption by ATP-asic pumps, firstly the Na^+/K^+ pump (Figure 1).

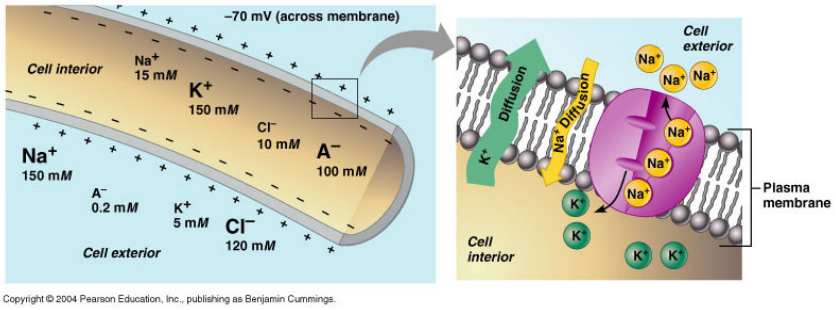

Figure 1. *Resting potential of a neuronal cell, **in which the electrochemical gradient of** K^+ **and** Na^+ **across the plasma membrane is balanced by** the action of the Na+/K+ ATPase pump. In resting condition, the neuronal membrane potential is approximately -70mV and the cells is in a "non-conducting" state.*

In most types of cells, the membrane potential is fairly constant and stable. However, excitable cells are electrically active, in sense their membrane potentials fluctuate over time. In neurons and muscle cells, the voltage fluctuations frequently take the form of a rapid upward spike followed by a rapid fall (Figure 1). These up-and-down cycles are known as action potentials. In physiology, an action potential occurs when the membrane potential rapidly rises and falls (Hodgkin AL AND Huxley AF, 1952) and is mediated by the activation of channels permeable to sodium and potassium. In neurons, action potentials play a central role in cell-to-cell communication, allowing the signals propagation along the neuronal axon toward the synaptic bouton, situated at the end of the axon. These signals may connect assure the communication of a neuron with other neurons, muscle cells or glands.

In neurons, the types of ion channels in the membrane usually vary in the different parts of the cell, conferring to the dendrites, axon, and cell body peculiar electrical properties. As a result, some parts of the neuronal membrane may be excitable (capable of generating action potentials), whereas others are not. The most excitable part of a neuron is that portion just located after the axon hillock (the point where the axon leaves the cell body; Figure 3), which is called the trigger point, at the initial segment.

Spike initiation and action potentials phases

Neuronal resting potential can be perturbed by signals coming from other neurons that cause voltage fluctuations versus a more negative value (hyperpolarization, that is inhibitory signal) or a less negative value (depolarization, that is excitatory signal). An action potential is generated when the cell depolarizes, and the membrane potential goes up to a certain voltage value called threshold potential. Generally, in neurons, threshold potential is around -55mV but different subpopulations of neurons possess different thresholds.

Action potentials are generated by ion fluxes through specialized ion channels. Those ion channels are voltage-sensitive, meaning that change in their state from open-active to closed-inactive is triggered by changes in the membrane potential. Action potentials are characterized by four important properties. First, they need a threshold for initiation. Second, the action potential is an all-or-none event. Indeed, the size and shape of an action potential is irrespective by the trigger signal; a large depolarizing current induces the same action potential evoked by a current that just outreaches the threshold. Third, the action potential is conducted without current decrement. It has a self-regenerative feature that keeps the amplitude constant, even when it is conducted over great distances. Fourth, the action potential is followed by a refractory period. For a brief time after the action potential, the neuron capability to fire a second action potential is suppressed. The refractory period limits the frequency at which a nerve can fire action potentials, allowing the action potential propagation in one direction, thus regulating the capacity to carry information along the axon.

The course of a single action potential can be divided into five parts (Figure 2): the rising phase, the peak phase, the falling phase, the undershoot phase, and the refractory period.

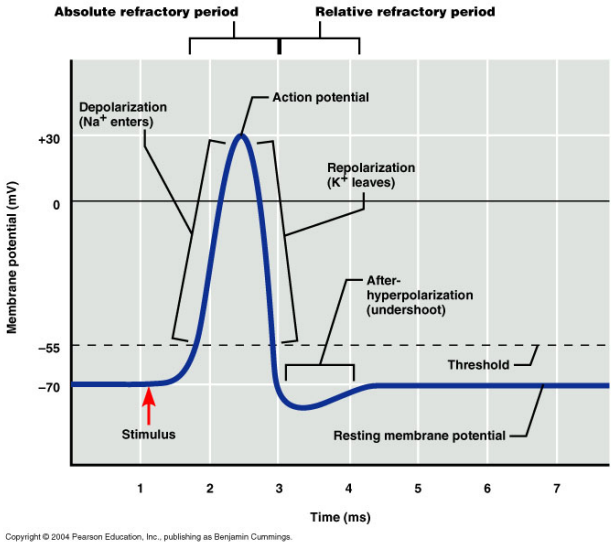

Figure 2. *Action potential phases: a depolarizing stimulus leads membrane potential to overcome threshold potential, Na_V opening induce strong depolarization. Before the peak phase, voltage-gated K^+ channels open. Membrane potential reach a maximum positive value in which Na_V close.*

The ending of sodium current and the persistency of K+ current lead to a hyperpolarization that leads the membrane potential to turn back to negative values. Potassium channel do not close immediately when the membrane reaches the resting potential of -70mV causing a further decrease in voltage, that is an undershoot condition. K+ channels close and membrane potential turn back to resting potential. This last phase is called relative refractory period.

1. <u>Stimulation and rise phase.</u> A typical action potential begins at the axon hillock when an inward gradual potential is sufficient to reach the trigger point, inducing a depolarization above the threshold potential. This trigger depolarization origins from ion currents generated by different external stimuli, depending on the neuron type, such as the release of excitatory neurotransmitters by a pre-synaptic neuron or an external stimulus from sensory neurons. The trigger depolarization is generally mediated by sodium inward.

   Several stimuli can reach the cell body and summate at the level of axon hillock, trigger point. If the depolarizing stimuli is weak the membrane repolarizes back to its normal resting potential, not generating an action potential because the basal outward potassium current (that is essential for the equilibrium potential maintenance) overwhelms the inward sodium current. Conversely, a strong sufficient depolarization, able to change the membrane potential (voltage membrane -V_m) over the threshold potential, causes the voltage-sensitive sodium channels opening, thus generating a strong inward current of Na^+. The influx of Na^+ through these channels causes further

depolarization. The additional depolarization causes stronger voltage-sensitive Na^+ channels opening and consequently induces more inward Na^+ current. This positive feedback cycle drives the membrane potential to the peak of the action potential that is around +55mV, equal to Na^+ equilibrium voltage (Hodgkin cycle; Bullock, Orkand & Grinnell, 1977; Purves et al., 2008; Schmidt-Nielsen, 1997; Junge 1981). Then, depolarization caused by Na^+ influx induces the opening of potassium channels, determining the potassium efflux.

2. Peak and falling phase. As soon as the membrane potential increases toward positive values, the open Na^+ channels slowly shut off, by closing their pores. Hence, the Na^+ channels become inactivated. This change in Na^+ permeability concurs to decrease the membrane potential, driving the voltage back towards the resting value. At the same time, then increase in membrane voltage let open the voltage-sensitive potassium channels. The increase in the membrane potassium permeability drives V_m towards E_K. Altogether, these changes in Na^+ and K^+ permeability cause V_m to drop quickly, repolarizing the membrane and producing the "falling phase" of the action potential. For this reason, the falling phase is also called repolarization phase.

3. Undershoot – After-hyperpolarization. The K^+ channels, opened during the repolarization phase, do not close completely when the membrane returns to its basal resting potential. Indeed, further K^+ channels are open, so that the intracellular concentration of K^+ ions is transiently and unusually low; this makes the V_m even closer to the K^+ equilibrium E_K. The membrane potential goes under the resting membrane potential, causing a so called

undershoot state. This hyperpolarization persists until the membrane K^+ permeability returns to its usual value, restoring the membrane potential at the resting state.

4. Refractory period. Each action potential is characterized by a refractory period, which can be divided into an *absolute refractory period*, during which it is impossible to evoke another action potential, and then a *relative refractory period*, during which a stronger stimulus is required to generate al action potential. These two refractory periods are caused by changes in the state of Na^+ and K^+ channels. After the peak shooting in action potential, the Na^+ channels are closed and enter an "inactivated" state, in which they cannot be opened regardless of the membrane potential. This gives rise to the absolute refractory period. Although a sufficient number of Na^+ channels turn back to their resting state, however, it frequently happens that a fraction of K^+ channels still remain open, driving the membrane potential to a hyperpolarizing state, thereby giving rise to the relative refractory period. The refractory period is responsible for the unidirectional propagation of action potentials along axons. Interestingly, the modulation of the neuronal membrane potential by mean of depolarizing currents, as discussed in this thesis, may substantially change its capability to generate a second action potential, resulting in train of action potentials during firing.

Action potential propagation

The action potential generated at the trigger zone (axon hillock) propagates as a wave along the axon. The currents flowing at a point on the axon during an action potential spread out along the axon, depolarizing the adjacent downstream membrane section. This depolarization provokes a similar action potential at the neighbouring membrane patches,

generating the axon potential propagation. This basic mechanism was demonstrated by Alan Lloyd Hodgkin in 1937 and it is described in figure 3.

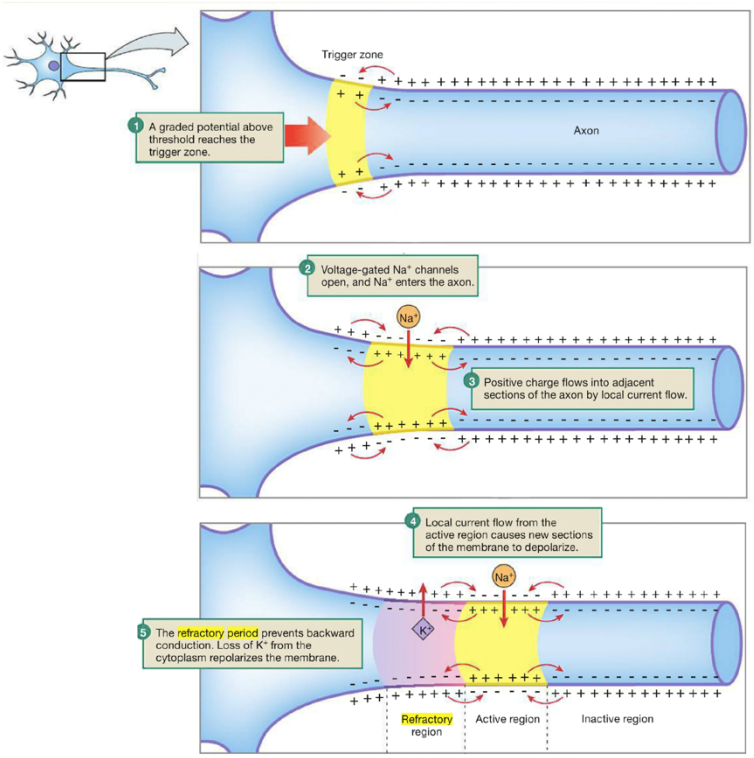

Figure 3. ***(1)*** *One or several depolarizing stimuli reach the axon hillock, called also trigger zone and,* ***(2)*** *if they reach the threshold potential, induce sodium influx and inversion of membrane potential from negative to positive voltage.* ***(3)*** *the depolarization, produced by sodium flux, induces the opening of further voltage-gated sodium channel in the neighbouring distal portion of axonal membrane and the subsequent depolarization till positive value also in this area.* ***(4)*** *local currents continue to propagate causing depolarization in new axonal section.* ***(5)*** *the physiological action potential phases induce potassium channel opening and repolarization of the apical segment. In addition, absolute refractory period prevents backward conduction of the action potential back to soma*

Action potential propagation speed is dependent by the anatomical properties of neuronal fibers, which may be distinguished in two different types: myelinated and unmyelinated fibers. In particular, fiber classification will be described in detail in chapter 3. However, unmyelinated fibers are characterized by slow action potential propagation, whereas myelinated fibers are on the opposite, being characterized by fast action potential propagation. The morphologic/biologic mechanism responsible for this difference is the presence of myelin in myelinated fibers.

Otherwise, the action potential propagation, illustrated in figure 3, represents the phenomena occurring in unmyelinated fibers, while in vertebrate nervous system the majority of neurons are characterized by the phenomena of so called “saltatory

conduction", allowed by the presence of myelin. As a general concept, action potential speed might be slightly improved by increasing the axonal diameter (Hursh JB, 1939), although this implicate unrealistic morphologic and anatomical changes. Therefore, myelination represent the evolutionary answer to the demand of more complex and fast nervous system, both at the central and peripheral level. Myelination, indeed, increases exponentially the mean action potential speed, ranges from 1 meter per second (m/s) to over 100 m/s.

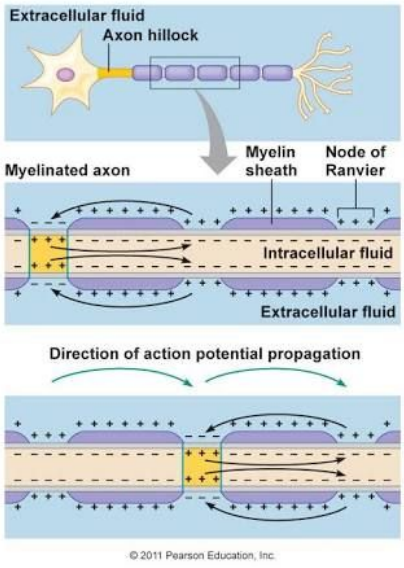

Figure 4. *schematic representation of saltatory conductance in myelinated axon.*

Myelin is a multilamellar sheath formed by cell membrane that enwraps the axon, organized in defined segments separated by intervals, known as nodes of Ranvier. It is produced by specialized cells, that is respectively Schwann cells (SC) in the peripheral nervous system (PNS), and oligodendrocytes in the CNS. Myelin sheath reduces membrane capacitance and increases membrane resistance in the inter-node intervals, thus allowing a fast, saltatory movement of action potentials from node to node (Zalc B, 2006; Poliak S and Peles S, 2006; Simons M and Trotter J, 2007). Myelin, indeed, prevents ions from entering or leaving the axon along myelinated segments and leaves small "free" membrane segments, able to conduct ion currents at the node of Ranvier.

The ionic current, from an action potential, at one node of Ranvier provokes the action potential propagation to the next node. This apparent "hopping" of the action potential from node to node is known as saltatory conduction. Although the mechanism of saltatory conduction was suggested in 1925 by Ralph Lillie, the first experimental evidence of this phenomenon came from Ichiji Tasaki and Taiji Takeuchi and from Andrew Huxley and Robert

Stämpfli. Since the ionic currents are confined to the nodes of Ranvier, far fewer ions "leak" across the membrane, saving metabolic energy. Such an energy preservation represents a significant selective advantage, since the human nervous system uses approximately 20% of the body's metabolic energy demand (Harline NK and Colman DR, 2007). Importantly, also the length of axons myelinated internodes is important to the success of saltatory conduction. They should be as long as possible to maximize the conduction speed, but not so long to avoid a weakening of the incoming signal, unable to provoke an action potential at the next node of Ranvier.

Action potential frequency and encoding

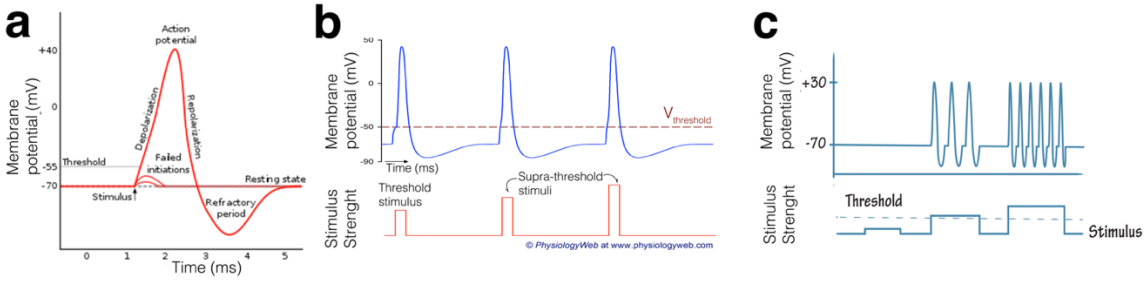

Figure 5. (a) (b) *Action potential has a fixed intensity despite different depolarizing stimulus.* ***(c)*** *Thus, stimuli of different intensities are encoded in different action potential frequency and not as action potential amplitude changes*

The amplitude of an action potential is independent by the amount of current that produced it. Namely, wide currents do not create wider action potentials. Indeed, action potentials are defined as **all-or-none** signals, because they occur fully or they do not occur at all (Sasaki T. et al., 2011; Aur D. et al., 2005; Aur D., 1960) (Figure 5.b). Otherwise, the strength of the stimulus is coded into the frequency of the action potentials that are generated (Figure 5.c). Therefore, the question about the strategies that neurons use to communicate different stimuli and intensities to their target may be raised. Neurons are able to generate train of

action potential, which are characterized by defined frequency and mean number of action potential. This phenomenon is named action potential coding, which can be classified as rate coding, temporal coding and/or population coding (Figure 5 and 6).

Rate coding is a traditional coding scheme, assuming that most, likely not all, information on the stimulus is encoded in the firing rate of the neuron. Therefore, the sequence of action potentials may be characterized by firing rates, rather than as specific spike sequences. In most sensory systems, the firing rate increases (generally non-linearly) as increases the stimulus intensity (Kandel, E et al., 1991)(Figure 5.c). Rate coding was originally shown by ED Adrian and Y Zotterman in 1926 (Adrian ED, Zotterman Y, 1926). In that simple experiment different weights were hung to a muscle. As the weight increased (that is the stimulus increased), the number of spikes recorded from sensory nerves innervating the muscle also increased in parallel. From these original experiments, Adrian and Zotterman concluded that action potentials are unitary events, and the frequency of events (but not the individual event magnitude) is the basis for most of the inter-neuronal communication via action potential. In the following decades, measurement of firing rates became the gold standard for describing the properties of all types of sensory or cortical neurons. This approach was partly based on the relative easiness of measuring the firing rates experimentally.

In addition, it has been identified also the temporal coding, which represents the precise spike timing or high-frequency firing rate fluctuations (Dayan P at al., 2001). A number of studies demonstrated that the temporal resolution of the neural code is based on a millisecond time scale, indicating that the precise spike timing is a significant element for the neural coding (Butts DA el al., 2007; Thorpe SJ, 1990). Such code, that signal the time between spikes are referred as interpulse interval codes. Temporal coding provides an alternative explanation for the “noise", measured in several electrophysiological assay. This

suggests that the random action potential, measured between classical firing trains, could encode information and effects of the neural processing. To translate this hypothesis, binary symbols can be used to convert a train of spikes to a specific code: 1 for a spike, 0 for no-spike. Temporal coding allows the sequence 000111000111 to mean something different from 001100110011, even though the mean firing rate is the same for both sequences, at 6 spikes/10 ms (Theunissen F; Miller JP, 1995).

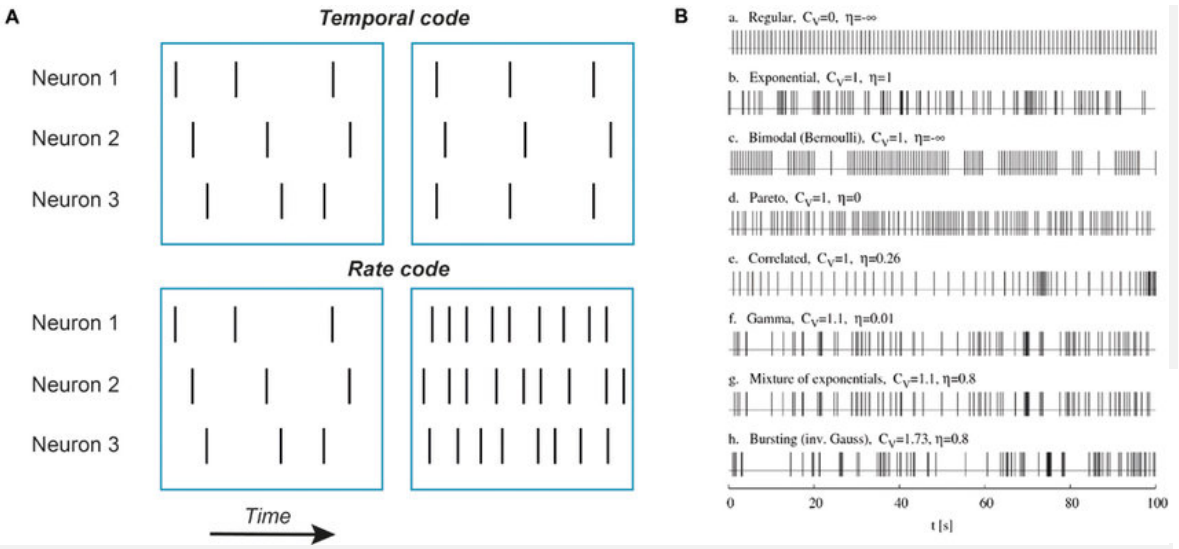

Figure 6. Examples of temporal codes. **(A)** Schematic representation of rate and temporal codes. Each vertical bar represents a single action potential. Top row: an example of temporal coding by three neurons. Note that there is no difference in action potential numbers between left and right blue boxes for all three neurons but on the right action potentials are aligned in time between the first and the third neuron, while in the second neuron the action potentials are delayed and fire after a constant time interval. Such an alignment in time (coincidence) or a constant time delay can be detected by neurons. Bottom row: an example of rate coding. No neuron fires action potentials in synchrony with other neurons, only the number of action potentials is increased. **(B)** Simulated trains of action potentials of the same mean firing frequency, but different variance and randomness. Potentially, all these action potential patterns can represent different temporal codes. Figure from Gytis B, 2015 and Kostal et al. (2007).

Population coding is another coding scheme that can add further information. In fact, certain stimuli can activate different subpopulations of neurons that are characterized by different threshold, conductance speed, desensitization process. Moreover, the integration or discrimination of action potential trains coming from different neurons sustain the nervous system for the interpretation of the signal. This phenomenon is strongly present in sensory system and also in pain perception, because the nociceptors are classified in different anatomical/functional subpopulations. Furthermore, population coding reduces uncertainty due to neuronal variability as well as the ability to represent a number of different stimulus attributed simultaneously. Population coding is also faster than rate coding and can reflect changes in the stimulus conditions nearly instantaneous (Hubel DH and Wiesel TN, 1959). Usually, individual neurons in such a population have different but overlapping selectivity, so that many neurons (necessarily not all) respond to a given stimulus.

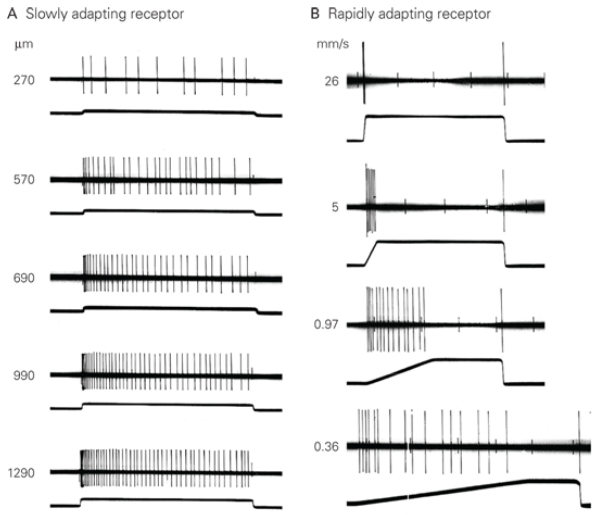

Figure 7. Example of different action potential coding by different neuronal subpopulations. Mechanoreceptors, which transmit different type of mechanical stimuli, are classified also by their rate of adaptation.

Chloride regulation of excitability

As previously described in this chapter, the ions mainly responsible for resting membrane potential and action potential, initiation and propagation, are Na^+ and K^+. Because of that, disbalance between those ions might induce dramatic changes in nervous and muscular cells, causing functional aberration such as conduction failure. For this reason, no voltage-dependent currents of additional ions could stabilize the cell membrane potential.

In cell biology, Cl^- ion is frequently described as an osmotic regulator, however in excitable cells it plays a fundamental role also in the regulation of excitability. Interestingly, is there a tight parallelism between its role in skeletal muscle, which has been fully characterized, and in neurons. As reported by Nielsen O.B. in 2018, Cl^- fluxes are fundamental for the stabilization of muscle membrane potential and for the maintenance of excitability during intense muscle activity. Transmembrane movements of Cl^- constitute up to 80% of the inhibitory currents in the membrane of muscle cells (Coonan JR. and Lamb GD., 1998; Hutter OF. and Warner AE., 1967; Lipicky RJ. Et al., 1971; Palade PT. and Barchi RL., 1977; Pedersen TH. Et al., 2005; Pedersen TH. Et al., 2004; Pierno S. et al., 2007), whereas the chloride channel type 1 (ClC-1) warrant most of the membrane Cl^- permeability (Lipicky RJ. Et al., 1971; Mehrke G. et al, 1988). This inhibitory effect of Cl^- on muscle excitability depends upon two properties. First, muscle fibers have high concentrations of Cl^- and membrane permeability, ascribing to the membrane a high Cl^- conductance. Second, the equilibrium potential for Cl^- is normally close to the resting membrane potential of the fibers, so that in resting condition the net current carried on by Cl^- is small (Figure 8.A). However, in case the membrane potential changes far from the Cl^- equilibrium potential, as during the initiation of an action potential, the Cl^- electrochemical driving force becomes larger; this elicits a Cl^- transmembrane movements toward the re-establishment of the membrane potential at the

Cl^- equilibrium. By this way, the high Cl^- conductance clamps the membrane potential close to the Cl^- equilibrium potential (Figure 8.B).

The physiologic correlation between Cl^- permeability and excitability has been demonstrated also through the observation of muscles hyperexcitability in mammals suffering from myotonia congenita. In this pathology a loss of function mutation in the ClC-1 channel dramatically lowers the resting membrane Cl^- permeability, facilitating the membrane hyperexcitation (Barchi RL.,1975; Bryant SH and Conte-Camerino D., 1991; Koch MC. Et al., 1992; Lipicky RJ. Et al., 1971; Lueck JD. Et al., 2007; Maduke M. et al., 2000; Pusch M., 2002). Conversely, large increases in ClC-1 channel opening leads to reduced excitability (Fink R. and Lüttgau HC., 1976; Pedersen TH. Et al., 2009).

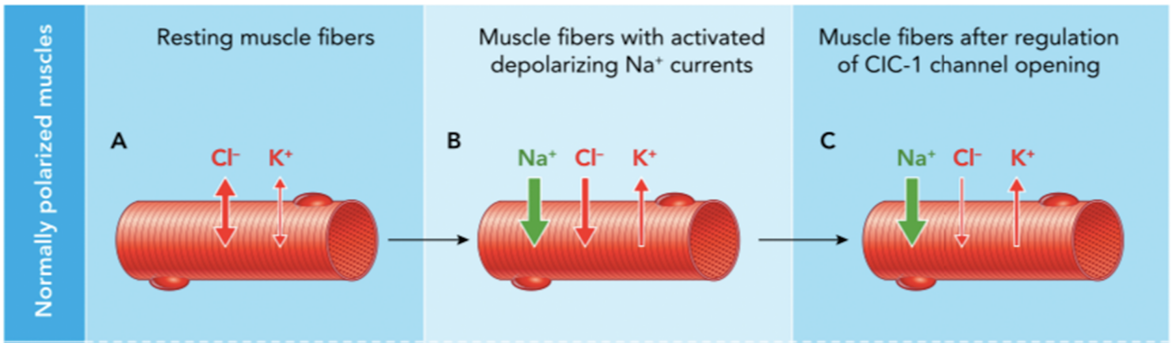

Figure 8. *Illustration of the balance between the excitatory Na^+ and the inhibitory Cl^- and K^+ current, before and after downregulation of ClC-1 channels in active muscle fibers.*
(A) *the resting membrane potential of muscles is stabilized by high conductance for Cl^- ion.* **(B)** *To start an action potential, Na^+ currents must overcome the repolarizing currents elicited by the Cl^- and K^+ channels. In muscles at elevated extracellular K^+, the K^+ conductance is increased and the Na^+ currents are decreased due to Na^+ channel slow inactivation leading to reduced fiber excitability.* **(C)** *In case the ClC-1 channel opening is inhibited, the balance between the excitatory and inhibitory currents is changed, and the excitability is increased.*

In active muscle fibers, as a consequence of K^+ currents during the repolarization phase of action potentials, K^+ accumulates extracellularly. The ensuing depolarization causes the slow inactivation of the voltage-gated Na^+ channels, which *per se* decreases the muscle fiber excitability, thus reducing the magnitude of the excitatory Na^+ currents eliciting the action

potentials. Suddenly, the imbalance between excitatory and inhibitory membrane currents leads to action potential failure, with compromised excitation-contraction and muscle fatigue. Therefore, maintenance of muscle function during exercise requires an activity-dependent counter regulation of muscle fiber excitability. Crucial player in these mechanisms are the Cl^- fluxes trough the muscular ClC-1 channels. In fact, muscle activity induces the inhibition of CLC-1 transporters, reducing the inhibitory Cl^- currents; this restores the balance between the excitatory Na^+ and the inhibitory K^+ currents (Figure 8.C). ClC-1 channels inhibition results in the maintenance of sufficient muscle excitability, reducing fatigue.

Importantly, the same processes occur also in neuronal axons during sustained activity. In this light, it should be underlined that Cl^- currents in neurons are mainly modulated by γ-amino-butyric acid (GABA) type A receptor ($GABA_AR$), extensively discussed in the next chapters.

The inhibition of ClC-1 during sustained activity and fatigue reduces Cl^- conductance up to 80% (de Paoli FV. et al., 2013). Interestingly, several studies have shown that, if the Cl^- conductance is reduced by ≧90%, it may be detrimental to muscle endurance (Cairns SP. Et al., 2004; Clausen T., Nielsen OB., 2007; de Paoli FV. et al., 2013; Dutka TL. Et al., 2008). This controversial effect likely relates to the ensuing loss of resting membrane potential stability (Maduke M., et al., 2000). It leads to larger depolarization in response to extracellular K^+ accumulation (Cairns SP. Et al., 2004), thereby to a stronger loss of excitatory Na^+ current, because of slow inactivation of Na^+ channels. In accordance, the depolarization of the muscle fibers during trains of action potentials may be exacerbated when the Cl^- conductance is reduced (de Paoli FV. et al., 2013; 36). Two opposite effects of Cl^- flux suggest that the optimal Cl^- conductance during intense exercise is determined by exchange

between the effects of the Cl^- conductance on excitability. This phenomenon is considered a biphasic correlation between Cl^- conductance and contractile endurance, exhibiting an improved muscle function up to 80% reduction in Cl^- conductance, but a reduced muscle function at >90% reduction (de Paoli FV. et al., 2013). Normally, the intrinsic downregulation of the Cl^- conductance in working muscles never exceeds 80%, therefore the resulting effect of Cl flux on muscle fiber excitability is prevalent (de Paoli FV. et al., 2013).

In summary, in excitable cells such as neurons, Cl^- currents are crucial in the stabilization of membrane conductance, both in resting condition and during sustained activity, in which Cl^- flux participate in the switch between excitable and/or inhibitor activities.

2. Electrophysiological measurements

Electrophysiology is the branch of physiology that studies the electric properties of cells and tissues. It involves measurements of voltage changes or currents, as well as electric manipulations, on a wide variety of scale, from single ion channels to whole organs, like the heart.

In neuroscience, electrophysiology measures the electric activity of neurons, in particular the action potential activity. Classical electrophysiological techniques actualize by placing electrodes into different biologic preparations, then recording electric activity from single cells, fibers or whole tissues.

Intracellular recording in single cell

An electrode sufficiently small in diameter (micrometres) can be inserted into a single cell, allowing the direct observation and recording of the intracellular electrical activity. In detail, it may be studied also by using a special form (hollow) of glass pipette, containing an electrolyte. Within this technique, the microscopic glass pipette tip is pressed against the cell membrane, to which it adheres tightly interacting with the membrane lipids. Applying a pulse of negative pressure to the pipette, the small patch of membrane encircled by the pipette rim may be fractured. Consequently, the electrolyte solution present in the the pipette may be delivered, in fluid continuity, with the cytoplasm (whole-cell recording). Alternatively, to set up an intracellular recording, the tip of a sharp microelectrode must be inserted inside the cell cytoplasm, so that the membrane potential previously described can be measured as illustrated in Figure 9.

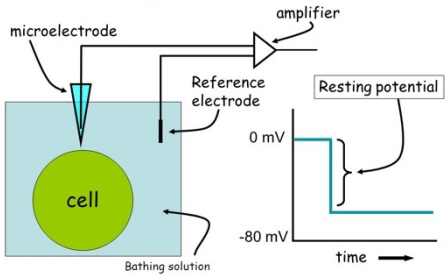

Figure 9. The system measures the voltage difference in voltage between a reference electrode, embedded in conducting solution, and a microelectrode. When both electrodes are plunged in the bath solution, the electric potential is equal to 0. When the electrode is inserted in the cell, indeed, it records the membrane potential, which drastically drops to -70 mV.

Extracellular compound action potential recording

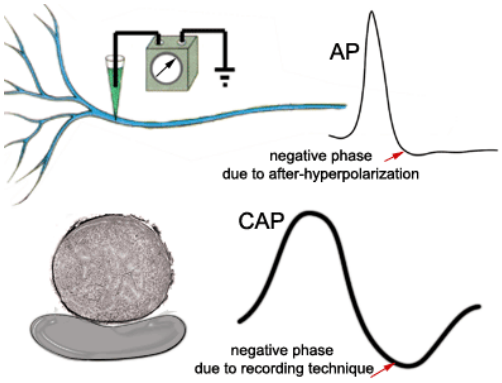

Figure 10. In the upper panel the schematic representation of action potential recording from single fiber. In the lower panel the schematic representation of CAP recording from entire nerve

Focusing the interest from the study of single neurons to organized neuronal tissues, the techniques suitable for *in vivo* or *ex vivo* recording on PNS may be distinguished in single fibers recording or compound action potential (CAP) recording (Figure 10). Single fibers techniques allows the measurement of intracellular voltage of a single axon or terminal, whereas CAP recording allows the recording of extracellular voltage from a whole nerve. In both cases, however, to measure the characteristic of action potential transmission in fibers, it is necessaire to record the neural activity generated by exogenous electrical stimulation. Notably, the CAP method relies on a suitable stimulus applied to the nerve or tissue, capable to evoke a CAP. Thereby, an exogenous stimuls is applied to the entire nerve, simultaneously and synchronously, recruiting many fibers. Depending either on the stimulus intensity or the fiber threshold, the resulting CAP response represents the summation of action potential generated by all activated fibers. Namely, more are the fibers recruited, bigger is the CAP amplitude recorded (lower panel of Figure 10).

Importantly, it should be underlined hat the shape of CAP, measured from a nerve, do not represent the classical action potential phases but the summation of several action potentials. CAP is resulting by assembling hundreds of individual neurons or nerve fibers. Differently from a all-or-none single action potential, CAP is a graded phenomenon; the stimulus producing the maximal response is the stimulus needed to recruit all axons.

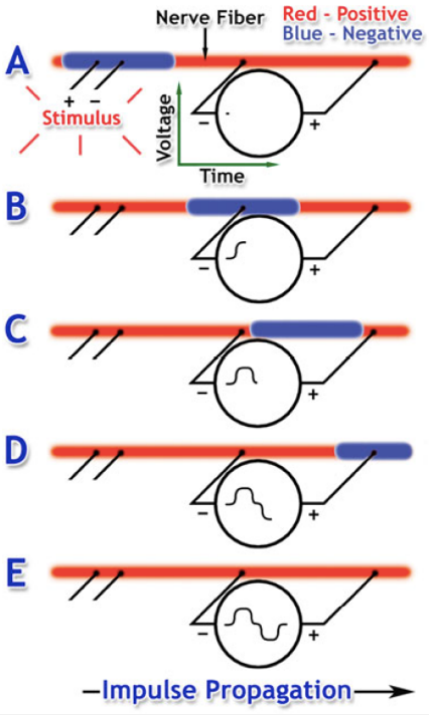

Figure 11. *CAP recording:* ***(A)*** *When a challenge, an external stimulus exceeds a defined threshold, an action potential occurs, creating the nerve impulse shown in blue. The polarity of the impulse is negative (-), because the recording is from outside (opposite polarity to that inside the cell). Since both recording electrodes at this instant are at the same voltage potential, the recording measure is 0 Volts. Regardless of the stimulus strength above threshold, the corresponding nerve impulse amplitude, duration and propagation velocity is the same.*
(B) *The nerve impulse propagates along the nerve with constant amplitude and velocity until it eventually passes over the negative ("-") recording electrode, resulting in a positive (upward) voltage recording.*
(C) *Propagation persists, as long as a point where the nerve impulse is between the "-" and "+" electrodes may be reached. This results in a 0 Volt recording (both electrodes at same voltage).*
(D) *Propagation continues and eventually pass over the "+" electrode, resulting in a negative (downward) voltage recording.*
(E) *At some point, the impulse propagation is complete, with the entire nerve fiber returned to its resting state. Since both electrodes are at the same voltage, the recorded voltage is 0 Volts.*

3. The somatosensory system

The somatosensory system is the set of neurons and neuronal pathways that perceive sensory stimulus and signal to the CNS. The sensory coding was studied electrophysiologically, first in the somatosensory system. Somatosensory information is provided by receptors distributed throughout the whole body, internal and/or on the cell surface. Indeed, the somatosensory system serves three major functions: proprioception, exteroception, and interception.

- *Proprioception* is the sense of oneself. Receptors located in skeletal muscle, joint capsules, and skin enable the capacity of conscious awareness of the body posture and movement, particularly of limbs and head.
- *Exteroception* is the sense of direct interaction with the external environment, as it impacts on the body. The principal modality of exteroception is the sense of touch, which includes sensations of contact, pressure, roughness, motion, and vibration, and is used to identify objects. Exteroception also includes the thermal senses of heat and cold. The sensory and motor components of touch are intimately connected in the brain and are important in determining the behaviour.

  Finally, exteroception includes the sense of pain, or nociception, a response to external events that damage or harm the body. Nociception is the prime challenge for actions aimed for survival, such as flight or fight.
- *Interoception* is the sense of the function of the major internal organ/systems of the body. Although most of the events recorded by intero-receptors in the viscera do not become conscious, information conveyed by these receptors is crucial for regulating autonomic functions, particularly for the cardiovascular, respiratory, digestive, and renal systems. (Crain AD., 2002)

Somatosensory information from the skin, muscles, joint capsules, and viscera are conveyed to the CNS area through the dorsal root ganglion (DRG) neurons, innervating the limbs and trunk, or through cranial nerves, such as the trigeminal sensory neurons, that innervate cranial structures (the face, lips, oral cavity, conjunctiva, and dura mater), or the sensory neurons forming the facial, glossopharyngeal and vagus nerves. These sensory neurons perform two major functions: the transduction and encoding of sensory stimuli into electrical signals and the transmission of those signals to the CNS.

Therefore, the DRG neurons generally represent the primary sensory neuron in the somatosensory system (Figure 12). The cell body of a DRG neuron lies in a ganglion on the dorsal root of a spinal nerve. Individual neurons in a DRG respond selectively to specific types of stimuli because of morphological and molecular specialization of their peripheral terminals. DRG neurons originate from the neural crest and are intimately associated with the nearby segment of the spinal cord. DRG neurons are a type of bipolar cell, called pseudounipolar cells. The axon of a DRG neuron has two branches, one projecting to the periphery and one projecting to the CNS (Figure 12).

Figure 12. *The DRG neuron is the primary sensory cell of the somatosensory system. The neuronal soma is located in a dorsal root ganglion, adjacent to the spinal cord. DRG neurons are pseudounipolar afferent neurons, T-shaped, which axon has two branches, one projecting to the periphery and the other projecting to the spinal cord (forming dorsal roots), where the afferent signals are processed. The distal branch conveys afferent somatosensory signals from peripheral specialized sensory receptors or free endings (nociceptors).*

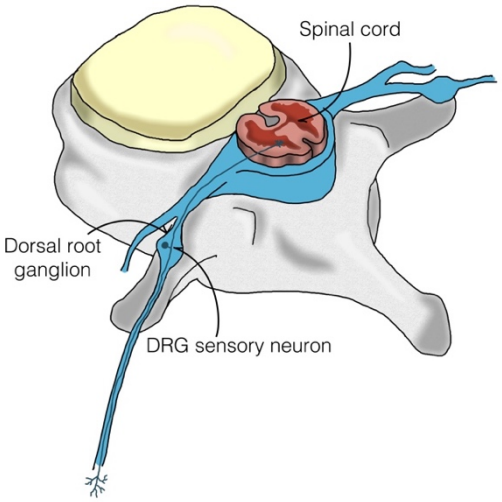

The peripheral terminals of different sensory neurons innervate the skin, muscle, joint capsules, or viscera whereas they end with specialized receptors for particular kinds of stimuli. These receptors differ in morphology and stimulus selectivity (e.g. Ruffini, Pacini. Merkel, Meissner corpuscoli). The central branch, or DRG root, enter the spinal cord, forming the first synapse of the somatosensory ascending pathways: the dorsal lemniscal system or the anterolateral system (see the Chapter below)

Thus, the axon of each DRG cell serves as a single transmission system, which is directional from the peripheral receptor terminals toward the CNS. Therefore, this system is called the primary afferent fiber. Individual primary afferent fibers innervating a particular region of the body, for instance the fingers, are grouped into fascicles of axons, forming the peripheral nerves. However, a lot of peripheral nerves are mixed nerves, because they also include the motor axon, innervating nearby muscles, blood vessels, glands, or viscera.

Classification of peripheral somatosensory fibers

The diverse modalities of somatic sensations are mediated by peripheral nerve fibers that differ in diameter and conduction velocity. Mechanoreceptors for touch and proprioception are constituted by DRG neuronal fibers with large-diameter and myelinated axons, that convey rapid action potentials. Thermal receptors, nociceptors, and other chemoreceptors are formed by small-diameter axons, that are either unmyelinated or thinly myelinated; these nerves conduct impulses more slowly. The different conduction velocity allows signals of touch and proprioception to reach the spinal cord and higher brain centers faster than noxious or thermal signals.

Large-diameter fibers conduct action potentials rapidly because the internal resistance to current flow along the axon is low. Moreover, the presence of myelin sheets further increase the action potential speed because of saltatory conduction, in addition to a larger distance between nods of Ranvier.

Peripheral nerve fibers are classified in groups based on properties related to axon function (sensory or motor), diameter, myelination and conduction velocity. One experimental method for classifying peripheral nerve fibers is based on electrical stimulation of whole nerves. This is a very common diagnostic technique, by which nerve conduction velocities are measured using pairs of stimulating and recording electrodes placed on the skin on top of a peripheral nerve. With this method is possible to classify different classes of fibers, based on conduction velocity and excitability threshold. The recorded signal (Figure 13) represents the action potentials of all nerve fibers excited by the stimulus pulse and is equivalent to CAP (as reported in chapter 2). It increases in amplitude in correlation with the increasing number of stimulated nerves fibers. Therefore, the summed activity is roughly proportional to the total number of active nerves fibers. During this analysis, peripheral

nerves are gradually stimulated with growing stimulus intensities, generating action potential in fibers when they reach their specific excitability threshold (Figure 13) (Mano T. et al., 2006; Valbo AB. et al., 1979; Eric R. et al., 2013).

Based on this measurements, peripheral fibers may be classified as Aα, Aβ, Aδ ad C fibers.

- **Aα fibers:** The earliest signal recorded by the CAP recording occurs in Aα fibers, characterized by conduction velocities greater than 90 m/s. This signal reflects the action potentials generated in motor neurons innervating skeletal muscle, that are generated by myelinated large diameter fibers.
- **Aβ fibers:** A second signal originate from largest diameter afferent fibers, present primarily in nerves that innervate the skin and deputed to tactile sensation. When indeed Aβ fibers are active, the subject will sense tingling non-painful sensation.

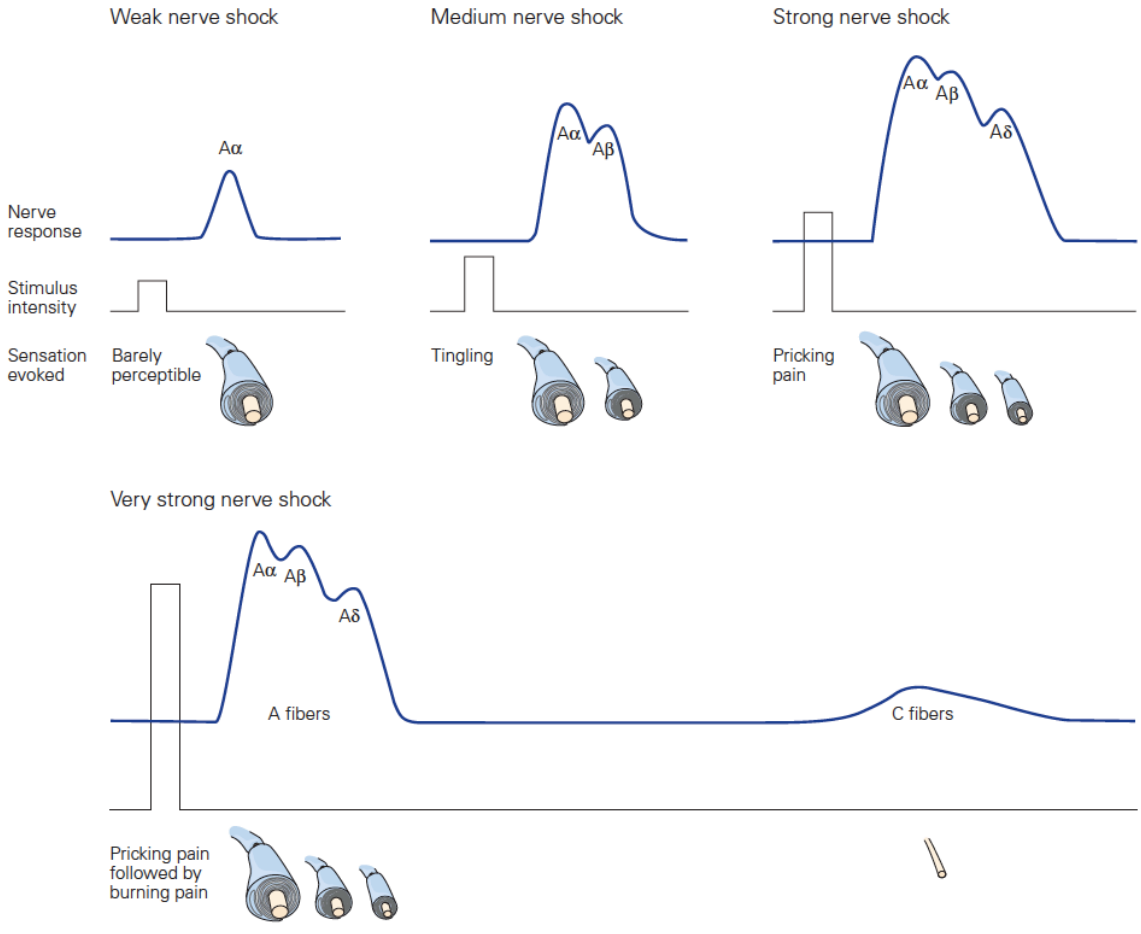

Figure 13. Measurement of conduction velocity of peripheral nerves. Nerve conduction velocities are measured increasing gradually the stimulus intensity. A pair of stimulating and recording electrodes are placed on the skin on top of a peripheral nerve.

- Aδ fibers: At higher voltages, when axons in the smaller Aδ range are recruited, the stimulus becomes painful. Those fibers are small diameter myelinated fibers. Nociceptors carrying information from peripheral mechanoreceptors and thermoreceptors to the dorsal horn of the spinal cord. Aδ fibers serve to receive and transmit information primarily relating to acute pain (sharp, immediate, and relatively short lasting). This type of pain can result from several classifications of stimulants: temperature-induced, mechanical, and chemical-induced. They are characterized by higher threshold compared with Aβ fibers, because deputed to distinguish a noxious/dangerous signal compared with simple tactile sensation. (Skljarevski, V.; Ramadan, N. M., 2002; Striedter GF, 1961, Purves D 2012). Moreover, Aδ fibers are slower then compared to Aβ fibers, because the possesses a smaller diameter.
- C fibers: A voltage sufficient to activate unmyelinated C-fibers evoke sensations of burning pain. C-fibers are indeed the fibers deputed to nociception, with the higher threshold and characterized by the slowest conduction velocity. C-fibers are unmyelinated nociceptors present in nerves of the skin and in deep somatic and visceral structures. C fibres has a diameter smaller than 2 mm and are characterized by conduction velocity of less than 2 m/s. C-fiber axons are grouped together into structures called Remak bundles. These occur when a non-myelinating Schwann cell bundles a group of axons. The Schwann cell isolate each axon, squeezing its cytoplasm among them and hindering axon-to-axon contact. Interestingly, not all unmyelinated fibres are nociceptors: some respond to heat in the non-noxious range and some are activated by non-noxious mechanical stimuli. These fibers are classified as “C touch” fibers.

Sensory neurons can be classified also by their physiologic function, depending on the specialized receptor present at their terminal. The particular receptor class expressed in the nerve terminal of a sensory neuron determines the type of stimulus detected by the neuron. The peripheral axons of the sensory neurons that mediate touch and proprioception (for instance, the Pacini or Meissner corpuscole) terminate with a non-neural capsule. They sense mechanical stimuli that physically deform the receptive surface. In contrast, the peripheral axons that detect noxious, thermal, or chemical events terminate with unsheathed endings and multiple branches. A variety of morphologically specialized receptors underlie the various somatosensory sub modalities. Based on receptor type, fiber type and physiologic function, sensory neurons can be classified as reported in the following table (Lumpkin EA. And Caterina MJ., 2007)

RECEPTOR RYPE	FIBER TYPE	FUNCTION
Cutaneous and subcutaneous mechanoreceptors:		touch
Meissner corpuscle	Aβ fibers	stroking and flutter
Merkel disk receptor	Aβ fibers	pressure and texture
Pacinian corpuscle	Aβ fibers	vibration
Ruffini ending	Aβ fibers	skin stretch
Hair-tylotrich, hair-guard	Aβ fibers	stroking and fluttering
Hair-down	Aδ fibers	light stroking
Field	Aβ fibers	skin stretch
C mechanoreceptor	C fibers	Gentle/erotic touch
Thermal receptors		temperature
Cool receptors	Aδ fibers	Skin cooling (< 25°C)
Warm receptors	C fibers	Skin warming (>35°C)
Heat nociceptors	Aδ fibers	Hot temperature (>45°C)
Cold nociceptors	C fibers	Cold temperature (< 5°C)
Nociceptors		Pain
Mechanical	Aδ fibers	Sharp, pricking pain
Thermal-mechanical (heat)	Aδ fibers	Burning pain
Thermal-mechanical (cold)	C fibers	Freezing pain
Polymodal	C fibers	Slow, burning pain
Muscle and skeletal mechanoreceptors		Limb proprioception
Muscle spindle primary	Aα fibers	Muscle length and speed
Muscle spindle secondary	Aβ fibers	Muscle stretch
Golgi tendon organ	Aα fibers	Muscle contraction
Joint capsule receptors	Aβ fibers	Joint angle
Stretch-sensitive free endings	Aδ fibers	Excess stretch or force

Nociceptors

The receptors that respond selectively to stimuli that may damage the tissue or organ are called nociceptors (Latin *nocere*, to injure). They respond directly to mechanical and thermal stimuli, and indirectly to other stimuli by means of chemicals released from cells in the injured tissue. In principle, the physiologic function of nociceptors is to limit the tissue injury and, more importantly, provide a constant reminder of tissues that must be protected.

Unlike mechanoreceptors, that are formed by specialized receptors at their endings, nociceptors are formed by peripheral free nerve endings, that need a transduction process for the conversion of a noxious stimulus (mechanical, chemical or thermal) into an electrical signal. Nociceptors involves a number of ion channels that are sensitive to different exogenous stimuli (Figure 14).

Nociceptors in the skin, muscle, joints, and visceral receptors fall into two broad classes, based on the myelination of their afferent fibers. Nociceptors forming Aδ fibers produce short-latency pain, that is described as sharp and pricking. The majority are called mechanical nociceptors because are excited by sharp objects that penetrate, squeeze, or pinch the skin (Figure 14). Many of these Aδ fibers also respond to noxious heat, burning the skin.

Nociceptors forming the C fibers produce dull burning pain, that is diffused on a wide area and poorly tolerated. The most common types are polymodal nociceptors that respond to a variety of noxious mechanical, thermal, and chemical stimuli, such as pinch or puncture, noxious heat and cold, or irritant chemicals applied to the skin. Electrical stimulation of these fibers in humans evokes prolonged sensations of burning pain. In the viscera nociceptors are activated by distension or organ swelling, producing sensations of intense pain. (Craig AD., 2004; Han ZS. Etal., 1998; Iggo A., 1960; Eric R. et al., Principles of Neural Science 2013).

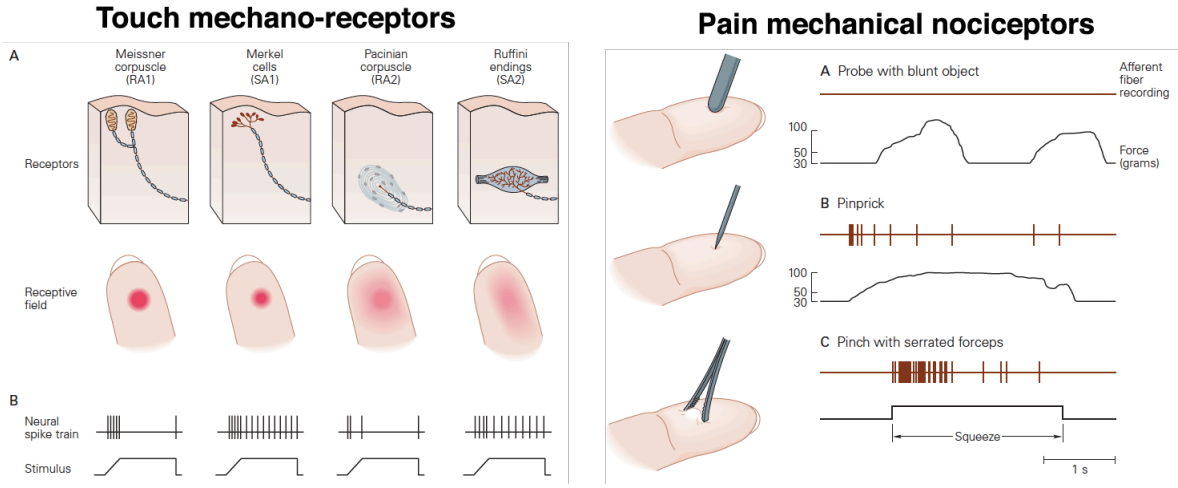

Figure 14. *Morphological and functional differences between mechanoreceptors and mechanical nociceptors. Specialized structural receptors are responsible for touch transduction, while nociceptors are characterized by free ending and higher threshold.*

Spinal and cranial nerves

Sensory information reaches the CNS either through the 31 spinal nerves, which enter through openings between the vertebrae of the spine, or through the 12 cranial nerves, which enter through openings in the cranium, at the brain stem level. The afferent and efferent axons within a spinal nerve arise from the dorsal and ventral roots of the spinal cord.

Individual spinal nerves terminate on neurons located in specific zones of the spinal cord grey matter. The spinal neurons that receive sensory input are either interneurons, which terminate upon other spinal neurons within the same or neighbouring segment, or projection neurons that serve as the cells of origin of major ascending pathways to higher centers in the brain.

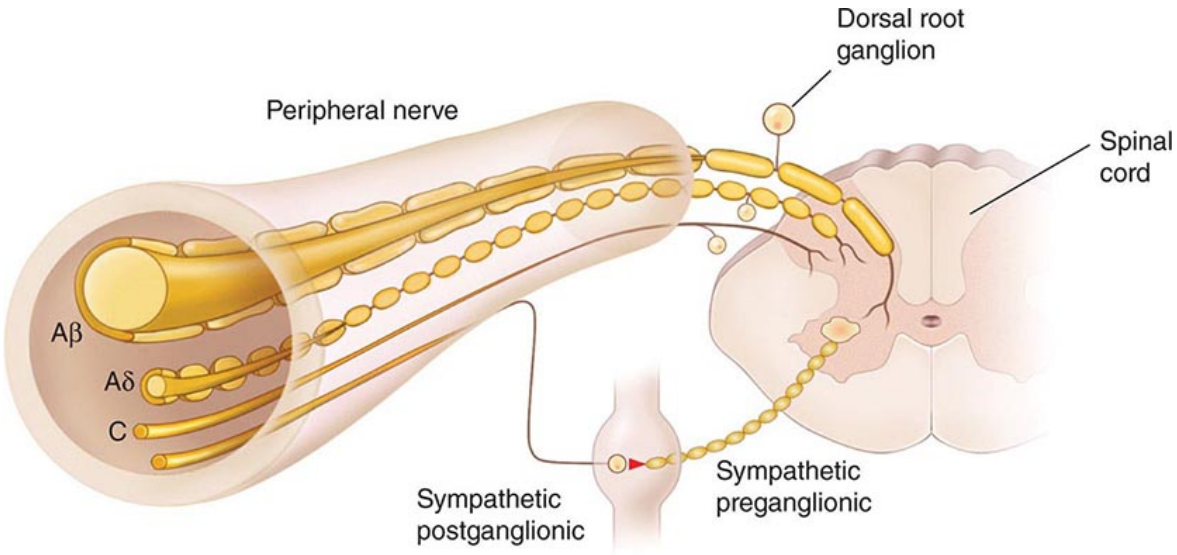

Figure 15. *Components of a typical cutaneous nerve. There are two distinct functional categories of axons: primary afferents with cell bodies in the dorsal root ganglion, and sympathetic postganglionic fibers with cell bodies in the sympathetic ganglion. Primary afferents include those with large-diameter myelinated (Aβ), small-diameter myelinated (Aδ), and unmyelinated (C) axons. All sympathetic postganglionic fibers are unmyelinated.*

Majority of spinal nerve contain both afferent and efferent fibers. After entering the spinal cord, the afferent fibers become further segregated, according to their physiologic modalities, and terminate on different functional sets of neurons in the grey matter of the same or adjacent spinal segments (Boyd IA. And Davey MR., 1968; Eric R. et al., Principles of Neural Science 2013).

Somatosensory ascending pathways

Tactile and noxious pathway travel along different path to reach the sensory cortex in the brain. The tactile specialized afferent fibers, Aα and Aβ, enter the spinal cord dorsal column on each side, forming the medial lemniscal system, that is the ascending gracile and cuneate fascicles.

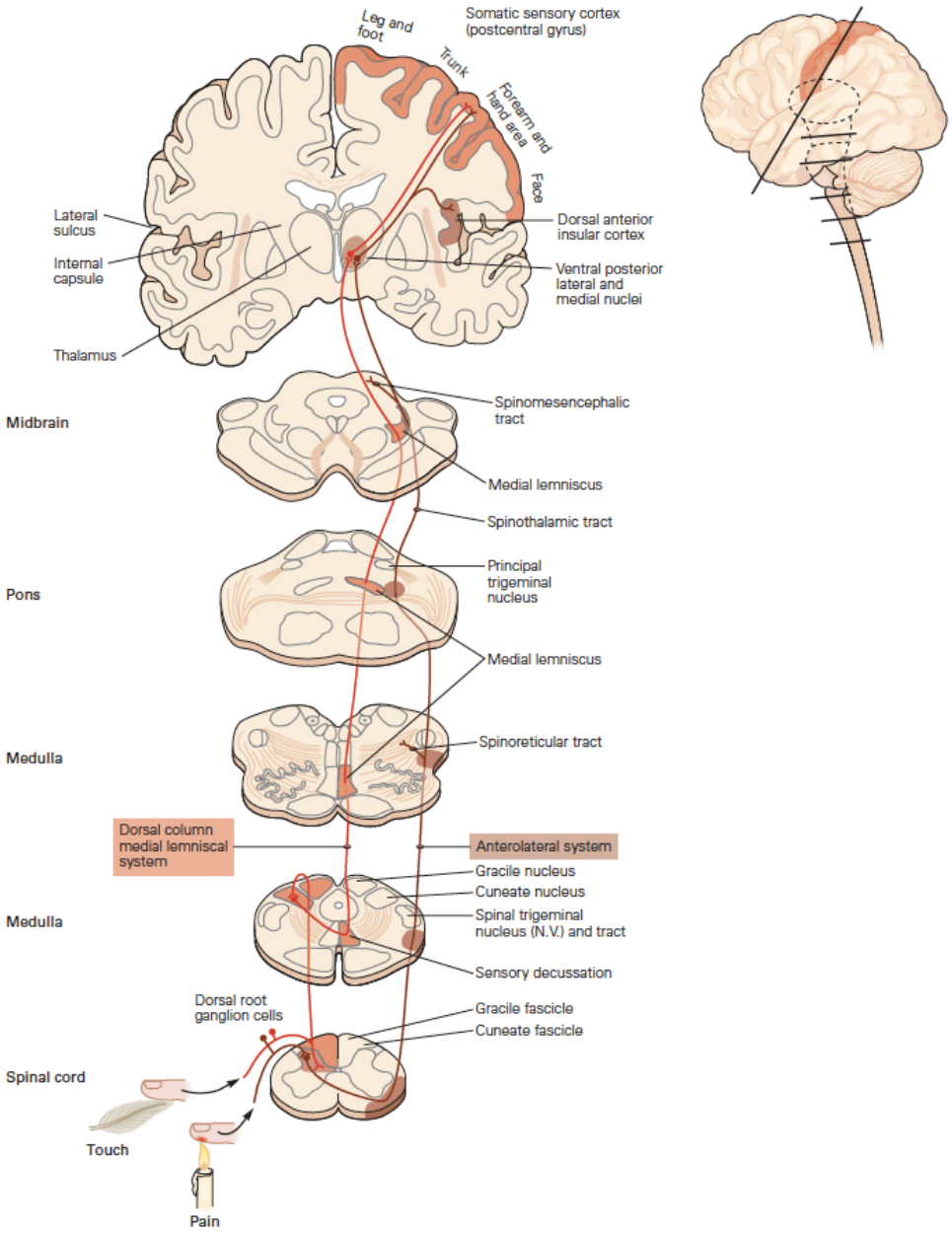

Figure 16. Somatosensory information from the limbs and trunk is conveyed to the thalamus and cerebral cortex through the ascending pathways.

They ascend up to the medulla oblungata, where first sensory decussation occurs, forming the major ascending pathway for tactile and proprioceptive information that project to the brain stem nuclei, that is the thalamus. From thalamus the somatosensory information is conveyed to the parietal cerebral cortex (Figure 16; red path). When the fibers reach the brain stem they are sorted into a coherent map, with the anogenital skin of the ipsilateral side of the body most medial and the skin of the ipsilateral neck and head most lateral.

In parallel, the pathway of pain signalling, originating with peripheral Aδ and C fibers, make the first synaptic contact directly in the spinal cord, with a projection neuron crossing the spinal cord on the contralateral side. After this initial decussation, the pain signals travel along the spinothalamic tract. Indeed, the spinothalamic tract is the principal pathway transmitting noxious, thermal and visceral information to the thalamus and cerebral cortex. It originates from neurons in laminae I, V, and VII, the main targets of the small-diameter fibers with sensory information intended for conscious perception. These neurons have distinctive physiological properties based on their sensory inputs. Spinothalamic tract ends in thalamus, like tactile fibers forming the medial lemniscal system, and similarly project to the parietal somatosensory cortex (Figure 16; brown path).

(Al-Chaer ED. et al., 1996; Hodge CJ. Jr and Alkarian AV., 1990; Kaas JH., 2008; Eric R. et al., Principles of Neural Science 2013).

4. Pain

The International Association for the Study of Pain (IASP) has defined pain as *'...an unpleasant sensory and emotional experience associated with actual or potential tissue damage or described in terms of such damage'*. In consequence, the perception of pain and its threshold are the result of complex interactions between sensory, emotional, and behavioural factors.

Pricking, burning, aching, stinging, and soreness are among the most distinctive of all the sensory modalities. As with the other somatic sensory modalities (touch, pressure, and position sense) pain serves an important protective function, alerting the body to injuries that require flight, evasion or treatment. In children born with a pathology bearing the insensitivity to pain, severe injuries often go unnoticed and can lead to permanent tissue damages.

When pain is experienced it can be acute, persistent, or in cases chronic. Persistent pain characterizes many clinical conditions and is usually the reason for which patients seek medical attention. Surprisingly, chronic pain appears to have no clinical goals or physiological significance; it only alienates patients in a miserable condition. Pain perception is highly subjective and personal, hence is rather difficult to be defined objectively and to treat clinically.

Many organs in the periphery, including skin and subcutaneous structures such as joints and muscles, possess specialized sensory receptors that are activated by noxious insults. As already reported in the previous chapter, unlike the specialized somatosensory receptors for light touch and pressure, most of these nociceptors are free nerve endings of primary

sensory neurons. There are three main classes of nociceptors: thermal, mechanical, and polymodal as well as a more enigmatic fourth class, termed silent nociceptors.

- *Thermal nociceptors* are activated by extreme temperatures, typically greater than 45°C (115°F) or less than 5°C (41°F). They are the peripheral free endings of small diameter, thinly myelinated Aδ axons that conduct action potentials at speeds of 5 to 30 m/s.
- *Mechanical nociceptors* are activated optimally by intense pressure applied to the skin. Also, these receptors are the endings of thinly myelinated Aδ axons.
- *Polymodal nociceptors* can be activated by high-intensity mechanical, chemical, or thermal (both hot and cold) stimuli. This class of nociceptors is found at the ends of small-diameter, unmyelinated C axons that conduct slowly, at speeds less than 1.0 m/s. These nociceptors respond to heat, intense cold, intense mechanical distortion (such as a pinch) changes in pH, particularly acid condition. In addition, it has been demonstrated that polymodal nociceptors and sensitive to chemical irritants, including adenosine triphosphate (ATP), serotonin, bradykinin, and histamine.
- *Silent nociceptors*. Although each nociceptor responds to a variety of possible threshold levels of stimuli, some do not respond at all to chemical, thermal or mechanical stimuli unless injury occurred. These are typically referred to as silent or sleeping nociceptors since their response comes only on the onset of inflammation of the surrounding tissue (Jessel TM et al., 1991). Recently, this peculiar type of nociceptor became a hot topic in the field of study of chronic pain and peripheral neuropathies, because it has been demonstrated playing a crucial role in the phenomena of pain sensitization and chronicization.

Thermal, mechanical and polymodal nociceptors are widely distributed in skin and deep tissues and are often coactivated. For example, when an injury occurs, the initial feeling is a sharp pain ("first pain"), followed by a more prolonged aching and sometimes burning pain ("second pain"). The fast-sharp pain is transmitted by Aδ fibers that carry information from damaged thermal and mechanical nociceptors. The slow dull pain is transmitted by C fibers, that convey signals from polymodal nociceptors.

Noxious stimuli depolarize the free nerve endings of afferent axons and generate action potentials that are propagated centrally, without the presence of any specialized structure deputed to transduction, as mechano-receptors (Figure 14). In nociceptor, the membrane of free endings contains receptors that convert the thermal, mechanical, or chemical energy of noxious stimuli into a depolarizing electrical potential. The major family of receptors expressed by nociceptor are the so-called transient receptor potential (TRP) ion channels. The first subtype discovered was TRPV1, a receptor able to respond to thermal stimuli and chemicals (as capsaicin, the drug in chili pepper, *capsicum*) (Principles of Neural Science 2013).

Noxious ascending pathways

These sensory pathways are part of the somatosensory ascending system and were described in previous chapters. However, all information generated in the periphery by nociceptors are transmitted to CNS through several steps of integration and modulation. Pain is conveyed along three neuron sub-pathways (first, second and third order neurons) that transmit noxious stimuli from the periphery to the cerebral somatosensory cortex. Indeed, peripheral transmission reaches spinal transmission, ascending tracts and finally supraspinal processing. The first step is represented by the transmission of primary afferent

of DRG neurons to second order neuron in the dorsal horn of spinal cord. Second order neurons are either nociceptive-specific or wide dynamic range (WDR). Noxious signal is then transmitted through the spinothalamic tract to the contralateral side of the spinal cord and then to the thalamus, whereas it synapses with the third order neurons that send fibers to the somatosensory areas in the parietal cortex.

Gate control theory

As previously reported, the first synapse of pain ascending pathway is in the spinal cord, whereby it represents the first step of pain modulation. The mammalian dorsal spinal cord processes information related to a variety of sensory modalities, including pain, itch, temperature, and touch (Braz J et al., 2014; Todd AJ, 2010). At this level is present an important inhibitory mechanism mediated by interneurons located in *substantia gelatinosa* of the spinal cord. This mechanism is at the base of the so called “gate control theory” of pain. Gate control theory asserts that non-painful signals shut the nerve "gates" off to painful input, preventing pain sensations from traveling to the CNS.

For instance, it is very common to observe that when a person experiences pain from a bump or a bite, a common reaction is an attempt to constrain the negative feeling, by rubbing or scratching the painful area. These are clear examples of gate control theory.

Gate control theory asserts that activation of nerve fibers such as Aβ afferents, which do not transmit pain signals may interfere with signals from painfull C-fibers, thereby concurring to inhibit pain. In a simplified version of this theory, it was proposed that both C-fibers (Figure 17; yellow) and Aδ fibers (touch-, pressure-, and vibration- transmitting; Figure 17, purple) carry information from the site of the injury to the projection neuron in the spinal cord,

which carry the pain signals up to the brain. Those Aδ and C-fibers make synapses also with inhibitory interneuron, that block the transmission cell activity (Figure 17).

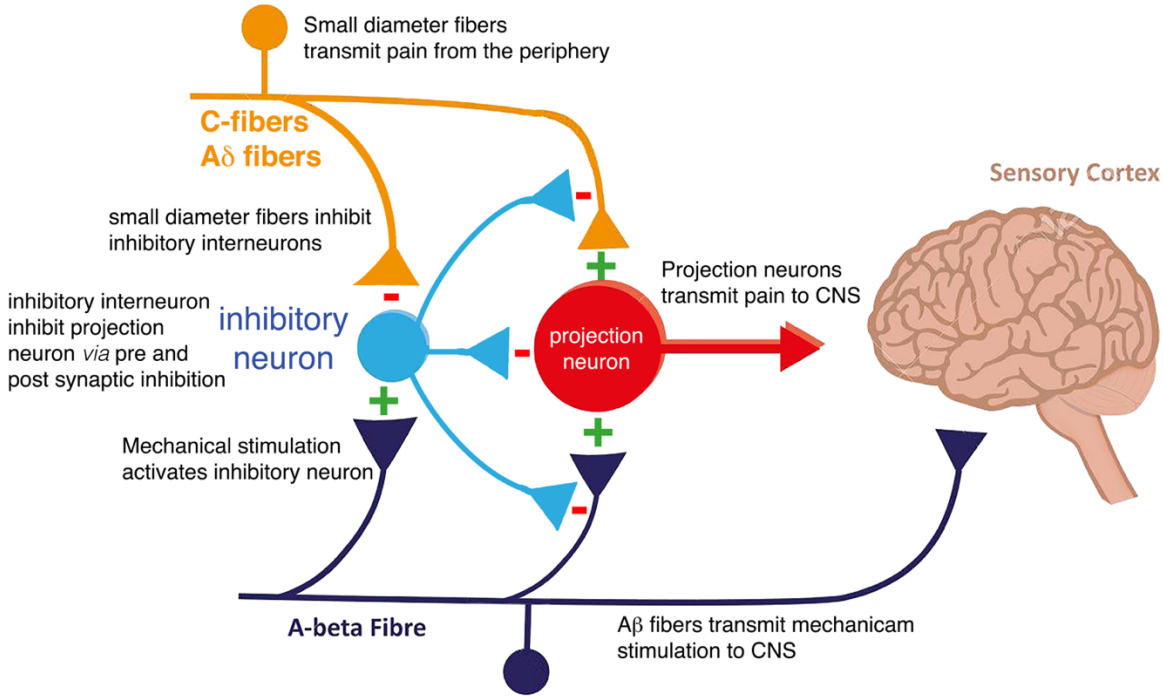

***Figure 17**. Gate control theory of pain. This model proposes that inhibitory interneurons (light blue) located in the substantia gelatinosa would control whether nociceptive input from the periphery are relayed through the spinal transmission system (projection neuron in red) to higher CNS areas, where pain sensation is consciously perceived.*

Therefore, mechanical perception is able to inhibit pain via the activation of inhibitory interneurons, that in turn inhibit second order neurons in the spinal cord. These mechanisms are mediated by the release GABA neurotransmitter, that will be further described in the next chapters.

Pain and peripheral neuropathies

It should be mentioned that the normal process of sensory signalling may be dramatically altered when peripheral tissues are damaged, resulting in an increase in pain sensitivity. This condition can be elicited by sensitizing peripheral nociceptors, through repetitive exposure

to noxious stimuli. The sensitization is triggered by a complex mix of chemicals released from damaged cells that accumulate at the site of tissue injury. This cocktail contains peptides and proteins such as bradykinin, substance P and nerve growth factor (NGF), as well as molecules such as ATP, histamine, serotonin, prostaglandins, leukotrienes and acetylcholine. Many of these chemical mediators are released from distinct cell types, but together they act to decrease the threshold of nociceptor activation, increasing pain sensitivity.

Therefore, the activation of nociceptors is associated with several pathological conditions. Allodynia and hyperalgesia are two common pain states that reflect changes in nociceptor activity. Patients with allodynia feel pain in response to stimuli that are normally innocuous. For instance, a light touch of sunburned skin or the joints movement in patients with arthritis rheumatoid, all produces allodynia. Nevertheless, patients with allodynia do not feel pain constantly. In the absence of a peripheral stimulus there is no pain. In contrast, patients with hyperalgesia, which is considered an overstated response to noxious stimuli, perceive persistent pain in the absence of sensory stimulation.

Persistent chronic pain can be subdivided into two broad classes, nociceptive and neuropathic. *Nociceptive pain r*esults from the activation of nociceptors in the skin or soft tissue in response to tissue injury. Usually it arises from an accompanying inflammation. For instance, tissue sprains and strains produce mild forms of nociceptive pain, whereas arthritis or a tumor invading soft tissues produce a much more severe nociceptive pain. Neuropathic pain results from direct injury to nerves in the PNS or CNS and is often accompanied by burning or electric sensations. Unfortunately, the pathogenesis of molecular mechanisms that induce neuropathic pain is still not completely understood.

Chronic pain dramatically reduces the quality of life of one fifth of adult European citizen and the 26% on Italians (WHO, 2007; Institute for clinical systems improvement, 2008; Ospina M and Harstall C., 2003; Scascighini l. et al., 2008). Pharmacological treatments for these patients are only palliatives and mostly unable to reduce successfully the symptomatology. For that reason, studies addressed to unveil the pathogenesis, chronicization onset and maintenance of chronic pain are needed, in order to identify novel and promising pharmacologic targets.

2. GABAergic system

The GABAergic system

GABA is the main inhibitory neurotransmitter of the nervous system, where it acts to reduce neuronal excitability. It was firstly characterized in 1950 By Roberts and Frankel (Roberts and Frankel, 1950). GABA is able to bind specifically two types of receptors: the ionotropic $GABA_A$ receptor ($GABA_AR$), permeable to chloride and bicarbonate, and the metabotropic receptor $GABA_B$ ($GABA_BR$), associated with both G_i ang G_o proteins. GABAergic signalling plays a major role in brain physiology, in fact dysfunction of GABAergic signalling can result in a pathologic condition such as epilepsy, which is generated when the balance between excitation and inhibition is impaired (Andersen P. et al., 1964; Eccles JC. 1966 and 1969; Eccles JC. Et al., 1966; Ito M. 2002; Roberts E., 1974; 1986 and 1986).

GABA is synthetized by the enzyme glutamic acid decarboxylase (GAD), that entails glutamate decarboxylation via a highly specific interaction. GAD is present in different isoforms, the main two being GAD 67 and GAD 65 (Erlander et al., 1991). GAD 67 is evenly distributed throughout the cell, while GAD 65 is mainly localized in the cytoplasm of axon terminals (Pinal and Tobin, 1998). Moreover, GAD is not equally distributed in the CNS. Indeed, it is present at high concentration in brain areas like substantia nigra, globus pallidus, hypothalamus, hippocampus, quadrigeminal bodies, cerebral cortex, cerebellum and the spinal cord. GAD enzymes have been found also in DRG, peripheral nerves and importantly also in peripheral glial cells, SCs (Corell M. et al.,2015; Magnaghi V. et al., 2010; Bowery N.G. et al., 1976).

After synthesis, GABA is stored in vesicles by the action of a specific transporter coupled to a vesicular protonic pump. GABA release in the synaptic space requires vesicles to fuse with

plasma membrane. This event can occur spontaneously or following depolarization caused by Ca^{++} influx (Hablitz et al., 2010). It has been demonstrated that GABA is also released in CNS tonically *via* a non-vesicular pathway. Presently, there is a growing debate about the origin and mechanism of GABA tonic release in CNS. In this light, it has proposed that tonic inhibition in the cerebellum may be due to GABA released from glial cells, by permeation through the Bestrophin 1 (Best1) anion channel (Lee S et al., 2010).

Once released, GABA can bind its specific receptors $GABA_AR$ and $GABA_BR$. Otherwise, GABA may be re-uptaken by neurons and glia, by the action of specific GABA transporters (GAT) GAT1 and GAT-3, that co-transport GABA with sodium (Na^+) and chloride (Cl^-) ions (Carver and Reddy, 2013). There is evidence suggesting that GAT-3 transporter, mainly expressed by glia, has a prominent role in the maintenance of low GABA synaptic levels, compared with GAT-1 contribution. Following the reuptake by neurons and glia, GABA is then degraded by the enzyme GABA transaminase (GABA-T), present both in pre- and post-synaptic neurons and in glia. GABA-T catalyses the reaction of GABA deamination to succinate semialdehyde. Interestingly, recent papers demonstrated the presence of functional metabotropic $GABA_BR$ in nociceptors soma and their free endings (Hanack C. et al., 2015). Moreover, it is also known the $GABA_BR$ role in the modulation of peripheral glia (Magnaghi et al., 2004), although in this thesis the focus is mostly addressed to the study of $GABA_AR$

$GABA_A$ receptor

$GABA_AR$ consist of pentameric assembly of distinct subunits, forming a central ion channel permeable to Cl^- ion, and to a lesser extent, to bicarbonate anion. Each subunit has one long extracellular N-terminus that interacts with a variety of drugs, including benzodiazepines, barbiturates, and neurosteroids (NS in Figure 18). Currently, in the mammalian CNS have

been cloned 19 GABA$_A$R subunits, as follows: α1–6, β1–3, γ1–3, δ, ε, θ, π, and ρ1–3. This diversity offers a great potential heterogeneity of GABA$_A$R subunit composition, which is further increased by alternative splicing. The molecular composition of the GABA$_A$R has important functional consequences as it determines the properties, pharmacological modulation, and targeting of the native receptors (Chuang and Reddy, 2018).

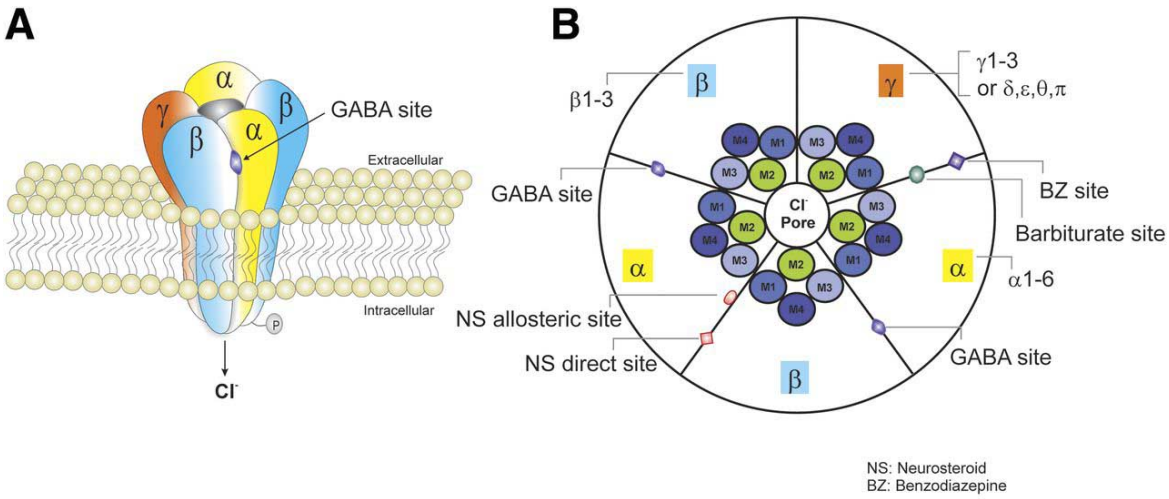

Figure 18. *Schematic representation of typical GABA$_A$R structure and subunit composition. (A) GABA$_A$R are heteropentamers forming a channel that is permeable to Cl$^-$ ion. (B) A top view of the pentameric GABA$_A$Rs which is composed from a repertoire of 19 known subunits: α1–6, β1–3, γ1–3, δ, ε, ϑ, π, and ρ1–3. The most general stoichiometry of GABA$_A$Rs contains two αs, two βs, and one γ; alternatively, the γ subunit can be substituted by δ, ε, ϑ, or π. Each subunit has four transmembrane (TM) domains. i.e.TM1–TM4. TM2s form a selective channel pore. GABA exerts fast inhibitory actions by activating postsynaptic GABA$_A$Rs in the brain, causing the influx of negatively charged Cl$^-$ ions and hyperpolarization of neurons, which serve to reduce neuronal excitability and firing. The GABA binding sites are located at the junction between subunit α and β, whereas benzodiazepines (BZs) bind at the interface between subunits α and γ. Barbiturates binding sites are distinct from the BZ binding site. Neuroactive steroids have two putative binding sites, including allosteric and direct binding site. The allosteric binding site is located at the α subunit TMs, whereas the direct binding site is within the TMs of the α and β subunits (Chuang S and Reddy D.S. 2018).*

The most general stoichiometry of GABA$_A$R contains two α subunits, two β subunits, and one γ or one δ subunit. GABA binding sites are located at the junction between subunits α and β, and benzodiazepines bind at the interface between subunits α and γ.

The γ-containing and δ-containing GABA$_A$R are classically associated with synaptic or extrasynaptic localization respectively. Those two receptors type possesses precise differences in subunit composition and distinct characteristics in their affinity and efficacy

to GABA, desensitization rate, as well as response to benzodiazepines and neuroactive steroids (Bianchi and Macdonald, 2002, 2003; Brown et al., 2002; Wohlfarth et al., 2002; Mortensen et al., 2012).

Extrasynaptic $GABA_AR$ are mainly a δ-containing type of receptors, which have high GABA affinity but low efficacy, low desensitization rate, low sensitivity to benzodiazepines and are highly potentiated by neuroactive steroids. Whereas synaptic $GABA_AR$ containing γ subunit and are the main mediators of fast and phasic inhibitory currents at the synaptic sites. These receptors are characterized by benzodiazepines sensitivity and lower potency (Sieghart and Sperk, 2002; Farrant and Nusser, 2005; Olsen and Sieghart, 2009). Activation of synaptic γ-containing $GABA_AR$ and extrasynaptic δ-containing $GABA_AR$ produce phasic and tonic inhibititory currents, respectively.

Rapid and transient phasic current inhibition is generated by presynaptic GABA release and subsequent binding of synaptic γ-containing $GABA_AR$, whereas tonic current inhibition is produced by persistent activation of perisynaptic or extrasynaptic δ-containing $GABA_AR$ by ambient GABA. Extrasynaptic $GABA_AR$ are tailored to regulate neuronal excitability by controlling the basal tone via shunting and tonic inhibition in neurons (Coulter and Carlson, 2007; Carver and Reddy 2013). Extrasynaptic receptors are found only in specific brain areas such as the hippocampus, amygdala, neocortex, thalamus, hypothalamus, and cerebellum (Stell et al., 2003; Jia et al., 2005; Drasbek and Jensen, 2006; Olmos-Serrano et al., 2010; Mortensen et al., 2012; Carver et al., 2014).

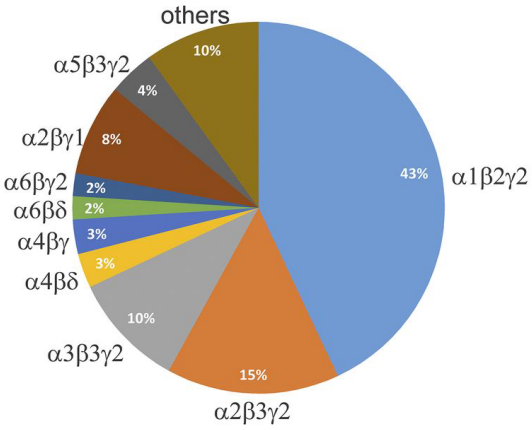

Cellular distribution	subunit isoforms	GABA potency (EC$_{50}$)
Synaptic	α1β2γ2	6.6 μM
	α1β3γ2	2.1 μM
	α2β3γ2	13.4 μM
	α3β3γ2	12.5 μM
	α4β3γ2	2.1 μM
	α6β3γ2	0.17 μM
Synaptic/Extrasynaptic	α5β3γ2	1.4 μM
Extrasynaptica6b3	α1β2δ	3.7 μM
	α3/5βδ	4.5 μM
	α3β3	0.97 μM
	α4β3	0.97-1.7 μM
	α4β2/3δ	0.076 μM
	α6β2/3δ	0.17 μM

Figure 19. *The diagram shows the estimated abundance of GABA$_A$R subtypes in the rodent brain. In the table are reported the GABA$_A$R potencies (EC$_{50}$) calculated by whole-cell voltage-clamp assay on HEK293 cell line expressing different GABA$_A$R subtype (Mortensen M et al., 2012).*

In general, GABA$_A$R subunits have discrete distributions among different brain regions. Approximately 90% of GABA$_A$R are γ-containing, while δ-containing receptors has more confined expression in parts of the brain such as the hippocampus, cerebellum, and thalamus (Figure 19). However, GABA$_A$R possess different potencies, depending on which α o β subunit composes the receptor. As reported by Martin Mortensen in 2012, GABA$_A$R EC$_{50}$ goes from 0.076 μM until 13.4 μM depending on subtype composition (Figure 19, Table). The prevalent synaptic location of αβγ GABA$_A$R depends on the specific binding with a number of intracellular proteins (such as gephyrin), regulating a set of GABA$_A$R properties, such as: transport to synaptic sites, anchoring at synapses, turnover and degradation, and possibly assembly of the whole receptor (Tretteretal.,2008,2011; Mukherjeeetal.,2011;,Wangetal.,1999; Kneussel et al., 2000).

Beside the "classic" synaptic and extrasynaptic GABA$_A$R receptors localization, in the last years has been proposed a more dynamic distribution. Indeed, GABA$_A$Rs seem to be characterized by constant diffusion within the neuronal plasma membrane, between synaptic and extra synaptic areas. Classical synaptic GABA$_A$Rs have been found in the

extrasynaptic domain (Bogdanov et al., 2006; Thomas et al., 2005), where they sustain tonic inhibition (Thomas et al.,2005; Bogdanov et al., 2006; Bannai et al., 2009; Hannan S. el al., 2019). In addition, it should be underlined that αβγ $GABA_ARs$ also diffuse laterally in the surface membrane (Thomas etal.,2005; TrillerandChoquet,2005; Bogdanovetal., 2006), where they may be found in significant number in extrasynaptic compartments of neurons (Kasugaietal.,2010).

$GABA_ARs$ are also expressed in glial cells, either in the CNS or in the PNS, being localized in astrocytes (Berger et al.,1992; Israel et al., 2003; Kettenmann et al.,1987), oligodendrocytes and SCs.

GABA$_A$R allosterical modulation and neuroactive steroids

GABA$_A$R are an important target for a variety of drugs including the benzodiazepines (used in the treatment of anxiety, epilepsy, sleep disorders and alcohol withdrawal, etc.) and a number of general anaesthetics such as propofol, etomidate and thiopental, that are used to induce anaesthesia (Sieghart, 1995; Sigel and Buhr, 1997; Belelli et al., 1999; Rudolph and Mohler, 2006). All these compounds act as positive allosteric modulators of GABA$_A$R, potentiating the inhibition mediated by the endogenous ligand GABA.

Interestingly, there are also endogenous allosteric ligands of GABA$_A$R such as the neuroactive steroids. These steroids are endogenous steroids that are synthesised *de novo* in the nervous system or come from steroidal precursors that are synthesized in endocrine tissues and then are metabolized in the nervous tissues (Figure 20) (Baulieu, 1981; Paul and Purdy, 1992; Reddy, 2003a,b). Among neuroactive steroids, the most important is the progesterone metabolite 5α-pregnan-3α-ol-20-one also called tetrahydroprogesterone (THP) or allopregnanolone (ALLO). ALLO can be synthesised *de novo* in the CNS and PNS, both in neurons and glia at levels sufficient to modulate the GABA$_A$R functions. It has been demonstrated, indeed, that ALLO plays an important physiological/pathophysiological role in the nervous system (Belelli and Lambert, 2005; Herd et al., 2007).

The interaction between ALLO and GABA$_A$R was investigated by mean of patch clamp studies, revealing that ALLO can act as positive allosteric modulation or direct agonist of GABA$_A$R, depending on concentration. In particular, at nanomolar concentration ALLO acts as an allosteric modulator, while at micromolar concentration is able to induce the Cl^- channel opening, even if endogenous GABA is not present (Callachan et al., 1987; Shu et al., 2004; Park-Chung et al., 1999; reviewed in Belelli and Lambert, 2005).

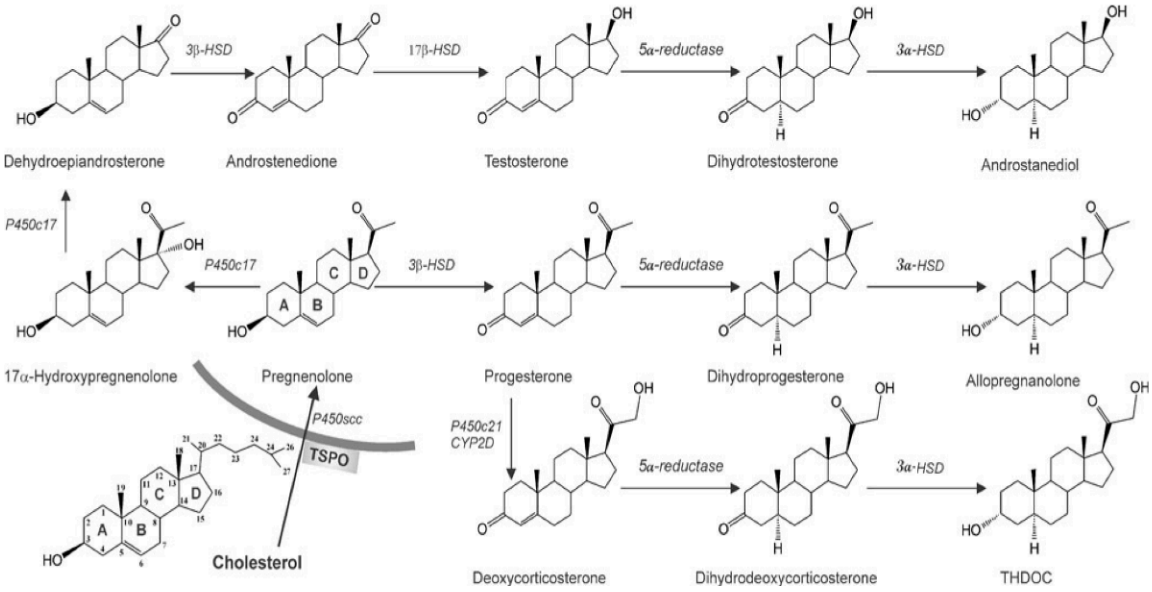

Figure 20. Neuroactive steroids synthesis. Cholesterol is converted to pregnenolone through the action of the P450 SCC enzyme, that is the substrate for the synthesis of other neuroactive steroids. The enzymes 5α-reductase and 3α-hydroxysteroid dehydrogenase convert the precursors in the neuroactive 3α-5α-metabolites. In particular, progesterone is converted in allopregnanolone, the main important NS in the nervous system. Adapted from Carver and Reddy, 2013.

Regarding the neuroactive steroids' biosynthesis, first the cholesterol is translocated across the mitochondrial membrane by TSPO (translocator protein 18 kDa, a key protein that controls the neuroactive steroids biosynthesis) and converted into steroid precursor pregnenolone by the cytochrome P450 side-chain cleavage enzyme, located in the inner membrane of mitochondria. Pregnenolone is subsequently converted respectively into the neuroactive steroids' precursors progesterone, deoxycorticosterone, and testosterone. Then these steroids undergo two sequential A-ring reduction steps and are converted into three prototype endogenous neuroactive steroids: ALLO (3α-hydroxy-5α–pregnan-20-one), tetrahydrodeoxycorticosterone (THDOC), and androstanediol by the catalysis of two key enzymes called 5α-reductase and 3α-hydroxysteroidreductase (5α-R-3α-HSD) (Reddy, 2003a, 2009a, 2011; Rupprecht, 2003; Belelli and Lambert, 2005; Carver and Reddy, 2013; Brown et al., 2015; Porcu et al., 2016).

GABA$_A$R phosphorylation and PKCε

Protein kinases are enzymes that can regulate the function of other proteins by phosphorylating hydroxyl groups. Importantly, protein kinase activity influences GABA$_A$R surface expression, trafficking, Cl^- conductance and sensitivity to neuroactive steroids. Several GABA$_A$R subunits, indeed, contain domains that can be phosphorylated by protein kinases, including α4, β, and γ2 subunits (Moss and Smart, 1996; Brandon et al., 2000). The serine residue (Ser-443), within the intracellular domain of the α4 subunit, is phosphorylated by protein kinase C (PKC) (Abramian et al., 2010).

PKC belongs to the AGC group of serine-threonine kinases and transduces signals derived from lipid second messengers. PKC is a family of kinases encoded by nine genes with distinct biological functions. Conventional PKC (cPKC), α, β, γ are activated by Ca^{++} and diacylglycerol (DAG). Novel PKC (nPKC) β, ε, η, θ are activated by DAG but not by Ca^{++}. Atypical PKC (aPKC) ζ and τ/γ are insensitive to Ca^{++} and DAG but are activated by other lipids and phosphorylation. In particular, PKCε plays important roles also in primary afferent nociceptor sensitization and mechanical hyperalgesia (Alley, 2001; Cang, 2009; Khasar, 1999; Srinivasan, 2008; Villarreal, 2009; Zhu, 2007).

Similarly, to other PKC isozymes, PKCε is regulated by four key mechanisms: cofactor binding, phosphorylation, protein-to-protein interaction and regulated degradation. PKC activation by DAG can be mimicked by the addition of other compounds that bind the C1 domain, such as tumour promoting phorbol ester (e.g.: phorbol-12-myristate-13-acetate – PMA). In fact, PMA is used as PKC activator in several studies. Moreover, PKCε must be primed through phosphorylation to display full enzymatic activity and to respond to allosteric regulators. Following activation, PKCε is delivered to specific subcellular compartments. This process involves the interactions with anchoring proteins like the

"receptors for activated C-kinase" (RACKs), which serve to anchor PKC isozymes in close proximity to their substrates. In particular, RACK2 binds preferentially the activated PKCε. The peptide εV1-2 is a specific PKCε inhibitor, derived from the first unique region (V1) of PKCε (amino acids 14–21). The peptide εV1-2 acts as a selective antagonist of PKCε translocation and function. Moreover, a similar mechanism of action is at the base of the PKCε specific agonist ψεRACK, that is a pseudo-receptor octapeptide for activated PKCε. It is able to bind activated PKCε, promoting its activity.

Beside its capacity to induce an acute increase of nociceptor excitability, PKCε is also crucial in establishing long-term sensitization, also termed hyperalgesic priming (Bogen et al., 2012; Ferrari et al., 2015). It should be underlined that long-term sensitization is a critical problem for the induction of chronic pain, such as that elicited by painful diabetic neuropathy. In this context, the comprehension of the role of PKCε in neuropathic pain might be of primary importance for the clinical management of chronic pain. Unveiling the role of PKCε in neuropathic pain is matter of recent investigations (like in this thesis) aimed to settle this stricking clinical problem. Notably, PKCε induces long-term sensitization of nociceptor by phosphorylating $GABA_AR$ and others ion channels involved in excitability regulation. In particular, PKCε targets the following receptors.

- **$GABA_AR$**. As already mentioned, PKCε phosphorylates $GABA_AR$. In particular, the phosphorylation of the $\gamma 2$ subunit of $GABA_AR$ reduces the $GABA_A$ response to ethanol and benzodiazepines. [Hodge, 1999]. Moreover, also the $GABA_AR$ trafficking is regulated by PKCε. Indeed, the activation of PKCε decreases the cell surface expression of $GABA_AR$ and attenuates $GABA_AR$ currents [Chou 2010].
- **TRPV1**. The receptor TRPV1 is a ligand-gated, non-selective, cation channel activated by capsaicin, heat, protons, leukotrienes and anandamide [Davis, 2000]. It is expressed by

small-diameter nociceptive neurons and integrates thermal and chemical stimuli as a polymodal receptor [Caterina,2000; Tominaga, 2004; Tominaga, 2005]. TRPV1 knockout mice show reduced sensitivity to noxious thermal stimuli and reduced inflammatory thermal hyperalgesia [Davis, 2000; Caterina, 2000]. PKC modulates TRPV1 function. A short treatment (<3 min) with phorbol esters reduces the TRPV1 thermal threshold and enhances its activation by capsaicin, anandamide, ATP and bradykinin. This effect is inhibited by PKC inhibitors [Sugiura, 2002; Crandall, 2002; Vellani, 2001]. Intracellular application of the PKCε inhibitor εV1-2 peptide (which inhibits PKCε binding to RACK2) reduces bradykinin-mediated enhancement of TRPV1 function [Sugiura, 2002]. Studies using the εV1-2 peptide also demonstrated that the activation of neurokinin-1 receptors [Qi, 2007] or protease-activated receptor 2 [Amadesi, 2006] enhances the TRPV1 function via PKCε.

- Na_V 1.8. In primary sensory neurons it was shown that increased levels and activation of PKCε, causes by repetitive inflammatory stimuli, determine the up-regulation of Na_V 1.8 expression [Villareal, 2009].

In general, for all these reasons, PKCε represents an interesting target of study for the comprehension of the mechanisms at the base of neuropathic pain aetiology and progression.

Developmental changes in chloride homeostasis

$GABA_AR$ mediated current is classically described as a hyperpolarizing current, induced by Cl- influx from the extracellular space to the intracellular cytoplasm of neurons. Interestingly, at early stage of life during development, in mammalian species and human brain structures, neurons have a higher intracellular Cl^- concentration. Consequently, in this condition the $GABA_AR$ activation leads to an efflux of Cl^-, thus exerting an excitatory action in immature neurons (Ben-Ari Y and Holmes GI., 2005) (Figure 21.A). Within neuronal maturation there is an excitatory to inhibitory developmental switch in GABAergic transmission (Ben-Ari Y, Gaiarsa J and Khazipov R 2007). Developmental changes in GABA signalling are determined by the progressive negative shift in E_{GABA}, that in turn reflects the reduction of intracellular Cl- concentration ([Cl-]i with development. In accordance, several electrophysiological and Ca^{++}-imaging experiments (also using Cl- indicator dyes) have demonstrated the excitatory effect of GABAAR opening and elevated $[Cl^-]_i$ in the immature neurons. By the use of the membrane-permeable MQAE and two-photon microscopy, it was shown that in immature CA1 pyramidal neurons (during the first postnatal week) the activation of $GABA_AR$ induces a Cl^- efflux; in the same neurons, but at the mature stage 2 postnatal weeks, it was demonstrated a chloride influx (Marandi N. et al., 2002).

Overall, it should be stated that $GABA_AR$ is depolarizing, excitatory, during development and turn to hyperpolarizing, inhibitory, in mature tissues.

Neuronal Cl^- homeostasis, however, is controlled also by the activity of other Cl- co-transporters, exchangers, and channels (Delpire E., French CR. Et al., 1990; Mercado A. et al., 2004; Payne JA. Et al., 2003; Plotkin MD. Et al., 1997). Among all Cl^- transporters expressed by neurons, cation-Cl^- cotransporters NKCC1 and KCC2 play a fundamental role in

the development changes of $[Cl^-]_i$. Indeed, NKCC1 accumulates Cl^-, while KCC2 extrudes Cl^- (Figure. 21).

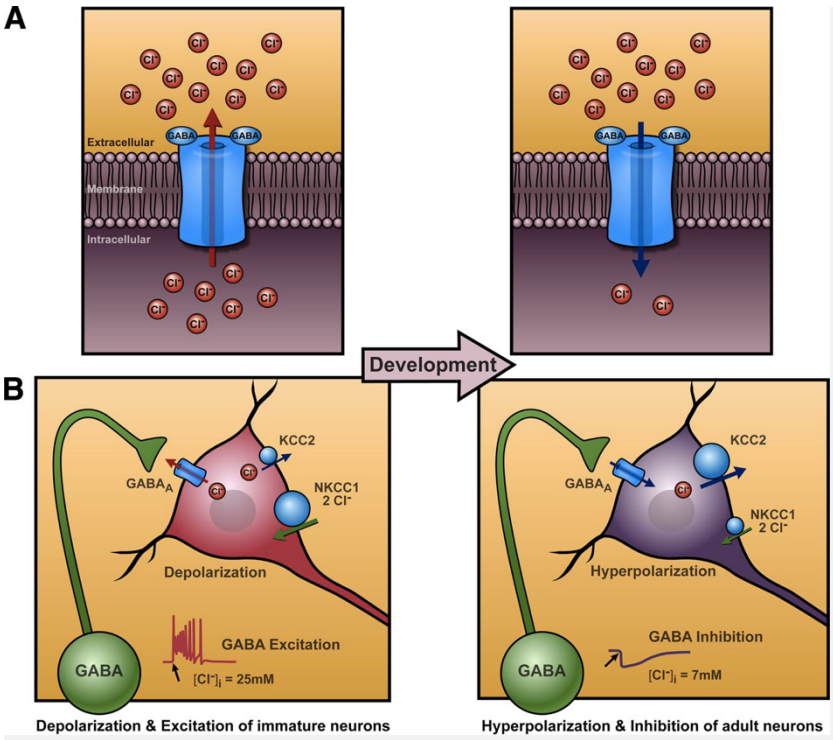

Figure 21. *Developmental changes in Cl^- homeostasis. (A) during development, the intracellular Cl^- concentration decreases. In the immature neurons, efflux of the negatively charged Cl^- ions produces inward electric current and depolarization. Conversely, In the mature neurons, Cl^- ion enters the cell and produces outward electric current and hyperpolarization. (B) developmental change in the intracellular Cl^- is due to the changes in the expression of the two major chloride cotransporters, NKCC1 and KCC2. NKCC1, which accumulates Cl^- in the cell, is more expressed in the immature neurons, while the Cl^- extruder KCC2 is expressed late in development (Ben-Ari Y. et al., 2007).*

NKCC is a membrane transport protein that mediates Cl^- uptake across the plasma membrane internalizing one Na^+, one K^+, and two Cl^- in electroneutral coupled fashion (Payne JA. Et al., 2003). The NKCC1 isoform is the so-called secretory isoform, best characterized in secretory epithelial cells. Notably, NKCC1 is expressed in all mammalian cells, where it plays a housekeeping role in control of cell volume homeostasis and cytosolic ion content. NKCC1 does not use ATP but acts using the electrochemical gradient for Na+ and K+ generated by the Na-K-ATPase pump. There is considerable evidence that uptake of Cl- in immature neurons is mediated by NKCC1. High expression of NKCC1 in immature neurons plays an important role in maintaining high intracellular Cl^- concentration (Delpire E.,2000; Dzhala VI. Et al., 2005; Fukuda A et al., 1998, Li H. et al., 2002; Mikawa S. et al.,

2002, Payne JA. Et al., 2003; Plotkin MD. Et al., 1997; Rohrbough J and Spitzer NC., 1996; Sung KW. Et al., 2000; Wang C. et al., 2002; Yamada J. et al., 2004).

KCC2 is the principal transporter working for Cl^- extrusion from neurons. KCC2 extrudes K^+ and Cl^- using the electrochemical gradient for K^+. Then, Cl^- extrusion is weak in immature neurons and increases with neuronal maturation (Khirug S. et al., 2005; Luhmann HJ, Prince DA., 1991; Zhang L., 1991). KCC2 is expressed in mature neurons, thus underlying the developmental changes in Cl- extrusion (Lu J. et al., 1999; Rivera C. et al., 1999; Shimizu-Okabe C. et al., 2002; Wang C. et al., 2002; Yamada J. et al., 2004), inducing the presence of low $[Cl^-]i$ in mature neurons (Deisz RA. And Lux HD., 1982; Jarolimek W. et al., 1999; Misgeld U. et al., 1986; Thompson SM et al., 1988a; 1988b; 1989).

Using single-cell PCR, Rivera et al. showed that KCC2 mRNA was barely detectable at birth (Rivera C. et al., 1999). A step increase in the expression was evident at post-natal day 5, reaching adult level at post-natal day 15. Interestingly, mature DRG neurons, that possess the depolarizing GABAAR (Deschenes M. et la., 1976) do not express KCC2.

In conclusion, at mature stage, almost neurons undergo a developmental switch characterized by NKCC1 downregulation and KCC2 upregulation, that entail a reduction of intracellular Cl^- and a consequent activation of the classical GABAAR-mediated hyperpolarization. However, olfactory and somatosensory neurons do not express KCC2 upon maturation, thus maintaining an elevated intra-cellular Cl^- concentration supported by a perdurable NKCC1 expression. This observation highlights the important dependency of GABA-evoked current from Cl^- gradient (regulated by NKCC1 and KCC2), not only in terms of flux direction but also in term of intensity.

Interestingly, the timing of the shift from depolarizing to hyperpolarizing depends on the species, gender, brain structures and neuronal type. In fact, rat brain excitatory to inhibitory

switch in GABAergic transmission occurred at 2-3 weeks post-natal (depending on the brain region), while in human cortex this switch occurs during the first year of life. For that reason, pharmacologic treatments of infant during the first year of age absolutely must take in account the opposite and potentially deleterious effects of GABAergic drugs on the nervous system.

In general, neurotransmitters have been shown to influence (directly or indirectly) several aspects of neuronal maturation (Barker JL. et al., 1998; Cameron HA. Et al., 1998; Edlund T. and Jessell TM. 1999, Landis SC., 1990; Lauder JM., 1993; Owens DF. and Kriegstein AR., 2002). In this light, GABA, like other neurotransmitters, is released by growth cones (Gao XB. and van den Pol AN., 2000) and may act on distal sites to generate GABAAR-mediated currents. In developing systems, the depolarizing action of GABA constitutes a common denominator to its actions on a wide range of processes. It has been hypothesized that the physiological significance of the excitatory GABAergic current in immature brain may be attributed to the capacity to promote synapses formation. GABA and GABAergic markers, indeed, are strongly expressed before synapses formation. Moreover, GABA is released at an early developmental stage, acting as a trophic factor to modulate some developmental processes, including neuronal proliferation, migration, differentiation, growth as well as synapse formation and network onset (Barker JL. et al., 1998; Kriegstein AR., 2005; Owens DF. and Kriegstein AR., 2002; Spitzer NC. Et al., 1993).

GABA$_A$R in PNS

GABA$_A$R has been largely characterized in CNS. Conversely, the GABA$_A$R functional role in PNS neurons is still matter of study. GABA evoked currents have been recently measured in peripheral sensory neurons soma (Zhang XL et al., 2015; Du X. et al., 2017), in their axons (Brown D.A. and Marsh S., 1978) and in central terminals in the spinal dorsal horn (Chen J.T. et al., 2014; Bardoni R. et al., 2013), suggesting the presence of functional GABA$_A$R in these structures. However, until few years ago, there were no coherent theories explaining the functional presence of GABA$_A$R in sensory neuronal soma and peripheral axons. Nor the possible source of GABA and/or agonists able to activate GABA$_A$R were known. Some authors suggested that no local sources of GABA might be present in the PNS (Gold M.S., 2013). Thus, GABA$_A$R in DRG soma and axons might be a side-product of receptor mis-trafficking toward the presynaptic terminals in the spinal cord, whereas GABA$_A$R normally mediate inhibitory "primary afferent depolarization" (Carlton S.M. et al., 1999; Curtis D.R. et al., 1977; Deschenes M et al., 1976). Interestingly, a more recent hypothesis tries to explain the functional presence of GABA$_A$R in DRG neuronal soma, suggesting that these neurons synthesize GABA acting like a autocrine/paracrine neurotransmitter locally within DRG neurons (Du X. et al., 2017). Additionally, up to now no studies considered the role of endogenous GABA$_A$R activation along sensory neuron axons and, eventually, the possible local cross-interaction with glial SCs.

By the way, it must be underlined that a consistent set of observations indicated a physiologic role of GABA$_A$R in SCs, where it participates in the regulation of myelination, myelin protein expression, SCs proliferation, migration and differentiation (Melcangi et al.,1999; Magnaghi et al., 2001; 2010; 2006; Melfi S. et al., 2017; Perego C. et al., 2012)

6. Schwann cells

SCs are highly specialized cells whose main function is the formation of the myelin sheath in the PNS. SC isolating property is fundamental for the transmission of the signal along the myelinated fibers. Indeed, SCs allow the saltatory conduction, except in areas comprised between two adjacent Schwann cells, known as nodes of Ranvier. However, SCs functions go much beyond that, being involved in an important cross-interaction with neuronal cells and having a fundamental role in axonal normal development and long-term survival (Taveggia, 2016). They have also an important role in regenerative processes following nerve lesions, being able to differentiate and stimulate nerve fibers regeneration (Glenn and Talbot, 2013b; Faroni et al., 2015). On the other hand, axons provide signals that regulate SCs proliferation, survival and differentiation, as well as myelin formation (Bozzali and Wrabetz, 2004; Simons and Trajkovic, 2006; Woodhoo and Sommer, 2008; Taveggia et al., 2010).

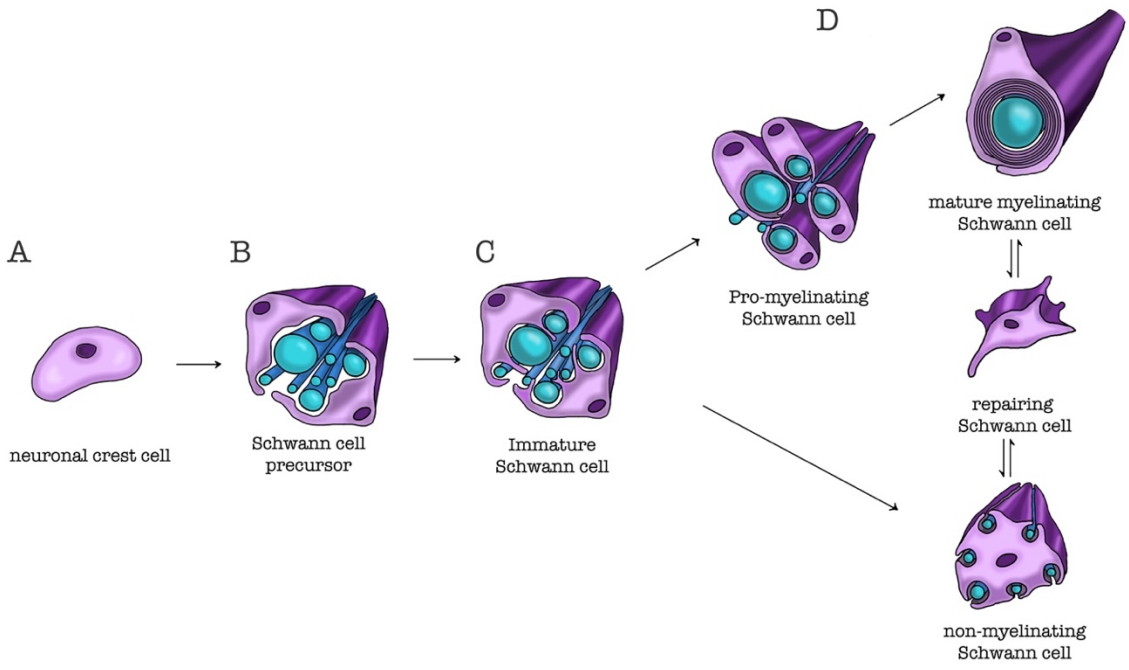

Figure 22. *Scheme of development, maturation and repairing of Schwann cells (SCs). SC development begins with neural crest cells (A). They later develop into SC precursors (B), then into immature SCs, which start the radial sorting process (C). After radial sorting, SCs alternatively mature into pro-myelinating SCs, which then*

originate myelinating SCs, or into non-myelinating SCs, which form Remak bundles. Mature SCs are characterized by remarkable plasticity, since following injury, they can differentiate into repairing SCs (D).

SC development starts from neural crest cells and leads to the formation of mature myelinating and non-myelinating SCs (Figure 22). The development process goes through different stages that require a dynamic control of SC morphology, with an accurate balance between proliferation and differentiation. These developmental stages include: neural crest cells, SC precursors, immature SCs, pro-myelinating SCs and mature myelinating and/or non-myelinating SCs (Monk et al., 2015). Neural crest cells (Figure 22.A) delaminate from the dorsal region of the neural tube. They possess high proliferative and migratory capacity, originating a wide range of cell types, including the cardiac cells, the skeletal and connective components of the head, the melanocytes, as well as neurons and glial cells of the PNS. Initially, the neural crest induction from the ectoderm requires some signals, such as the bone morphogenic protein (BMP), fibroblast growth factor (FGF) and the activation of the Wnt signaling pathway (Stuhlmiller and García-Castro, 2012). Successively, other factors seem to be fundamental for the differentiation of neural crest cells into SC precursors, including the transcription factor Sox10 (Woodhoo and Sommer, 2008), the neuregulin-1 (NRG-1) system (Shah et al., 1994), and the histone deacetylases (HDAC) isoforms 1 and 2 (HDAC1, 2) (Jacob et al., 2014). However, the molecular machinery required for these initial stages of SC differentiation has not been completely elucidated. Similarly, to neural crest cells, SC precursors (Figure 22B) are proliferative and migratory, and rely on axonal signals for survival. A determinant of SC precursor development is the NRG-1/ErbB2/3 signalling system (Raphael and Talbot, 2011). Successively, SC precursors develop into immature SCs, with a mechanism involving the activation of Notch signaling (Woodhoo et al., 2009). These

cells lose their migratory capacity. Differently from the previous stage, immature SCs are dependent on autocrine signalling for survival (Jessen and Mirsky, 2005).

Immature SCs (Figure 22C) are involved in the radial sorting process, during which axons separate based on their caliber. In rodents and humans, this physiologic process starts perinatally and continues during development, determining the morphologic aspect of the mature PNS, in which larger axons are myelinated (Feltri et al., 2016). During this phase, immature SCs undergo cytoskeletal remodelling, leading to the extension of filipodia and lamellipodia. These specialized structures enable SCs to surround axons of mixed calibers and to send cytoplasmic processes between axons, to progressively choose and segregate the larger axons at the periphery of the bundle (Feltri et al., 2016). Thus, immature SCs which enter in a 1:1 ratio with larger axons, and later proceed towards the pro-myelinating phenotype. SCs that contact small caliber axons, indeed, differentiate towards the non-myelinating phenotype (Figure 1D), leading to the formation of Remak bundles (Salzer, 2015; Feltri et al., 2016). Radial sorting is controlled by several factors, although the main determinants of this process are components of the extracellular matrix (e.g., laminin 211 and 411 or collagen XV), their specific receptors (e.g., integrins α6β1 and α7β1 or dystroglycan) (Monk et al., 2015) and the downstream intracellular-activated pathways, such as the Rho family kinases or the protein merlin..

Hereafter, pro-myelinating SCs progress towards the myelinating phenotype (Figure 22D), in which mature myelinating SCs form the myelin sheath around large caliber axons. A master regulator of this process is NRG-1 type III (Taveggia, 2016), although other molecules are equally involved. For instance, important functions are played by receptor belonging to the G-protein coupled receptors (GPCRs) family, such as GPR126 (Monk et al., 2009), GPR44 (Trimarco et al., 2014) and $GABA_BR$ (Procacci et al., 2012; Faroni et al., 2014).

After the differentiation program, the myelinating and non-myelinating SCs may run into pathophysiological condition such as the nerve injury, thus re-changing their differentiation state. The repairing SC phenotype (Figure 1D) is sometimes mistaken with the pre-myelinating immature SC phenotype. However, the two phenotypes present different peculiar characteristics. Repairing SCs present a series of typical biomarkers, such as Olig1, Shh and artemin, all under the control of the transcription factor c-Jun. These proteins are lightly or not expressed in immature SCs (Jessen and Mirsky, 2016). After nerve injury, the activated SCs proliferate to form a SC column, the so-called band of Büngner, which facilitates the axonal regeneration and the general PNS regrowth. A lot of molecules were found to be involved in the nerve regeneration process, including adhesion proteins, extracellular matrix, and neurotrophic factors.

Overall, the study of glia in CNS and PNS has largely improved in the last decades, given the progressive discovery of its important role in the neuron-glia interaction. Many studies suggest that glial cells, in particular astrocytes in the CNS, strongly modulate neurotransmitter trafficking and metabolism, possess neurotransmitter receptors and are capable of excitability oscillation in response to neuronal activity (Parpura V. and Verkhratsky A., 2011). Also SCs in the PNS has been found to possess some neurotransmitter receptors. However, their capability to quickly communicate with neurons via electrical signalling is still debated. Sensory neurons and SCs cannot interact in synaptic site because the only synaptic contact of DRG neurons is in spinal cord, where SCs are not present. For that reason, the communication between SCs and DRG neurons might occur only along peripheral axons, and this topic will be one of the main focus in this thesis.

AIMS

Neuropathic pain is a type of chronic pain caused by damage to the nervous system and characterised by a significant negative impact on a patient's quality of life. Pharmacotherapy is typically the first step in treating neuropathic pain consisting of antidepressant and anticonvulsant drugs. However, the majority of patients do not experience complete pain relief. Therefore, this condition represents a compelling medical need, not only for the treatment of symptomatology of pain but especially for the identification of a reliable therapy to treat the aetiology of the neuropathies.

Given that the mechanisms at the base of pathogenesis of neuropathic pain and the chronicization process are still not completely elucidated, first it is necessary to investigate nociception under physiological condition, with the aim to exploit the findings for the study of the neuropathic pain under pathologic condition.

Based on this concept, the main goal of this thesis is the investigation of new pathways involved in the conduction of noxious stimuli from the periphery, along axons, until the CNS. Namely, we focus our attention on the characterization of the GABAergic system along peripheral nociceptive fibers. In particular, the study of $GABA_AR$ in whole PNS is an old story, although its presence and functional role in DRG sensory neurons is still debated. Indeed, $GABA_AR$ inhibitory properties has been found in the primary afferents of DRG neurons in spinal cord, while little is known about $GABA_AR$ roles in the rest of the cellular components (i.e. soma and axon) of the DRG sensory neurons.

Therefore, the principal aim of this thesis was to investigate the presence and function of $GABA_AR$ in peripheral C-fibers, focusing on its putative role in the modulation of pain conductance. Moreover, our studies were aimed to evaluate the possible implication of axonal $GABA_AR$ in peripheral neuropathies. To address these aims, we used a combination

of *in vitro*, *ex vivo* and *in vivo* models (i.e. transgenic conditional mice), applying electrophysiological and biomolecular techniques.

At length, the aims pursued in this thesis can be summarized into three lines of research:

1. Firstly, we characterized the GABAergic system, primarily the $GABA_AR$, along unmyelinated sensory fibers. Then we investigated the subunit composition and the kinetic properties of the $GABA_AR$ subtype predominantly expressed in those fibers. Moreover, we focused on the study of the putative physiological and functional role of peripheral GABA-mediated currents in the modulation of noxious conductance. These studies were performed by mean of *ex vivo* electrophysiological studies on mice peripheral nerves.
2. Secondly, we investigated the putative role of peripheral GABAergic transmission on the onset, evolution and recovery of inflammatory pain sensitization and on nociceptor conductance in this pathological condition. To this end, *in vivo* mice model of inflammatory pain as been studied through behavioural tests. Contemporarily, *ex vivo* electrophysiological studies were performed on the peripheral nerves of the same mice.
3. Third, the axonal $GABA_AR$ involvement has been studied in regard to the peripheral neuron-glia interaction. Indeed, we investigated the capability of SCs to control the axonal $GABA_AR$ phosphorylation and desensitization, *via* the release of endogenous mediators. In particular, we studied the effect of the NS ALLO directly on axons and on SCs, that were able to release the neurotrophic factor BDNF and consequently to modulate the PKCε levels and activation in the peripheral neuronal compartment. This research has been achieved by mean of *in vitro* experiments, studying the interaction between rat primary SCs cultures and DRG neurons.

MATERIAL AND METHODS

Animals

Experiments were performed on adult male wildtype and conditional $GABA_AR$ β3-/- mice. Experiments were performed in compliance with the guidelines for the welfare of experimental animals as stipulated either by the Federal Republic of Germany (Heidelberg University) or the Animal Research Committee (University of Milan) and in accordance with European regulations concerning care and use of animals (Council Directive 2010/63/EU of the European parliament and the Council of 22 September 2010 on the protection of animals used for scientific purposes) and according to 3R's guidelines. Wildtype C57BL/6N outbred mice were purchased from Charles River Laboratories (Paris, France). Mice with a conditional deletion of β3 $GABA_AR$ were generated by crossing floxed Gabrb3fl/fl mice (JacksonLabs#008310) with either Advillin-Cre (S. Zurborg *et al., 2011*) or Sns-Cre (N. Agarwal et al.,2004) mice. The resulting Advillin-Cre;Gabrb3fl/fl and Sns-Cre;Gabrb3fl/fl lines are referred to here as Adv^{Cre};β3fl/fl and Sns^{Cre};$\beta3^{fl/fl}$. Littermate comparisons comprised either Advillin-cre or Sns-Cre or Gabrb3fl/fl mice and recordings from these mice were pooled and are referred to as "control" mice.

Electrophysiology

CAP recording setup

Sural nerves were removed by dissection immediately after mice were killed by rapid cervical dislocation subsequent to initial anaesthesia with sevoflurane (source). The epineurium was gently removed from ex vivo nerves to facilitate drug permeation. The desheathed nerve was mounted between suction electrodes in an organ bath and each end of the nerve was embedded in a suction electrode and sealed with vaseline to establish a mechanical and high resistance electrical seal (see Figure 23A). The organ bath was

perfused continuously at a rate of 6-8 ml/min with physiological solution of the following composition: NaCl 118 mM, KCl 3.2 mM, HEPES 20mM, CaCl2 1.5 mM, MgCl2 1 mM, D-Glucose 10.0 mM, bubbled with O2, to pH 7.4 (all obtained from Sigma-Aldrich, Steinheim, Germany). The temperature of the solution perfusing the bath was held constant at 30-32°C. The distance between stimulating and recording electrodes varied but was typically 6–11 mm.

Sural nerves were removed by dissection immediately after mice were killed by rapid cervical dislocation subsequent to initial anesthesia with sevoflurane (source). The epineurium was gently removed from ex vivo nerves to facilitate drug permeation.

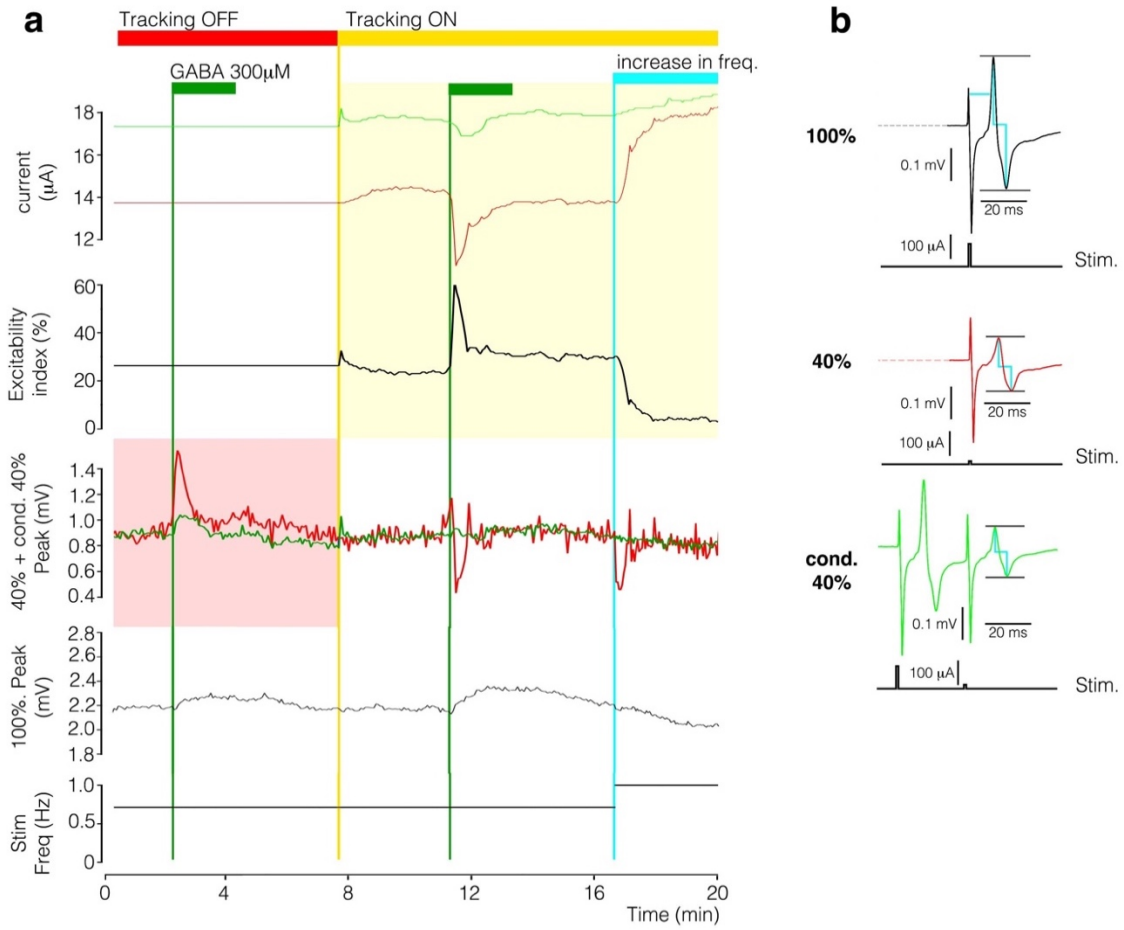

Figure 23. *Example to illustrate the technique of axonal threshold tracking as used here to monitor axonal excitability in sural nerve C fibres* ***(a).*** *Axonal excitability was assessed using repeat cycles of electrical stimulation presented sequentially in sets of 3 (b). The first stimulus in each set was at current intensity fixed at 10x threshold and this was used to evoke a maximal C-CAP designated as a 100% response (b, black trace raw signal). The peak-peak amplitude (a, 100% peak) and latency between stimulus onset and the 100% C*

*CAP response (a, 100% latency). The second stimulus of the set was delivered at a current strength adjusted to elicit a compound C CAP of 40% amplitude (a & b, red traces). i.e. 40% of the amplitude o the 100% C CAP response. The third stimulus in the set comprises an initial supra-maximal conditioning stimulus at 10xthreshold followed 30ms later by a second stimulus pulse adjusted to evoke a compound action potential response of 40% (**b**, 40% cond. green trace). This sequence was repeated continuously, and the parameters related to each stimulus monitored across time as shown in panel a. The stimulus frequency (a, lower trace) is the reciprocal of the interval between each stimulus in the sequence. To illustrate the use of threshold tracking the example recording in panel **(a)** shows the effect of GABA (100µM) on C fibre axons initially without tracking (a, tracking OFF) and subsequently using the tracking technique (a, tracking ON). With tracking OFF, i.e. 40% stimulus current strength fixed, application of GABA increases the amplitude of a C-CAP (a, red trace, red shading). Activating the tracking algorithm (a, tracking ON) and repeating application of GABA (100µM) the amplitude of the 40% C-CAP is held stable by adjustments, in this case a reduction, to the stimulus current strength (a, red trace yellow shading). Importantly, the profile of changes in the 40% stimulus amplitude during GABA (a, tracking ON yellow shading) mirror the increase in 40% C CAP (a, tracking OFF, grey shading). To illustrate the sensitivity of the technique to changes in axonal membrane potential, stimulus frequency was increased from 0.7 Hz to 1.0 Hz and an increase in the stimulus current required to maintain a 40% C CAP ensues (a, red trace, yellow square, increase in frequency).*

The desheathed nerve was mounted between suction electrodes in an organ bath and each end of the nerve was embedded in a suction electrode and sealed with vaseline to establish a mechanical and high resistance electrical seal (see Figure 23A). The organ bath was perfused continuously at a rate of 6-8 ml/min with physiological solution of the following composition: NaCl 118 mM, KCl 3.2 mM, HEPES 20mM, CaCl2 1.5 mM, MgCl2 1 mM, D-Glucose 10.0 mM, bubbled with O2, to pH 7.4 (all obtained from Sigma-Aldrich, Steinheim, Germany). The temperature of the solution perfusing the bath was held constant at 30-32°C. The distance between stimulating and recording electrodes varied but was typically 6–11 mm.

Compound action potentials in C fibers were evoked by stimulating the nerve with constant current rectangular pulses of 1ms duration (A395, WPI, Sarasota, FL, USA). A chlorided silver wire inside the stimulating suction electrode served as the anode and a second silver wire wound around the suction pipette in the organ bath served as the cathode. Extracellular compound action potential (CAP) signals were recorded over the sealing resistance of the suction electrode. Signals were amplified (N104 Neurolog, Digitimer, UK),

digitized (NI-600, National Instruments, USA) and processed on-line using QTRAC software (Digitimer, UK). To isolate the C-fiber component of electrically evoked CAP a digital window discriminator (Figure 23B) was implemented in QTRAC. In response to each electrical stimulus, the signal within this time window was analyzed on-line to determine the peak to peak amplitude (Figure 23B) and the latency from the time of stimulation to the first positive-crossing of the signal at an amplitude 50% of the maximum peak positive amplitude (Figure 23B).

We used axonal threshold tracking to monitor C-fibres responses to GABA. Brown and Marsh (D. A. Brown et al., 1978) first reported that GABA depolarizes C-fibres in rat vagus and this effect was accompanied by a decrease in the amplitude of a supra-maximal C-fibre compound action potential (C-CAP) response to electrical stimulation. Subsequent confirmation of GABA induced axonal depolarization showed that GABA increases sub-maximal C-CAP responses in rat dorsal root (R. B. Bhisitkul et al., 1987). We applied threshold tracking techniques to C-fibre CAP responses to assess axonal GABA responses (Figure 23). To illustrate the utility of this method we confirm the observation that GABA (100μM) increased the amplitude of a sub-maximal C-CAP (red trace, no tracking, Figure 1A). This change in amplitude for the sub-maximal C CAP can be alternatively quantified by maintaining a constant sub-maximal CAP amplitude (Figure 23A, tracking), in which case, the current required to stabilize the C CAP at 40% decreases during GABA application (current red trace, Figure 1B, tracked). In this configuration, changes in current intensity reflect changes in excitability. To relate changes in excitability to changes in membrane potential we further tracked changes in the excitability of the C-CAP response conditioned by a preceding supra-maximal stimulus 30ms beforehand (green trace, Figure 23B), as previously detailed (H. Bostock et al., 2003; R. W. Carr et al., 2010).

C-fibre axonal excitability was assessed using repeat cycles of electrical stimuli presented in a set of 3. Firstly, a stimulus current intensity was fixed at 10x threshold and this was used to evoke a maximal C-CAP designated a 100% response (100% black trace, Figure 23B). The second stimulus of the set was delivered at a current strength required to elicit a compound C-fiber response with an amplitude of 40% that of the preceding response to supra-maximal stimulation (40% red trace, Figure 23B). The third stimulus also adjusted the stimulus current to evoke a compound action potential response of 40% amplitude but at a time point 30 ms after a conditioning supra-maximal electrical stimulus (40% cond., green trace, Figure 23B). The stimulus current required to evoke a 40% amplitude C-fiber compound action potential (both unconditioned and conditioned) was continuously adjusted by QTRAC software based on the difference between the evoked CAP and the target value of 40% of the maximum amplitude. The current intensities required to elicit a 40% CAP for the conditioned and unconditioned cases (Stimuli 2 and 3 above) were used to derive an "excitability index". The excitability index is the ratio of the difference between conditioned and unconditioned currents to the current intensity for the unconditioned response expressed as a percentage. This experimental condition of CAP recording, at 1 Hz stimulation, has been used to assess acute pharmacological characterization.

Sustained 2.5 Hz activity challenge

Changes in axonal conduction and excitability were assessed during physiological challenge with elevated action potential activity. We standardized the electrical protocol for this to comprise an initial period of electrical stimulation at 0.5 Hz (every 2s) followed by a 3 min period of stimulation at 2.5 Hz before returning to 0.5Hz. During stimulation at 2.5Hz changes in axonal excitability together with the peak amplitude and latency of the C-fibre

CAP were monitored. Changes in axonal excitability are indicative of relative changes in axonal membrane potential (G. Moalem-Taylor et al., 2007) while changes in latency reflect changes in the number of available NaV and accumulation of intracellular sodium (R. De Col et al., 2008). This experimental condition of CAP recording, at 2.5 Hz stimulation, has been used to assess activity-dependent pharmacological modulation.

Pharmacological treatments.

The final concentration of each substance was achieved by dilution from stock into the solution perfusing the bath, or into culture medium on the day of each experiment. Substances used (Sigma-Aldrich where not otherwise stated) were: GABA [from 1 to 1000 µM], bicuculline [50 µM,] muscimol [100 µM], baclofen [100 µM], nipecotic acid (NPA) [1mM] , N0-711 [200 µM], gaboxadol (also called THIP) [from 100 to 200 µM], midazolam [100 µM], DCP-LA [200 µM], ALLO [10 nM/1 µM; by Steraloids Newport, RI, USA], human recombinant BDNF [1pM, 1nM, Millipore, Darmstadt, Germany], CYCLO [10 nM; generous gift by Prof. Michel M.M. Verheij. Inflammatory soup was composed by histamine [1 µM] bradykinin [5 µM], prostaglandin E2 (PGE2) [1 µM], serotonin hydrochloride [1 µM], all by Sigma-Aldrich. GABA treatments were performed adding the needed volume of GABA stock solution, prepared fresh every week, to the perfusing buffer for 2 min, then washed out with standard HEPES. For GABA 100 µM treatment, 7 min of washout were needed to completely restore standard conditions. Differentiated SCs primary cultures were treated for the indicated time after over-night serum free medium exposure.

High-performance liquid chromatography (HPLC) analysis

Endogenous GABA has been quantified by HPLC analysis. GABA amount in the collected samples was calculated as pmol/ml of HEPES buffer that was incubated in contact with de-sheated sural nerve. Endogenous GABA content was measured by high performance liquid chromatography analysis (Alliance 2095 module with remote control by the Millenium 32 Chromotography Manager Software; Waters Italia s.p.a, Sesto San Giovanni, Italy) coupled with a fluorometric detection system (Shimadzu RF-10AXL; excitation wavelength 350 nm; emission wavelength 450 nm) as previously described (Milanese et al., 2013). The collected samples were used as it is, without any dilution factor.

The methods consist in a pre-column derivatization of the sample with *O*-phthalaldehyde (Sigma-Aldrich, St. Louis, MO, USA) and gradient separation on a C18 reverse-phase chromatographic column (Agilent MicroSpher C18, S100x4.6, 3 µm; CPS Analitica, Milano, Italy) maintained at 30 °C. Homoserine was used as an internal standard (Sigma-Aldrich, St. Louis, MO, USA). The following gradient buffers were utilized: solvent A, 0.1 M sodium acetate (pH 5.8)/methanol 80:20; solvent B, 0.1 M sodium acetate (pH 5.8)/methanol, 20:80; solvent C, sodium acetate (pH 6.0)/methanol, 80:20. The gradient program was as follows: 100% C for 4 min from the initiation of the program; 90% A and 10% B in 1 min; 42% A and 58% B in 14 min; 100% B in 1 min; isocratic flow 2 min; 100% C in 3 min; flow rate 0.9 mL/min.

DRG neurons and SCs primary cultures.

DRGs were dissociated for 40 min in Ham's F12 medium (Life Technologies Italia, Monza, Italy), containing 0.125% (w/v) collagenase Type IV (Worthington Biochemical, Lakewood, NJ, USA), followed by 30 min digestion with 0.25% (w/v) trypsin (Worthington Biochemical)

and filtration with 100 µm membrane (BD Biosciences, Milan, Italy). Cells were suspended in Ham's F12 and purified on a gradient of 15% (w/v) bovine serum albumin (BSA; Sigma-Aldrich, Milan, Italy). The final neuronal pellet was suspended in Bottenstein and Sato's medium with minor changes [BSM; F12 medium plus N2 (100 µM putrescine, 30 nM sodium selenite, 20 nM progesterone, 0.1 mg/ml BSA, 1.3 mM transferrin and 10 pM insulin nerve growth factor 50 ng/mL), all Sigma-Aldrich] plus 10 µM arabinoside C (AraC; Sigma-Aldrich). A cell suspension ($1.5x10^4$) of neurons was seeded on a 35 mm petri dish coated with poli-L-lysin and laminin (Sigma-Aldrich). The cells grown at 37 °C, 5% CO_2 and 95% humidity. DRG neurons were characterized by immunofluorescence for neurofilament of 200 kDa (NF200, Sigma-Aldrich), as described (Melfi S*, et al.*, 2017).

Sciatic nerves from newborn rat used to prepare SCs, as previously described (Melfi S*, et al.*, 2017). Sciatic nerves were digested with 1% collagenase and 0.25% trypsin (Sigma-Aldrich), then mechanically dissociated, filtered through a 100 µm filter (BD Biosciences) and centrifuged 5 min at 900 rpm. Pellets were suspended in Dulbecco's modified Eagle's medium (DMEM, Serotec, Oxford, UK) plus 10% fetal calf serum (FCS; Life Technologies Italia) and plated on 35 mm Petri dishes. After 24 h, the medium was supplemented with 10 µM Ara-C (Sigma-Aldrich). Medium was then changed with DMEM-FCS 10% plus 10 µM forskolin (Sigma-Aldrich) and 200 µg/ml bovine pituitary extract (BPE; Life Technologies Italia). Cells became confluent in 10 days. Immunopanning for final purification was carried out incubating the cells 30 min with mouse anti rat Thy1.1 antibody (Serotec, Italy) followed by 500 µl of baby rabbit complement (Cedarlane, Burlington, Canada). Cell suspension ($6x10^4$ cells) was seeded on 35 mm petri dishes, in presence of 2 µM forskolin at 37 °C, 5% CO_2 and 95% humidity. At third *in vitro* passage, SCs were treated for 48 h with 4 µM forskolin, then used for different assays. At the time experiments begun SCs had equal cell

densities. SCs purity (more than 98%) was tested with a specific antibody against glycoprotein P0 (Nin MS et al., 2011).

RNA extraction and qRT-PCR.

RNA samples, from DRGs, nerves, DRG neurons cultures and SCs cultures were obtained using Trizol™ (Life Technologies Italia) according to the manufacturer's protocol, and quantified with NanoDrop2000 (Thermo Fisher Scientific, Monza, Italy). Pure RNA was obtained after DNAse treatment with a specific kit (Sigma-Aldrich). 1 μg of RNA was reverse-transcribed to cDNA using iScript™ Reverse Transcription Supermix for RT-qPCR (Bio-Rad, Segrate, Milan, Italy). Primers were designed by PrimerBlast software (NIH, Bethesda, MD, USA). Primer sequences for $GABA_A$-R subunits, PKCε and the housekeeper genes α-tubulin, 18s-rRNA and β2-microglobulin are reported in the Table S1. 10 ng of cDNA for each sample were used for Real Time PCR. qRT-PCR was performed by measuring the incorporation of EVA Green dye (Bio-Rad) with a CFX 96 Real Time System-C1000 touch thermal cycler (Bio-Rad). Data analysis was performed using the CFX Manager 2.0 software (Bio-Rad). The threshold cycle number (Ct) values of both the calibrator and the samples of interest were normalized to the geometric mean of Ct of the endogenous housekeeping genes. Data analysis was performed according to the Pfaff method and results are expressed as relative expression, normalized on the mean of housekeeper genes. As calibrator we used the RNA obtained from control samples. BDNF and trkB mRNA expression was analyzed by TaqMan qRT-PCR instrument (CFX384 real time system, Bio-Rad Laboratories) using the iScript™ one-step RT-PCR kit for probes (Bio-Rad Laboratories). Samples were run in 384 wells formats in triplicate as multiplexed reactions. Data were analysed with the comparative threshold cycle ($\Delta\Delta$Ct) method using β-Actin as reference gene. The primer efficiencies were experimentally set up for each couple of primers.

Primers and probe for BDNF, trkB and β-Actin were purchased from Eurofins MWG-Operon. Their sequences are reported in supplementary Table 1.

Immunofluorescence (IFL).

Nerves were explanted and de-sheeted. Then, nerves were fixed in 4% paraformaldehyde (PFA, Sigma-Aldrich), cryoprotected using sucrose solution at crescent concentration, embedded in OCT (Sakura, Leiden, The Netherlands) and cut in coronal sections. For dissociated nerves, a slight digestion was performed incubating nerves fragments in collagenase IV for 45 min, before fixing in 4% PFA (Sigma-Aldrich). Cells were fixed in 4% PFA and processed for immunostaining.

Primary antibodies used in this experiments were the following: guinea pig anti $GABA_A$-R α2 1:250 (generous gift by Prof. Fritschy, Univ. of Zurich, Switzerland), anti-βIII-tubulin-Cy3 (Sigma-Aldrich), anti $GABA_A$-R β3 (Abcam, Cambridge, UK), rabbit anti PKCε 1:200 (Abcam), rabbit anti phospho S729 PKCε 1:200 (Abcam), mouse anti Smi31 1:500 (Biolegend, San Diego, CA, USA), mouse anti Smi32 1:500 (Biolegend), rabbit anti trkB 1:200 (Santa Cruz Biotechnology, Dallas, TX, USA) and fluoromyelin 1:150 (Thermo Fisher Scientific). Specific secondary antibodies used were: Goat anti-rat (Millipore, Milano, Italy) Goat anti-rabbit (Sigma-Aldrich); goat anti-mouse (Sigma-Aldrich) Donkey anti-Guinea pig (Sigma-Aldrich).

After washing, slides and nerves were mounted using Vectashield™ (Vector Laboratories, Burlingame, CA, USA) and nuclei stained with 4,6-diamidino-2-phenylindole (Dapi). To ensure specificity, control slides were incubated in solutions lacking primary antibodies. Confocal microscopy was carried out using a Zeiss LSM 510 System (Zeiss, Gottingen, Germany) and images were processed with Image Pro-Plus 6.0 (Media Cybernetics,

Bethesda, MA, USA). IFL were repeated on negative samples to prove the antibodies reliability and specificity.

Western blotting.

Protein samples were extracted in lysis buffer (PBS, 1% Nonidet P-40 and 1mM EDTA; all by Sigma-Aldrich) containing a cocktail of protease inhibitors (Sigma-Aldrich). Samples were heated 20 min at 55°C to denaturate secondary structures, then 15 µg were loaded onto a SDS-PAGE gel (Criterion TGX; Bio-Rad) and run at 200 V for 40 min in running buffer. Gels were electroblotted to PVDF membrane (GE Healthcare, Milan, Italy). Membranes were blocked with 10% not-fat dry milk (Bio-Rad) in TBS before incubation with the primary antibody against BDNF diluted in the blocking solution (1:500, Santa Cruz Biotechnology). Results were standardized using β-actin (1:10000, Sigma-Aldrich) as reference. Membranes were incubated with appropriated HRP-conjugated secondary antibodies (Cell Signaling Technology Inc., Italy). Immunocomplexes were revealed by enhanced chemiluminescence (GE Healthcare), visualized using the Chemidoc MP Imaging System (Bio-Rad) and analyzed by the Image Lab software (Bio-Rad).

Data and statistical analysis

Electrophysiological data were analyzed with scripts in Igor Pro 7.01 (Wavemetrics, Lake Oswego, OR, USA). GraphPad Prism 6.00 (San Diego, CA, USA) was used for Figures and statistical tests including *t*-tests, ANOVA and associated *post hoc* tests. Group data are expressed as mean ± s.e.m. The level of significance to designate an effect was set at $p<0.05$.

Data were statistically evaluated using the statistical package GraphPad Prism 6.00 (San Diego, USA), with independent or paired two-tailed samples *t*-tests, one-way, two-way or repeated measures ANOVA followed up by *post hoc* tests (see figure legends). All data were expressed as mean ± s.e.m. of the determinations performed, and significance was set at $p<0.05$. Experiments were repeated at least 3 times. In pharmacological experiments, cell culture samples were allocated to groups randomly, organizing the treatments on multi-well device. Graphs were created with GraphPad Prism 6.00, while electrophysiological traces were analyzed with Igor Pro 7.01 (WaweMetrics, Lake Oswego, OR, USA).

RESULTS

CHAPTER 1

Physiological role of axonal $GABA_AR$ in sensory C-fibers axons

GABA depolarizes unmyelinated axons in peripheral nerve

Intracellular recordings from unmyelinated axons in peripheral nerve is precluded by their small diameter and physical barriers of the ensheathing tissue. Therefore, in order to assess axonal membrane currents, we adopted a threshold tracking technique to record changes in axonal excitability. The threshold tracking method relies on the assumption that for CAP, any given sub-maximal amplitude corresponds to the summed response of a fixed number of single axons, all of each contribute as all-or-none action potential. Under this assumption, adjustments to the intensity of stimulus current required to maintain a CAP amplitude at 40% of maximum, reflect changes in axonal excitability. An increase in the excitability of some single axons needs a reduction in stimulus current to maintain a 40% C-CAP amplitude (Figure 24). The increase in axonal excitability reflects a depolarizing membrane current.

Therefore, we used ex vivo threshold tracing technique to test weather GABA depolarizes unmyelinated C-fibers axons in a predominant sensory nerve such as the sural nerve of wildtype mice. Addition of GABA (100 µM) to the solution decreased the stimulus current required to elicit a 40% C-CAP response (Figure 24.a,b). This increase in C-fibre excitability in response to GABA produced a parallel increase in axonal conduction velocity, measured as a decrese in C-CAP latency (latency trace, Figure 24.a,c), without any decline in the C-CAP amplitude to supra-maximal stimulation. Altogether these data showed that the increase in axonal excitability and conduction velocity are both consistent with axonal depolarization in unmyelinated C-fiber axons (Brown DA & Marsh S, 1978; Bhisitkul RB at

al. 1987). GABA-evoked axonal depolarization increased in a concentration-dependent fashion between 1 and 1000 µM with an EC_{50} of 36.86 µM (Figure 24 d; n= 73).

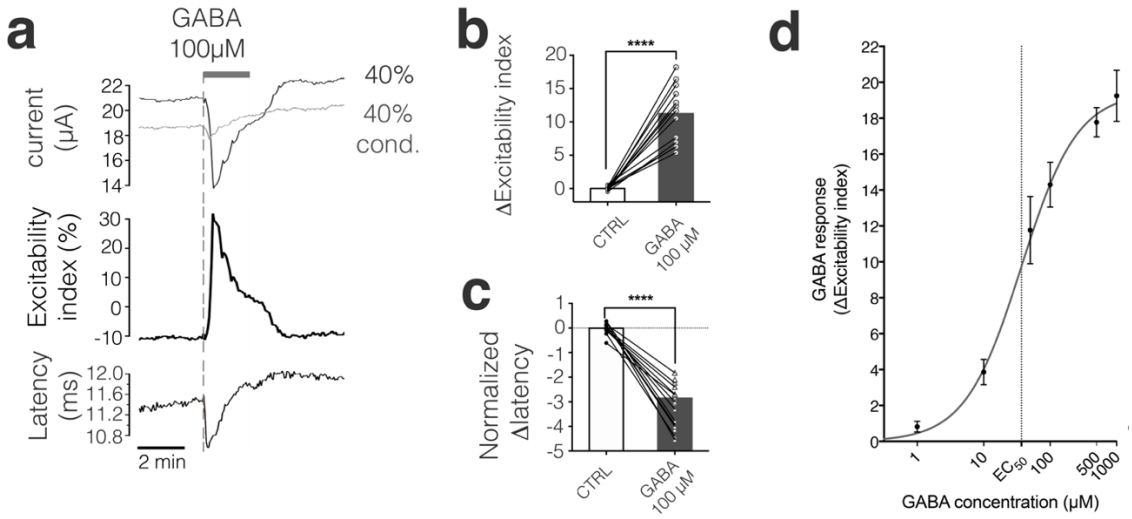

FIGURE 24. (a) *GABA (100 µM) increased axonal excitability, i.e. less current was required to evoke a 40% C-CAP.* ***(b,c)*** *The increase in excitability index (pairs n=13, p < 0.0001, paired t-test) and the concomitant increase in C-fiber conduction velocity measured as a reduction in latency (pairs n=12, p < 0.0001, paired t-test) are consistent with axonal depolarization.* ***(d)*** *GABA increased axonal excitability in a concentration dependent manner with an EC_{50} of 36.86 µM (n= 73, goodness of fit degree of freedom 70; lack of fit was: p= 0.9663).*

The pharmacology of C-fiber axonal responses to GABA was consistent with $GABA_AR$ specific activation. GABA responses were blocked by the competitive $GABA_AR$ antagonist bicuculline (50µM, Figure 25.a) and mimicked by the $GABA_AR$ agonist muscimol (100µM, Figure 25.b). In addition, allopregnanolone (ALLO, 1 µM), a positive allosteric modulator of $GABA_AR$, enhanced the amplitude of axonal responses to GABA (Figure 25.d). Although some evidence implicates axonal $GABA_B$ in C-fibre sensitization (Bhisitkul RB at al. 1987), we did not observe any acute effect of the $GABA_BR$ agonist baclofen (100µM) on axonal excitability, conduction latency nor peak amplitude of the C-CAP (Figure 25.c).

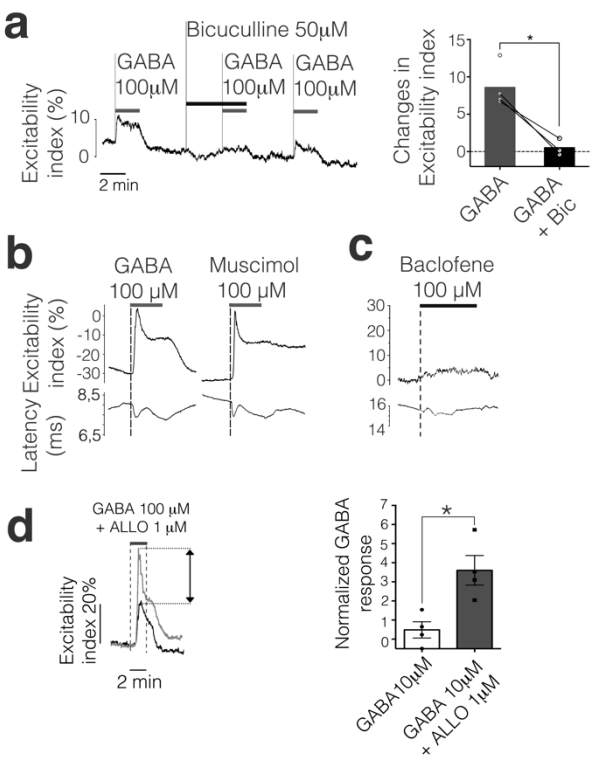

Figure 25. *We tested speficic $GABA_AR$ pharmacology.* ***(a)*** *Axonal GABA (100µM) responses were blocked by the specific $GABA_A$-R antagonist bicuculline 50µM (pairs n=3, p=0.0194 t=7.076 df=2, paired t test)* ***(b)*** *mimicked by the specific $GABA_AR$ agonist muscimol (100µM)* ***(c)*** *but not by the specific $GABA_BR$ agonist baclofen (100µM)* ***(d)*** *and enhanced by the neuroactive steroid ALLO (1µM, GABA n=3, GABA + ALLO n=4, p=0.0123, t; unpaired t test).*

To establish whether GABA induced changes in C-fibre excitability were mediated by outward chloride currents, bumetanide (20 µM) was used to block NKCC1 inward chloride transport. While simple repetition of GABA showed no decline in response amplitude (Figure 26.a,b) NKCC1 blockade resulted in a progressive decrease in GABA response amplitude (Figure 26.a,b). The suppression of axonal GABA responses by bumetanide, together with the use of HEPES rather than a CO_2 bicarbonate buffered solution, implies that the current responsible for the axonal depolarization was carried by chloride with minimal outward movement of bicarbonate (HCO_3^-).

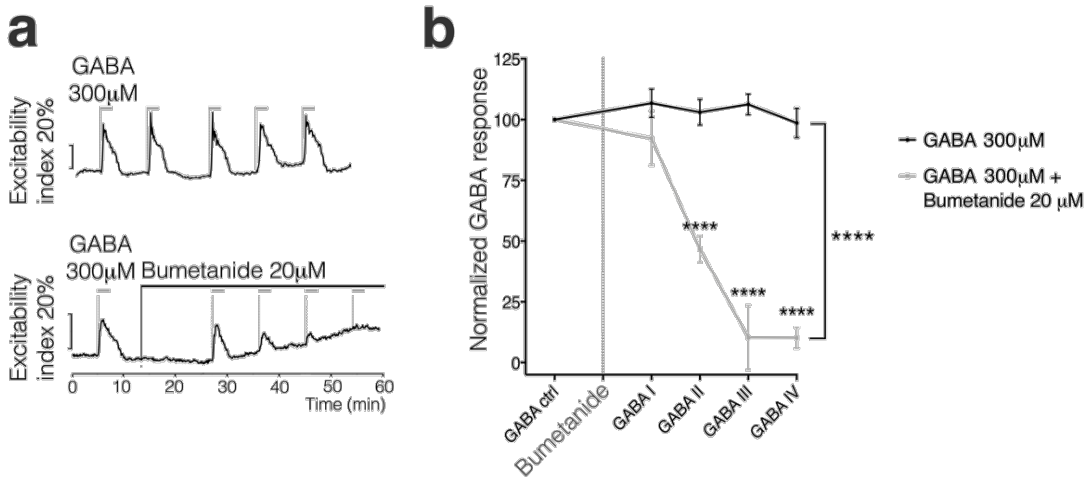

Figure 26. (a) *Repeat applications of GABA (300µM) evoked reproducible increases in C-fibre axonal excitability (upper trace) while GABA response were suppressed by the contemporaneous application of NKCC1 blocker bumetanide (20 µM, lower trace) leading to complete blockade of GABA response on the further application.* ***(b)*** *Pooled data showing the progressive inhibition of GABA depolarization amplitude in presence of bumetanide (GABA n=20, GABA+bumetanide n=14, interaction p<0.0001 F(4,24)=21.39 , treatment factor p<0.0001 , F(4,24)=21.55, 2 way ANOVA; post-hoc GABA vs GABA + bumetanide, GABA II p<0.0001 t=4.691, GABA III p<0.0001 t=9.237, GABA IV p<0.0001 t=8273).*

$GABA_AR$ subunit composition in unmyelinated axons

To examine the possible subunit composition and functionality of $GABA_AR$ in peripheral unmyelinated axons, we combined *in vivo* transgenic models, mRNA analysis, pharmacology and immunofluorescence. We also tested GABA sensitivity of conditional KO (cKO) *AdvCre;β3$^{fl/fl}$* mice, lacking β3-$GABA_AR$ subunit in almost all DRG neurons. Nerves from cKO mice showed undetectable responses to GABA (up to 1mM) on C-fibre excitability, latency or peak amplitude (Figure 27.a,b) consistent with the absence of functional $GABA_AR$ along C-fibers axons. We confirmed that GABA induces depolarization specifically *via* $GABA_AR$ and that the presence of the β3 subunit is essential for the most common $GABA_AR$ composition (Nguyen QA & Nicoll RA, 2018). To explore the distribution of $GABA_AR$ in C-fibre axons subtipes, we restricted the deletion of β3-$GABA_AR$ subunit to nociceptive neurons expressing the TTX-resistant NaV1.8 sodium channel by generating

Sns^{CRE};β3$^{fl/fl}$ mice and this genetic manipulation similarly rendered GABA uncapable to exert any effect on axonal excitability in C-fibre axons (Figure 27.c,d).

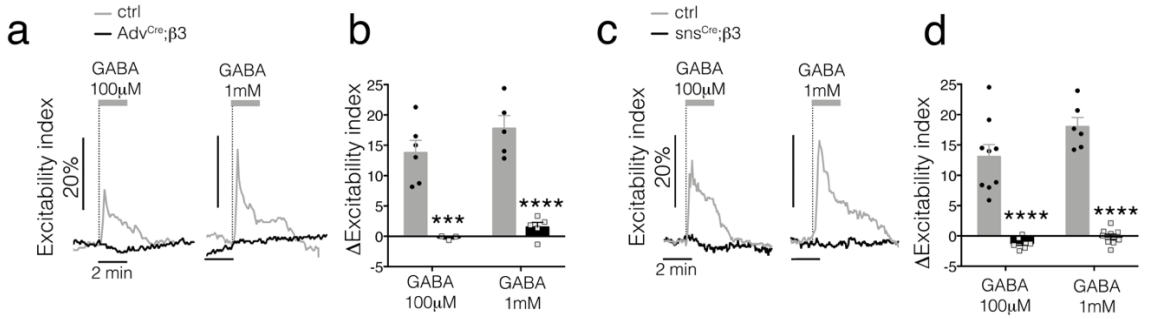

Figure 27. (a) *Axonal responses to GABA were absent in AdvCre;-β3-/- null mice, characterized by the conditional deletion of the $GABA_AR$ β3 subunit in DRG neurons;* ***(b)*** *pulled data (ctrl n=11, Adv/β3 KO=7, 2way ANOVA genotype factor p<0.0001 F(1,15) 68.02; post-hoc GABA 100μM p=0.0003, t=5.120; GABA 1mM p<0.0001, t=6.67).* ***(c)*** *GABA were absent also in snsCre;-β3-/- null mice;* ***(d)*** *pulled data (ctrl=28, snsCre;β3-/-=27, genotype factor p<0.0001, interaction F(1,27)=141.2 ; 2way ANOVA; post-hoc GABA 100μM p<0.0001 t=7.576, GABA 1mM p<0.0001 t=9.199; data are mean ± s.e.m.).*

Altogether these data further confirm: (1) specific $GABA_AR$ involvement; (2) the necessity of β3-$GABA_AR$ subunit in the functionality of axonal $GABA_AR$; (3) the selective expression on this receptor in nociceptive neurons within all C-fibers.

Having established the requisite presence of β3 for functional axonal $GABA_AR$ we performed qRT-PCR on whole DRG explants to characterize further the subunit composition of axonal $GABA_AR$. Data showed a mRNA profile with a prevalence of α2, β3 and γ2 subunits, while β1 mRNA levels were lower than in cultured DRG neurons (Faroni A*, et al.*, 2019). Commonly, this subunit composition characterizes the low affinity, phasic inhibitory postsynaptic $GABA_AR$ (Essrich et al., 1998; Fritschy and Brunig,2003; Schweizer et al., 2003). Conversely, δ subunit expression resulted close to the detection limit, suggesting its absence in DRG explants. The δ subunit is indeed characteristic of the high affinity, tonic inhibitory extra-synaptic $GABA_AR$ (Saxena and Macdonald, 1994; Haas and Macdonald, 1999; Bianchi et al., 2002; Lagrange et al., 2007). To confirm this data, we

tested the functional absence of δ–containing $GABA_AR$ in axons, using its specific agonist THIP (gaboxadol), which is selective for $GABA_AR$ containing δ subunits at concentrations below 1 μM (Meera P, Wallner M, & Otis TS, 2011). Consistent with the faint δ mRNA levelsin DRG explants (Figure 28.a) THIP was inefficient at nanomolar concentration. However, THIP resulted active at higher micromolar concentrations (Figure 28.b), whereas THIP become unspecific, in accordance with other authors (Meera P, Wallner M, & Otis TS, 2011).

The presence of α2 mRNA in DRG explant, and presumably in DRG neurons, was confirmed by immunostaining of teased fibre preparations of sciatic nerve. The α2 subunit was found along both myelinated and unmyelinated axons. In myelinated axons, which are surrounded with fluoromyelin positive glia (red, Figure 28.c; right bottom panel), α2 subunit co-stained with heavy neurofilament markers (yellow, Figure 28.d). In unmyelinated axons, which are not surrounded by fluoromyelin immunopositive glia (Figure 28.c; right top panel), α2 subunit immunopositivity did not co-stained with heavy neurofilament (green, Figure 28.d).

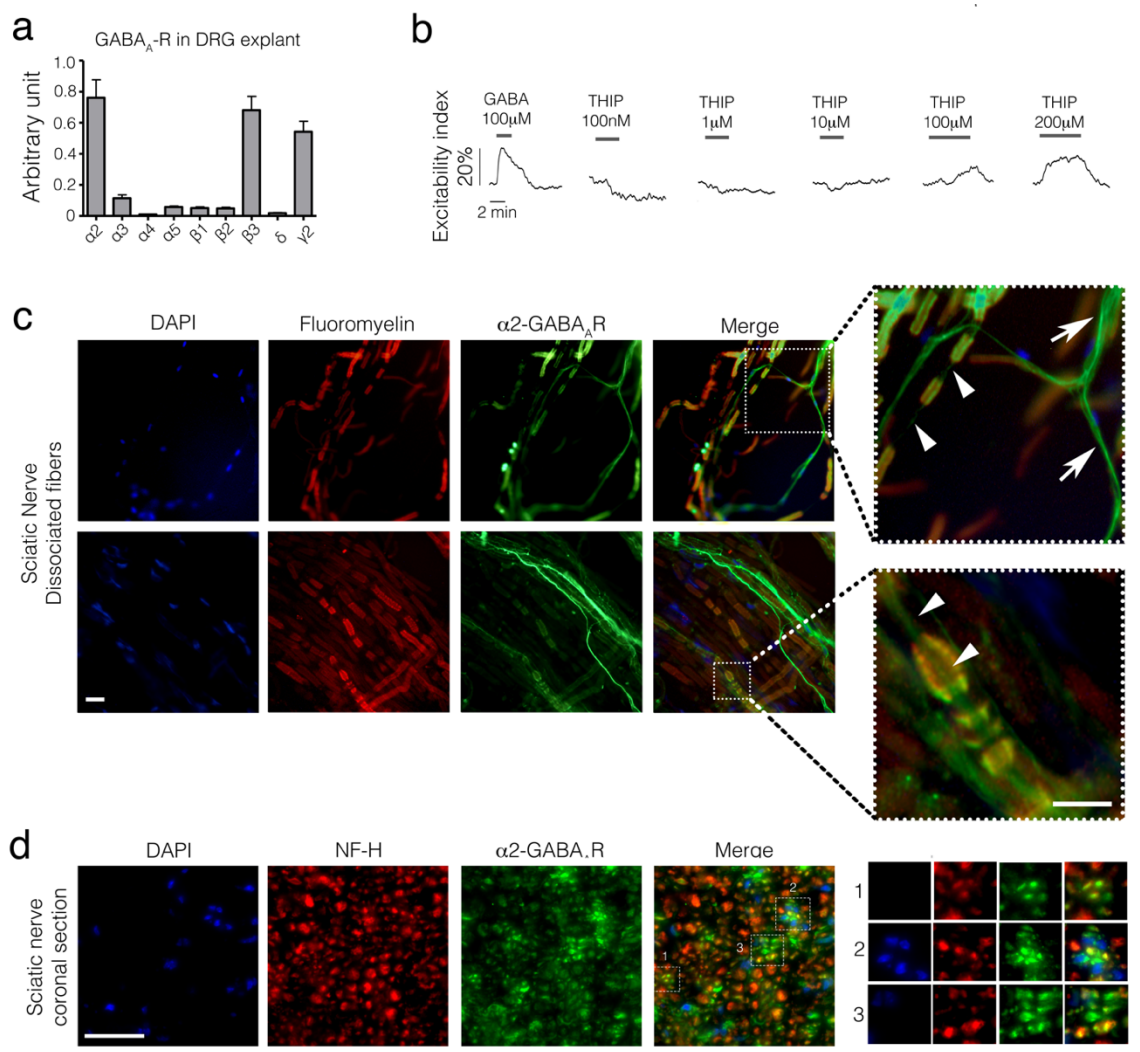

Figure 28. (e) *qRT-PCR analysis of acutely isolated whole DRG tissue for $GABA_AR$ subunits α2, α3, α4, β1, β2, β3, δ and γ2. Expression levels are shown relative to the housekeeping genes α-tubulin and 18s.* ***(f)*** *Assessment of axonal C-fibre responses THIP/gaboxadol at concentrations range from 100nM to 200μM, compared with GABA (100μM) response. THIP induced a modulation of excitability index starting from 100μM concentration, without effect in the nanomolar range, wherese THIP activation is indicative of the presence of δ subunit.* ***(g)*** *Immunolabelled images of mouse sciatic nerve in longitudinal teased fibre preparations* ***(h)*** *and nerve cross section. Teased fibres co-stained with $GABA_AR$ α2 (green) and fluoromyelin (red), showed that both unmyelinated (arrows, upper right-most image, pure green signal without red-marked glia) and myelinated (arrowheads, right-most image, green signal surrounded by red-marked glia) dissociated fibers expressed $GABA_A$-R α2 (dapi in blue). Scale bar 20μm (bar 10μm in the magnification).* ***(h)*** *Similarly, Immunostaining for $GABA_A$-R α2 (green) and heavy neurofilament NF-H (red) on sciatic cross section showed α2 presence in unmyelinated (green in merge) and myelinated fibers (co-labeled with NF-H, yellow in merge). Right-most insets 1, 2 and 3 show expanded views as indicated in the merge image (Scale bar 20μm).*

NKCC1 regulates intra-axonal chloride and thereby axonal GABA response amplitude

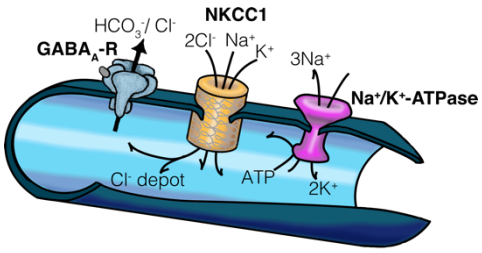

Figure 29. *Scheme of the intercoupling of the Na/K-ATPase, NKCC1 co-transporter and $GABA_AR$ in peripheral axons.*

Axonal C-fibre response to GABA, monitored using threshold tracking techniques, show a distinct time profile, comprising an initial transient (phasic) increase in excitability that decreased to a tonic sustained plateau, maintained for the duration of GABA application (Figure 30.a).

We speculated that this profile of excitability changes reflected $GABA_AR$ mediated chloride currents constituted by 2 different components. An initial phasic current characterized by a fast outward of chloride, driven by axonal chloride gradient, till chloride concentration depletion; this results in a subsequent decrease in GABA evoked depolarization during GABA treatment. The second component of GABA response was a residual tonic current, that is maintained for all GABA treatment, and that might result from a steady-state between NKCC1 chloride influx and $GABA_AR$ mediated chloride efflux during prolonged GABA application.

We tested this hypothesis by blocking NKCC1 with bumetanide (20µM) and we observed a loss of the tonic component of axonal C-fibre responses to prolonged GABA application (Figure 30.b), together with a strong reduction in the amplitude of the phasic response to a second GABA applications (Figure 30.b and Figure 26). This observation demonstrated the contribution of NKCC1-mediated chloride current to tonic GABA response and the depletion of chloride gradient, occurring after the phasic response.

Varying the time between successive GABA applications we studied the kinetics of intra-axonal chloride depletion and NKCC1 mediated axonal chloride loading (Figure 30.c). Using 5 sec GABA applications every 2 min, to probe the intra-axonal chloride concentration, lead

to a progressive reduction of the phasic response (Figure 30.c) consistent with a depletion of intra-axonal chloride. Notably, by mean of this protocol, the phasic GABA response amplitude decreased progressively until an amplitude comparable with the tonic response to GABA observed during earlier long GABA treatment (light blue, Figure 30.c). Subsequent recovery of the phasic response to GABA occurred upon increasing the interval between successive GABA applications from 2 up to 6 min (light green, Figure 30.c). Similarly, following prolonged 3 min GABA treatment recovery of the phasic GABA response requires several min, at least 7 min (dark green, Figure 30.c), possibly reflecting the time required by NKCC1 to restore the chloride gradient in the axon. The independence of tonic axonal GABA responses, upon preceding GABA application, is consistent with the hypothesis that the tonic increase in axonal excitability reflects steady-state equilibrium between NKCC1 mediated chloride influx and $GABA_AR$ chloride efflux.

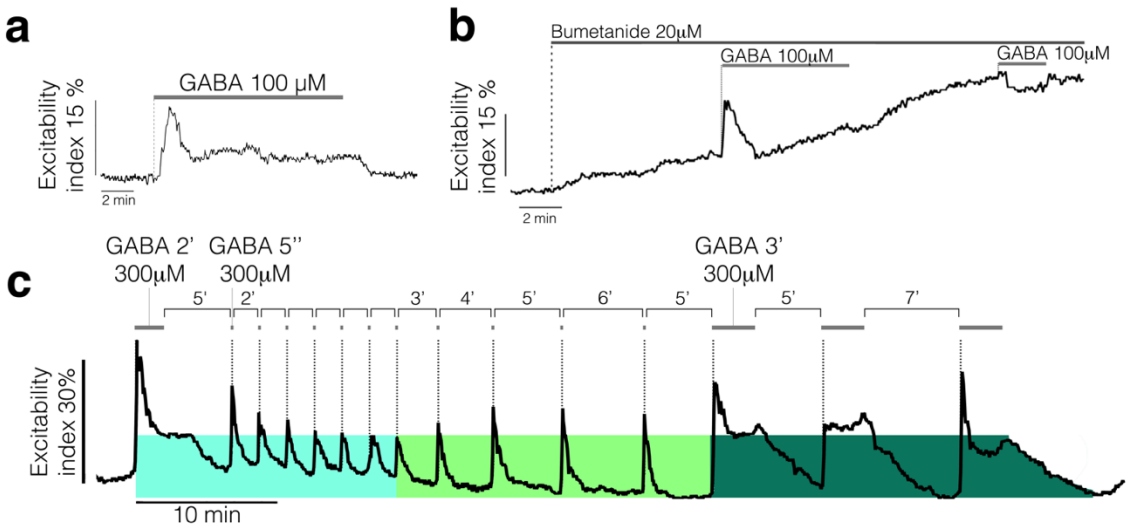

Figure 30. (a) *Axonal GABA (100µM, 10min) responses are characterized by an initial phasic and subsequent tonic component that persists during, and subsides after, GABA application.* ***(b)*** *In the presence of the specific NKCC1 blocker bumetanide (20µM) the tonic component of the axonal GABA (100µM, 6min) response were absent and subsequent GABA (100µM) responses were absent indicating the depletion of intra-axonal chloride.* ***(c)*** *The dependence of the phasic component of GABA responses on NKCC1 activity is illustrated by a progressive reduction in phasic amplitude in response to 5 second applications of GABA at 2 mine intervals. Notably, the phasic amplitude of GABA responses decreases to a level comparable with the tonic response to GABA, observed during the initial 2 min GABA application (light blue). The phasic GABA response is restored upon extension of the interval between successive 5 second GABA applications from 2 out to 6 min (light*

green). In confirmation of this, repeated 3-minute GABA (300µm) applications produced an initial GABA response with both phasic and tonic components following which a 7 min period was required to re-establish the phasic component of the GABA response (dark green).

Action potential activity stimulates NKCC1 mediated chloride loading of axons

Observation from the literature (Brumback AC & Staley KJ, 2008), correlated the activity of NKCC1 to the action potential firing in immature CA1 pyramidal neurons. This phenomenon has been hypotetized to occur also in somatosensory C-fibres (Price TJ et Al., 2009). Therefore, to examine a possible nexus between action potential firing and NKCC1 activity we investigated axonal GABA responses at different rates of electrical stimulation from 0.5 to 1.7 Hz (Figure 31.a). As stimulus rate increased, a corresponding axonal GABA response amplitude increases accordingly (Figure 31.a); this was consistent with previous reports (Carr RW et Al., 2010). Furthermore, the subsequent reduction of stimulation rate back to 0.5 Hz resulted in the maintenance of GABA sensitization (Figure 31.a, III GABA application). This observation demonstrated that the increase in GABA response amplitude was not induced only by a shift in membrane potential, but that there is a second phenomenon that is modulating chloride flux intensity. We than hypothesized that the increase in GABA responses might depend on an intra-axonal accumulation of chloride, that resulted in a bigger chloride gradient and subsequent chloride flux trough $GABA_AR$.

Interestingly, axonal GABA responses at low stimulus rate (0.5 Hz) were increased also following a single (Figure 31.b) and successive bouts (Figure 31.c, d) of high frequency stimulation, consistent with an action potential driven accumulation of intra-axonal chloride (Figure 31.c, d).

We then further demonstrated that axonal GABA responses remained elevated in comparison to the condition before 2.5Hz stimulation, even 30 min after electrical stimulation (Figure 31.f, g). Confirming the exclusion of membrane potential shift

involvement in GABA potentiation and indicating that the mechanism responsible for the chloride gradient modulation was long-lasting in time. Since the main regulator of chloride inward in DRG sensory neurons is NKCC1, we hypothesized that, electrical high frequency stimulation, may positively modulate NKCC1 activity with a long-lasting mechanism, enhancing intra-axonal chloride gradient. In accordance with our hypotheses, NKCC1 blockade significantly curtailed the enhancement of GABA responses in the period after electrical activity (Figure 31.h, i). Interestingly, GABA response enhancement by 2.5Hz stimulation was restored upon washout of bumetanide and without the necessity of a further stimulation, suggesting that NKCC1 activity is necessary to increase intra-axonal chloride concentration. However, the sensitization process of NKCC1, occurred during firing even if the transporter was blocked. For this reason, we suggest that NKCC1 might be activated by phosphorylation during firing. This phosphorylation induced the transporter upregulation, causing a long-lasting increase in chloride influx rate that induce the increase in chloride gradient and subsequently rise in GABA evoked currents. We further studied this phenomenon, excluding other possible mechanism that might induce potentiation in GABA responses. The enhancement of GABA responses was not due to the simple GABA repetitive applications, which did not affect the amplitude of depolarization (Figure 31.l, m). Secondly, we evaluated whether $GABA_AR$ might be directly activated during the firing stimulation. We treated nerves with the $GABA_AR$ antagonist bicuculline (50µM) during the 2.5Hz stimulation. This blockade did not alter the enhancement of GABA responses subsequent to electrical stimulation (Figure 31.n, o) demonstrating that $GABA_AR$ was not directly sensitized to GABA.

Taken together, this set of data showed that GABA responses in C-fibre axons are enhanced by elevated NKCC1 activity, associated with action potential firing.

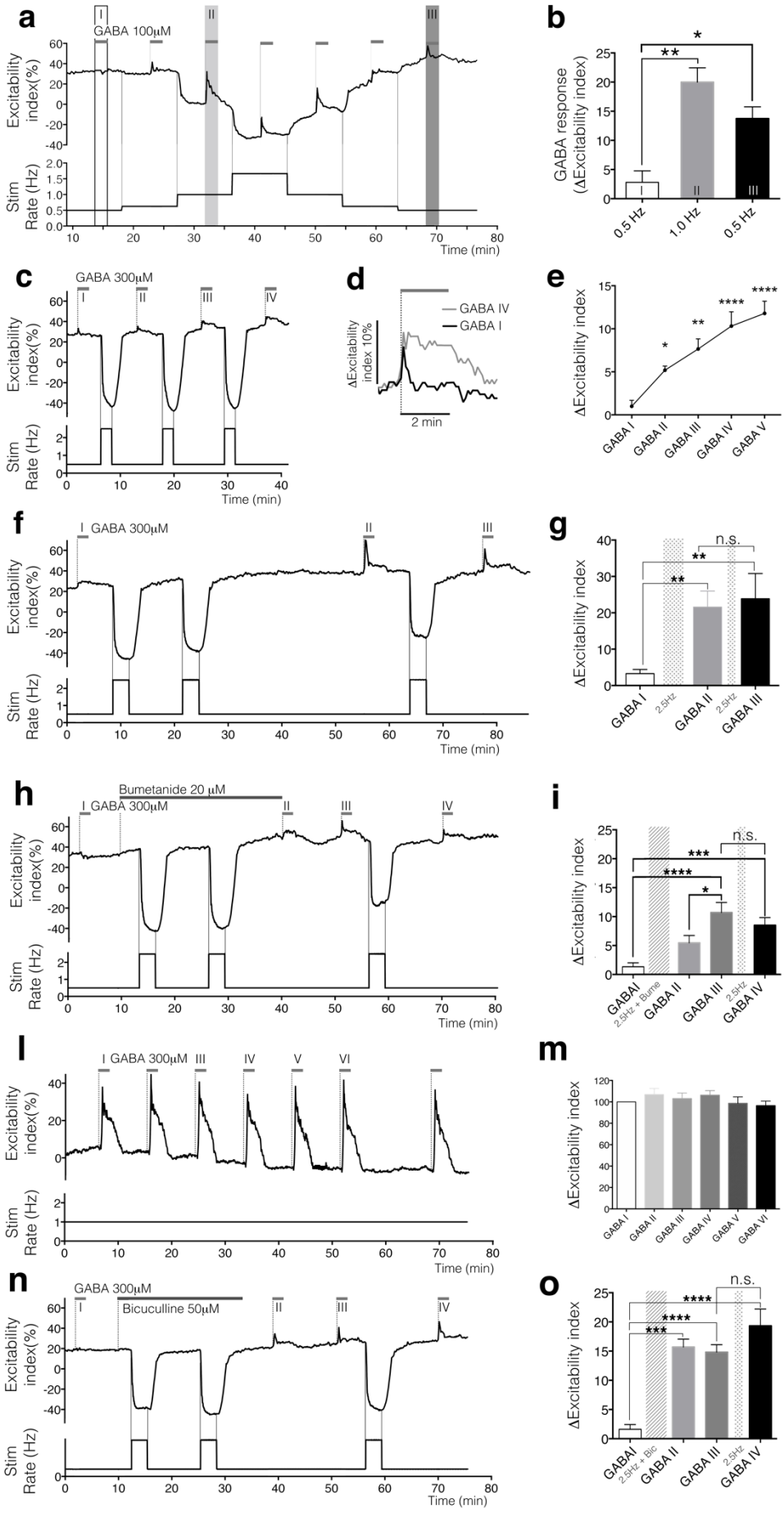
a
GABA 100µM
Excitability index(%)
Stim Rate (Hz)
Time (min)
b
GABA response (ΔExcitability index)
0.5 Hz
1.0 Hz
0.5 Hz
c
GABA 300µM
d
GABA IV
GABA I
ΔExcitability index 10%
2 min
e
ΔExcitability index
GABA I
GABA II
GABA III
GABA IV
GABA V
f
I GABA 300µM
g
n.s.
2.5Hz
h
Bumetanide 20 µM
i
GABA I
2.5Hz + Bume
l
m
n
Bicuculline 50µM
o
2.5Hz + Bic

Figure 31. (a) *The peak amplitude of axonal GABA responses (100μM) increases at higher rates of electrical stimulation, from 0.5 to 1.7Hz. The increase in amplitude persists upon returning to the initial stimulus rate of 0.5Hz* ***(b)*** *as indicated in the pooled data* ***(I*** *n=3, II n=3, III n=3; p=0.0037 F(2,6)= 16.34; Ordinary one-way ANOVA; post-hoc I 0.5Hz vs- II 1.0Hz p= 0.0032 q=7.987, I 0.5Hz vs. II 0.5Hz p=0.0266 q=5.081).* ***(c)*** *Repeated bouts (3min 2.5Hz) of electrically induced action potential, increased GABA responses amplitude following subsequent applications of GABA (300μM)* ***(e)*** *as indicated in the pooled data (n=19, p<0.0001 F(4,14)=22.4; Ordinary one-way ANOVA; post-hoc GABA I vs. others, GABA II p=0.0161 q=3.345, GABA III p=0.0005 q=5.215, GABA IV p<0.0001 q=7.233, GABA V p<0.0001 q=7.153),* ***(d)*** *including an increase in the tonic component.* ***(f)*** *Activity-induced increase in the response to GABA (300μM) is long lasting and persists over 30 min beyond the end of 2.5 Hz stimulation but does not further increase after a subsequent high frequency stimulation;* ***(g)*** *pooled data (n=18, p=0.0004 F(2,15)=13.71, Ordinary one-way ANOVA, post-hoc GABAI vs GABA II p=0.0035 q=5.569; GABAI vs GABA III p=0.0013 q=6.268; GABA II vs. GABA III n.s. p=0.9106 q= 0.5849).* ***(h)*** *The presence of the NKCC1 blocker bumetanide (20μM) during the bouts of 2.5 Hz stimulation abrogates the activity-induced increase in axonal response to GABA (300μM). Following washout of bumetanide, an activity-induced increase in the axonal response to GABA (300μM) was evident and this does not increase further with an additional bout of 2.5 Hz stimulation; pooled data in* ***(i)*** *(n=27, p<0.0001 F(3,23)=0.3837, Ordinary one-way ANOVA; post hoc GABA I n= 12, GABA II n=5, GABA III n=5, GABA IV n=5; GABA I vs. others; not statistically significant GABA II p=0.0564 q=3.833; statistically significant GABA III p<0.0001 q= 8.686, GABA IV p=0.0005 q=6.653; GABA II vs. GABA III p =0.0386 q=4.085).* ***(l)*** *During repeated application of GABA (300μM) at 7 min intervals between treatments, there is no change in response amplitude;* ***(m)*** *and pooled data.* ***(n)*** *The increase in axonal excitability response to GABA (300μM) is not affected by $GABA_AR$ blockade with bicuculline (50μM, black bar upper trace) during bouts of 2.5 Hz stimulation, and not further increased by a subsequent bouts of 0.5 Hz stimulation in absence of bicuculline;* ***(o)*** *and pooled data (n=17, p<0.0001 F(3,13)=38.33, Ordinary one-way ANOVA; post-hoc GABA I vs. others; GABA II p=0.0001 q=6.108; GABA III p<0.0001 q=6.723; GABA IV p<0.0001 q=9; GABA II vs GABA III not statistically significant p=0.9880 q=0.4545).*

$GABA_AR$ modulation of activity-dependent changes in C-fibre axonal excitability

Given the clear observation that the action potential activity was coupled to chloride loading in axons, we exanimated the functional role of $GABA_AR$ chloride currents on C-fibers conduction during sustained activity. We hypothesized that depolarizing $GABA_AR$ chloride currents could limit the reduction respectively in axonal conduction speed (Serra J et Al. 1999) and excitability (De Col R et Al., 2012), during sustained activity in C-fibers (De Col R, et Al., 2008; Thalhammer JG et al., 1994). We studied C fibers during 2.5 Hz for 3 min stimulation, monitoring their increase in conduction time (i.e. reduction in conduction speed). We first studied the differences occurring between control and cKO mice for β3 subunit in nociceptive neurons, sns^{CRE}:β3-/- previously characterized. In nerves from control mice, the activity-dependent C-fibre conduction slowing was reduced by exogenous

application of GABA (1mM), while axonal slowing was strongly enhanced in sns:β3-/- mice (Figure 32.a, b). We then confirmed the data obtained in sns^{CRE}:β3 cKO mice by pharmacological experiments, treating wild type nerves with specific antagonist. In the presence of bumetanide (20µM), axonal slowing was similarly enhanced (Figure 32.c,d). Axonal conduction slowing in C-fibres was also increased by bicuculline (50µM; Figure 32.e,f). Furthermore axonal conduction slowing was decreased by the positive allosteric modulator ALLO (1 µM; Figure 32.g,h). These pharmacological treatments demonstrated that $GABA_AR$ is endogenously activated during sustained electrical activity and that its activation enhanced C- fiber conductance speed allowing unmyelinated axons to respond better to the high frequency stimulation.

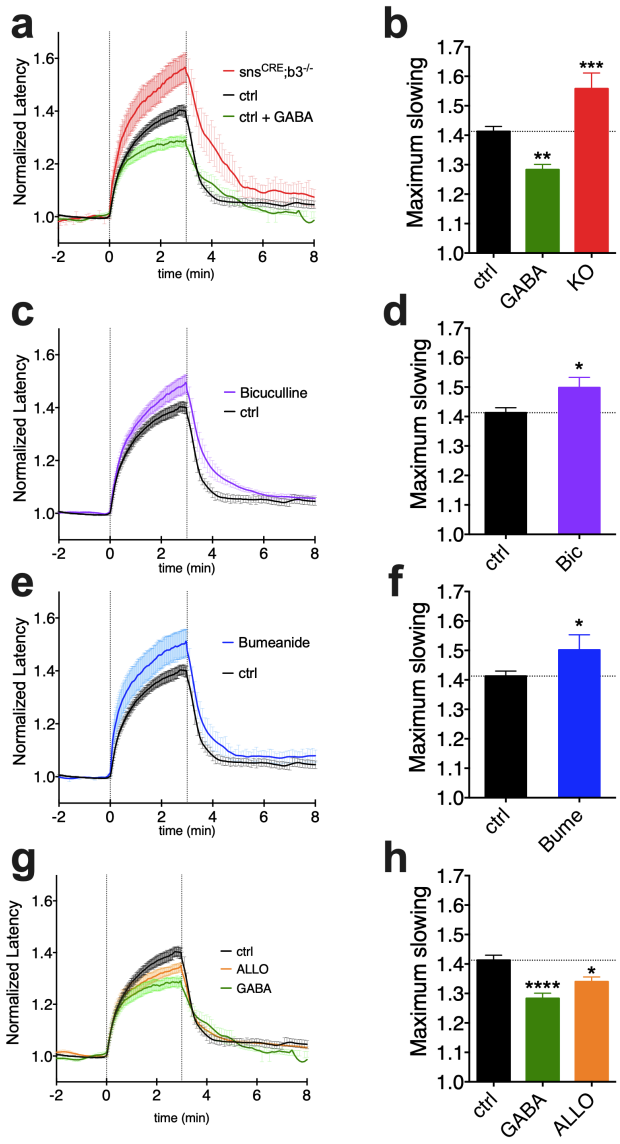

Figure 32. *Electrical stimulation of C-fibers at 2.5Hz for 3 min decreased axonal velocity, measured as an increase in conduction latency* ***(a)*** *and this was enhanced in Sns^{Cre};β3 mice (dark grey trace) and reduced by application of GABA (1mM, light grey trace).* ***(b)*** *Pooled data for the average increase in conduction latency over the last 30 seconds of 2.5Hz stimulation (ctrl n=13, Sns^{Cre};β3 n=6 GABA n=9; p<0.0001 F(2,25)=22.07 Ordinary one-way ANOVA; post-hoc ctrl vs. GABA p=0.0016 q=3.797, ctrl vs. Sns^{Cre};β3 p=0.0020 q=3.723).* ***(c)*** *Activity-induced axonal slowing was increased in the presence of the specific NKCC1 blocker bumetanide (20µM)* ***(d)*** *pooled data (ctrl n= 13, bumetanide 20 µM n=5; unpaired t test p=0.0491 t=2.129 df=16).* ***(e)*** *slowing was increased also in the presence of the specific $GABA_AR$ antagonist bicuculline (50µM, p= 0.0242 t=2.474, df=17 unpaired t test).* ***(g)*** *In contrast, the neuroactive steroid and positive allosterical modulator of $GABA_AR$ ALLO reduced axonal slowing during 2.5Hz stimulation* ***(h)*** *(ctrl n= 13, GABA 1mM n=9, ALLO n=5; p<0.0001 F(2,24)=14.68, Ordinary one-way ANOVA; post-hoc ctrl vs. ALLO p<0.0001 q=5.371, ctrl vs. ALLO p=0.0379 q=2.480).*

GABA is present in sciatic nerve

In order to analyse the putative presence of endogenous ligands of $GABA_AR$ in unmyelinated fibers, we measured GABA levels released by de-sheated surale nerve in HEPES buffer by mean of HPLC assay. HPLC analysis of the solution in which segments of whole sural nerve were deeped for 10 min, revealed micromolar concentrations of GABA (Figure 33.C,D). Importantly, the concentration of GABA was not significantly altered following 10 min of electrical stimulation at 2.5Hz (Figure 33.D), confirming that GABA activity-dependent sensitization, described above, was mediated by chloride enhancement and not by increase in endogenous ligand release.

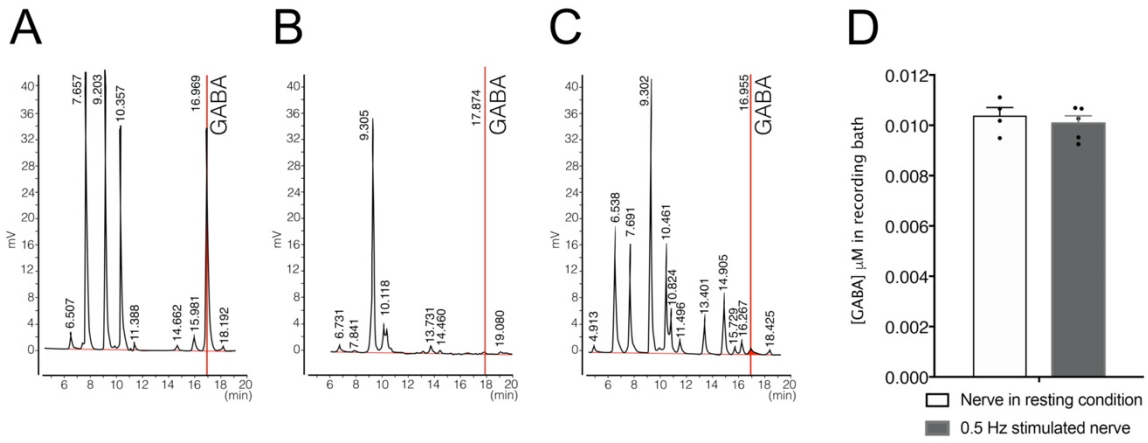

Figure 33. (A) *example of chromatogram trace for GABA determination in a standard reference solution.* ***(B)*** *chromatogram trace of a blank sample formed by HEPES buffer that was not in contact with a nerve.* ***(C)*** *chromatogram trace for GABA determination in HEPES bathing a segment of the sural nerve. GABA peak highlighted in red.* ***(D)*** *HPLC quantification of the solution bathing a segment of sural nerve revealed nanomolar concentrations of GABA (12.16±0.81 nM). GABA release was not modulated following 10 min of electrical stimulation at 2.5 Hz (9.82±0.353 nM). The GABA quantification is expressed as the mean ± SEM of nine (n=9) independent determinations.*

CHAPTER D.1 DISCUSSION

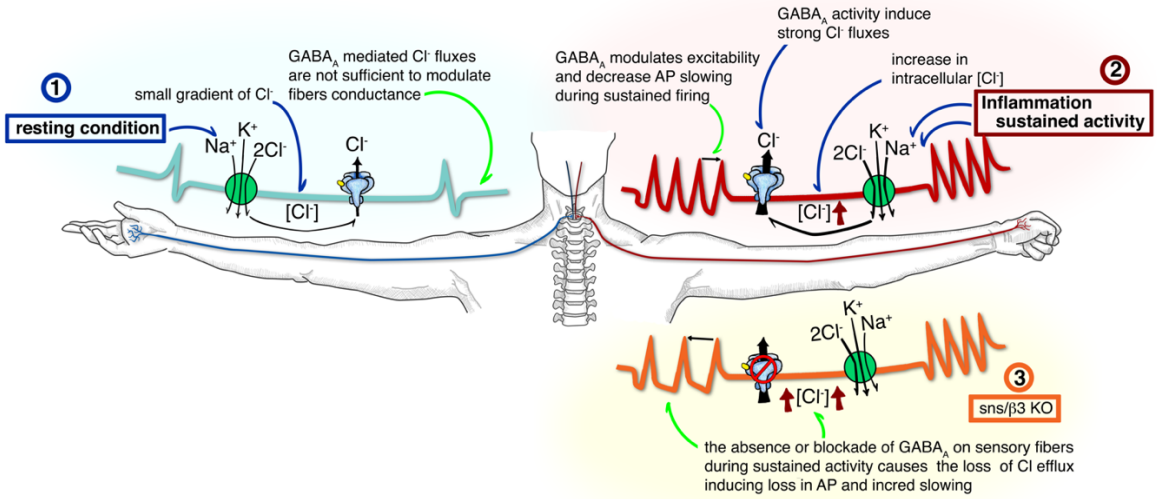

Figure 34. Schematic representation of $GABA_AR$ physiological role in PNS. ***(1)*** *chloride gradient in resting condition is close to membrane resting potential and $GABA_AR$ opening do not cause a strong chloride current, resulting in a weak depolarization.* ***(2)*** *During sustained activity (firing) or after inflammation, NKCC1 increases its activity inducing an increase in intracellular chloride concentration. The increase in chloride gradient cause the potentiation of GABA-induced currents, resulting in a strong depolarization. During sustained activity, $GABA_AR$ activation maintain C-fibers a higher conductance velocity.* ***(3)*** *Nociceptors lacking functional $GABA_AR$ are characterized by a strong loss of conductance velocity during sustained activity.*

The presence and function on $GABA_AR$ in peripheral sensory neuron have been recently discovered and studied in different cellular compartments (Du X. et al., 2017; Chen JT et al., 2014), although its presence in axons and putative role in pain transmission from periphery to CNS is still uncertain. As reported in the introduction, modulation in conduction velocity and fiber threshold can change action potential trains pattern, thus altering the coding process. For this reason, the chloride current capability of modulating conduction velocity could be crucial in the physiological transmission on pain. In addition, morphological conformation of DRG sensory neurons, characterized by the predominance of axonal structure, in comparison with the smaller extension of soma and afferent roots, makes the conduction velocity modulation more critical for the central interpretation of

pain. For all these reasons, small differences in action potential frequency occurring along axons, due to conduction velocity modulation might be translated in big alteration in the signal reaching the synapses in spinal cord.

Threshold tracking techniques were used to characterize for the first time the axonal $GABA_AR$ currents in unmyelinated somatosensory C-fibres. Depolarizing GABA currents in C-fibre axons were mediated by axonal $GABA_AR$ expressed selectively by nociceptors. We further identified, by mean of pharmacological and biomolecular approaches, that the predominant axonal $GABA_AR$ composition is $\alpha2\beta3\gamma2$, which is characterized by fast kinetics, low affinity to GABA (μM range) and mandatory requirement of $\beta3$ subunit to be functional. GABA induces depolarization through chloride efflux, and for this reason $GABA_AR$ activity is strictly dependent by intra-axonal chloride concentration regulated by NKCC1 activity. We demonstrated here that NKCC1 activity is strongly modulated by C-fibers electrical activity (Figure 8) and by inflammatory mediators (Funk K. et al., 2008), that cause its acceleration. NKCC1 indeed, is able to quickly restore intra-axonal chloride concentration after $GABA_AR$ mediated depletion. Furthermore, NKCC1 increases chloride inward rate during and after electrical stimulation, causing the increase in chloride gradient and subsequent GABA evoked currents intensity. Overall this phenomenon resulted in an interesting activity-dependent modulation on C-fibers conductance by $GABA_AR$. $GABA_AR$ activation stabilizes axonal excitability during firing, reducing speed loss and allowing pain transmission from the periphery to the CNS. Moreover, we demonstrated that $GABA_AR$ is physiologically activated by endogenous agonist with a tonic kinetics, because its activity disappeared in the nerves of conditional null mice, in presence of competitive antagonists and in presence of NKCC1 blockers, while it was enhanced by the treatment with allosteric positive $GABA_AR$ modulators.

Intracellular recordings from unmyelinated axons in peripheral nerve is precluded by their small diameter and physical barriers of the surrounding tissue. Therefore, in order to assess axonal membrane currents, we adopted a threshold tracking technique to record changes in axonal excitability. The threshold tracking method relies on the assumption that for CAP, any given sub-maximal amplitude corresponds to the summed response of a fixed number of individual axons, each one contributing with an all-or-none action potential. Under this assumption, adjustments to the intensity of stimulus current required to maintain a CAP amplitude at 40% of maximum reflect changes in axonal excitability, that is an increase in the excitability of each, or at least several, individual axons necessitates a reduction in stimulus current to maintain a 40% C-CAP amplitude (Figure 23). By tracking changes in stimulus current required to maintain a 40% C-CAP we observed that GABA produced a large and reproducible increase in axonal excitability. The increase in axonal excitability reflects a depolarizing membrane current. The absence of axonal GABA response in mice lacking β3 (Figure 27) and the pharmacological outcomes (Figure 25) confirm that GABA currents in peripheral C-fiber axons were mediated by $GABA_AR$, without any prominent $GABA_B$ contribution (Figure 25.c).

The subunit composition of $GABA_AR$ in unmyelinated axons has not been determined. Analysing mRNA from whole DRG we found a preponderance of α2 β3 and γ2 subunits (Figure 28.a). This $GABA_AR$ subunit composition is correlated with low affinity to GABA and fast kinetic. Indeed, we tested the hypothesis that axonal $GABA_AR$ might be composed reflecting mRNA levels detected in DRG, finding that GABA currents in axons were induced only by micromolar concentration of GABA, muscimol and THIP, indicating the absence of the high affinity δ–containing $GABA_AR$. In accordance, previous in-situ hybridization (Ma *et*

al., 1993), RT-PCR (Maddox *et al.*, 2004) and immunohistochemical data (Lorenzo *et al.*, 2014) identified accordingly α2, β3 and γ2 in adult DRG neuronal soma.

α2β2/3γ2 composed $GABA_AR$ is typically associated with the synaptic $GABA_AR$ type (Nusser *et al.*, 1996), for instance in hippocampal CA1 pyramidal neurons (Prenosil G.A. et al., 2006; Kasugai Y. et al., 2010) whereas, α2 subunit association with gephyrin is fundamental to target the receptor to the post synaptic domain (Tretter et al 2008). However, the central terminals of DRG neurons do not express gephyrin (Lorenzo *et al.*, 2014) suggesting the presence of different association proteins or an α2 independent trafficking to central primary afferents and possible mis trafficking of synaptic receptor to extra synaptic domain. $GABA_ARs$ are, indeed, highly dynamic and diffuse within the neuronal plasma membrane, between synaptic and extra synaptic areas. In accordance, classical synaptic $GABA_ARs$, has been found in the extra synaptic domain (Bogdanov et al., 2006; Thomas et al., 2005), to support tonic inhibition (Thomas et al.,2005; Bogdanov et al., 2006; Bannai et al., 2009; Hannan S. el al., 2019). All these reasons might explain the presence of a "synaptic" $GABA_AR$ at an extra-synaptic site, along peripheral axons. Herein this theory, was confirmed by IFL analysis, revealing the presence of the α2 subunit, typically described as synaptic subunit, along myelinated and unmyelinated axons of mice sciatic nerve.

Conditional deletion of β3 subunit suppressed completely GABA responses in C-fibre, confirming that peripheral $GABA_AR$ along axons needs β3 subunit to be functional. However, the absence of axonal GABA responses found in $sns^{Cre};\beta3^{-/-}$ mice diverged from the previous report, which showed a substantial reduction but not a complete absence of GABA currents in the soma of DRG neurons (Chen et al., 2014). We hypothesized that this inconsistency in GABA sensitivity might be due to compensatory mechanisms occurring *in vitro*, in which DRG neurons sprout and made de novo receptor synthesis. Accordingly, we

previously showed that primary culture of DRG neurons expressed a wider composition of $GABA_AR$ subunits, within β1 upregulation (Faroni et al., 2019). This $GABA_AR$ composition might compensate for the absence of β3 subunit, restoring in part the GABA sensitivity. The analysis of chloride currents kinetic provided evidence that the intra-axonal chloride concentration in nociceptors was controlled by the balance among NKCC1, Na^+/K^+-ATPase and $GABA_AR$ activity. Depolarizing chloride currents mediated by $GABA_AR$ opening, indeed, are counterbalanced by the fast capacity of NKCC1 (5-7 min) to restore intra-axonal chloride gradient, exploiting the Na^+ gradient driving force maintained by Na^+/K^+-ATPase. The kinetic correlation between $GABA_AR$ chloride efflux and NKCC1 chloride inward was confirmed through the bumetanide co-treatments, which showed that $GABA_AR$ opening, under this condition, depleted completely the chloride gradient, leading to abrogation of subsequent GABA-evoked currents. The kinetic of NKCC1 chloride loading along axons has been tested by the repetitive application of exogenous GABA for different times (Figure 30.c). Interestingly, extra-synaptic axonal GABA responses were characterized by the combination of a phasic phase, followed by a prolonged tonic phase (Figure 25.a,b,d; Figure 30.1,c) (if GABA was kept in the perfusing bath long enough to evidence both components). A similar kinetic was previously reported in DRG neuronal soma (Akaike *et al.*, 1987; Zhang *et al.*, 2015). Short-interval application of quick GABA treatment caused the gradual decrease in responses amplitude, until a minimum intensity. This residual effect was characterized by an intensity corresponding to tonic component of prolonged GABA treatment and reflects a persistent depolarization maintained by an inward chloride current, that may be counterbalanced to some degree by NKCC1 activity. Prolonged application of high concentration of GABA confirmed this hypothesis, showing a transient phasic phase induced by chloride efflux and a consequent loss of chloride gradient

(recovery phase during GABA exposure); then the persistence of a tonic stable response that was absent in co-treatment with bumetanide (Figure 30.a,b). Thus, we hypothesize that GABA phasic phase origins from Cl^- gradient depletion, whereas the subsequent tonic phase resulted from the achievement of a steady-state between NKCC1 and $GABA_AR$ receptor Cl^- fluxes.

In resting condition, C-fibers showed a weak response to exogenous GABA application that was strongly increased after electrical activity. This observation is crucial for the understanding of the physiological role of GABAergic system in PNS. Indeed, $GABA_AR$ in C-fibers axons might play an important role in the modulation of action potential conductance during sustained activity, as demonstrated also in CNS, whereas $GABA_AR$ modulates the degree of synchronization of complex spike activity in Purkinje cells (Lang et al. 1996; Llinas and Sasaki 1989). We showed that modest electrical stimulus frequency application (2.5 Hz stimulation for 3 min) is sufficient to sensitize axons to GABA for a long period of time (figure 31) and that this process might be due to NKCC1 acceleration and subsequent increase in chloride gradient. After C-fiber activity-depended sensitization, GABA was able to increases dramatically C-fiber excitability and to reduce the loss of conductance during high frequency stimulation. In other words, GABA modulation in peripheral axons is able to balance the intrinsic desensitization of C-fiber that occur during intense nociceptive stimulation.

We postulated the hypothesis that the increased effect of GABA was due to an increased intra-axonal chloride gradient, mediated by NKCC1 transporter, as demonstrated by the effect of its blockade with bumetanide (Figure 31.h,i). We excluded the hypothesize that this phenomenon was due to voltage membrane shift (Figure 31.a,b,f,g) or $GABA_AR$ direct sensitization (figure 31.l,m,n,o). Similarly, it has been similarly demonstrated that action

potentials train can induce the increase in intracellular chloride concentration in CNS immature neurons, due to the reset of the thermodynamic equilibrium for NKCC1, secondary to Na^+/K^+-ATPase activity changes (Brumback and Staley, 2008). Interestingly, GABA sensitization observed, caused by intra-axonal chloride shift in peripheral axons was characterized by long-lasting kinetics, which persisted even after more than 30 min from stimuli, suggesting that the possible mechanism of action might by the transporter phosphorylation.

A central question related to the localization of $GABA_AR$ at extra-synaptic sites along peripheral unmyelinated axons, concerns their physiological and possible pathophysiological role. Using the axonal conduction slowing as an index of excitability loss we observed that sns^{CRE}; $\beta3^{-/-}$ are characterized by a more pronounced loss of conduction speed during firing (Figure 32.a,b) , and the same slowing profile has been observed in wild type mice nerves treated with bumetanide (NKCC1 blockers that induce loss of chloride gradient) and bicuculline ($GABA_AR$ specific competitive antagonist) (Figure 32.c,d,e,f). These data indicate that $GABA_AR$ is constitutively active in axons and modulates C-fiber conduction speed during activity. In addition, we traded the nerve with the allosteric $GABA_AR$ positive modulator ALLO, demonstrating that it was able to increase conduction speed similarly to exogenous GABA (Figure 32.g,h). Recently, it has been demonstrated that $GABA_AR$ is characterized by spontaneous opening, not requiring GABA binding to get into active state (Nathanael O'Neill and Sergiy Sylantyev, 2019). However, our pharmacological outcomes suggest a direct activation of axonal $GABA_AR$ by local GABA, corroborating the occurrence of local paracrine mechanism. By accomplishing this hypothesize, HPLC analysis revealed the presence of GABA in whole sural nerve perfusate at low micromolar concentration, that were unchanged by sustained electrical stimulation (2.5Hz, for 10 min;

Figure 33). In addition, these observations confirmed the endogenous and local regulation of axonal excitability via $GABA_AR$ in peripheral nerves. Hanack and colleagues (Hanack *et al.*, 2015) suggested that axons themselves may be a source of GABA in the periphery. In addition, we showed that Schwann cells in peripheral nerves possess large metabolic resources and could be a local source of $GABA_A$ agonists, in the form of GABA itself or the neuroactive steroids ALLO (Robert *et al.*, 2001; Magnaghi *et al.*, 2010). Schwann cells possess, indeed, GABA synthetic machinery (Magnaghi *et al.*, 2010); Procacci *et al.*, 2012; Magnaghi et al., 2007)

In conclusion, we propose a new physiologic control mechanism of nociceptors, mediated by $GABA_AR$ chloride currents. $GABA_AR$ is able to control the activity-dependent loss of conductance velocity, allowing the physiological transmission of pain signal to the CNS. We show that the activation of axonal $GABA_A$ becomes effective only during or subsequent to axonal firing. Nociceptors firing drives NKCC1 to load axonal chloride and rising $GABA_AR$ depolarizing modulations upon action potential conductance. During activity, endogenous $GABA_AR$ activation confer to C-fibers the capacity to follow sustained firing through chloride currents.

CHAPTER 2

Pathological involvement of axonal $GABA_AR$ in sensory C-fibers axons:

1. Inflammation modulates axonal $GABA_AR$ activity

$GABA_AR$ in unmyelinated axons regulates mechanical pain threshold

Considering the endogenous activation of $GABA_AR$ and its capability to modulates nociceptor activity-dependent slowing, we tested the basal behavioural perception of pain in the cKO mouse line sns^{CRE};β3, where the ablation of $GABA_AR$ β3 subunit was restricted to a smaller neuronal subpopulation. We observed that sns^{CRE};$β3^{-/-}$ mice, lacking β3 subunit only in sensory neurons, showed sensitivity to mechanical pain (Figure 35). We tested their sensitivity to mechanical stimuli applying forces at different intensities, from a not painful (from 0.008g to 0.07g) to a painful stimuli (from 0.16g to 1.4g) using Von-Frey test (2way RM ANOVA interaction *p=0.0007 F(8,168)= 3.593*, genotype factor *p<0.0022 F(1,21)=12.18*. Tukey multiple comparison test; sns^{CRE}; $β3^{fl/fl}$ vs. sns^{CRE}; $β3^{-/-}$ at 0.02 g *p=0.0201*, 0.04g *p=0.0056*, 0.07g *p= 0.0487*, 0.16g *p<0.0001,* 0.4g *p=0.00438*). Sns^{CRE}; $β3^{-/-}$ showed to be less sensitive to the same force intensity compared to control littermates, indicating a higher mechanical threshold. These observations demonstrate $GABA_AR$ involvement in mechanical-induced pain perception.

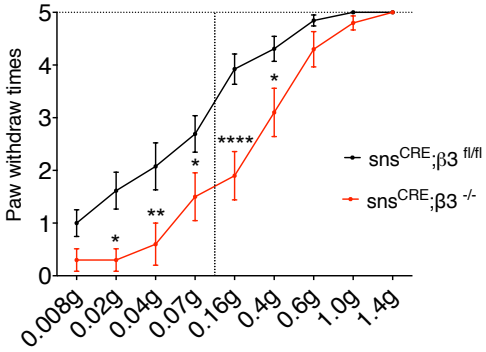

Figure 35. *Von-Frey test on sns^{CRE};$b3^{fl/fl}$ mice line. cKO mice showed higher mechanical threshold to different forces applied; both canonic tactile stimuli (from 0.008g to 0.07g) and pain stimuli (over 0.16g). Von-Frey filament was applied 5 times on mice paw, and we measured the number of times the mouse retracted the limb.*

Inflammatory mediators induce C-fibers sensitization to GABA

Given the implication of $GABA_AR$ in physiological perception of pain, we explored its possible role in pathological condition. Since NKCC1 is known to be modulated by inflammatory mediators (Cramer SW at al., 2008; Delpire E et al., 2010; Kahle KT et al., 2005; Darman RB et al., 2002), inducing the intra-axonal increase of chloride concentration, we hypotesized that $GABA_AR$ activity in C-fiber axons may be regulated by inflammatory condition. We exposed sural nerves to inflammatory soup for 10 min (histamine 1 µM, bradykinin 2 µM, PGE_2 1 µM and serotonin 1 µM), a mixture known to sensitize C nociceptors (Kessler W. et al., 1992) and phosphorylate NKCC1 (Funk K*, et al.,* 2008). Inflammatory mediators lead to a prominent increase in the amplitude of axonal GABA responses (100 µM, Figure 36); this might be in accordance with a putative increase in NKCC1 mediated axonal chloride loading.

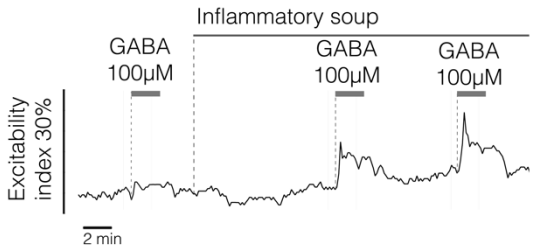

Figure 36. *GABA 100µM was applied to desheated nerve in "resting condition" 0.5Hz without electrical sensitization (2.5Hz application) showing a small increase in excitability; the nerve was then incubated 10 min with inflammatory soup, composed by histamine 1µM, bradykinin 2µM, PGE_2 1µM and serotonin 1µM. In presence of Inflammatory mediator, the same GABA concentration induced a strong depolarization.*

Effect of inflammation in *in-vivo* models – acute inflammation

To extend our observation to *in vivo* model, we tested the pain perception in presence of complete Freund's adjuvant (CFA)-induced inflammatory pain in a model of conditional KO (cKO) mouse line $sns^{CRE};\beta3$. Intraplantar unilateral injection of CFA is known to rise the noxious sensitivity to heat as well as increase the sensitivity to mechanical stimulation. We tested mechanical pain threshold in $sns^{CRE};\beta3$ mice by using Von Frey test. We confirmed that 2 days after CFA injection, control mice (CTRL; $sns^{CRE};\beta3^{fl/fl}$) showed a significant lower

threshold to mechanical stimuli (Fig 37.b; CTRL CFA (blue) vs. CTRL contralateral (black); statistic Fig 37.d) and in particular to gentle tactile stimuli (from 0.008g to 0.07g force applied), canonically described as allodynia. As reported above, cKO ($sns^{CRE};\beta3^{-/-}$), were characterized by a constitutive higher threshold to mechanical pain, (cKO contralateral (red) vs. CTRL contralateral (black) Figure 35, Figure 37.b) and were also affected by the inflammatory insult (cKO CFA (orange) vs. cKO contralateral (red)). However, cKO mice showed a different intensity and phenotype compared with controls. Controls mice, in fact, presented a sensitization curve that was particularly intense with low forces applied but and less intense with strong forces, resulting in a minor slope (figure 37.b). Conversely, cKO mice are characterized by a constant inflammatory-mediated sensitization that involve also intense painful stimulation (from 0.16g to 1.4g), determining a curve parallel to the contralateral response (Figure 37.c). This observation suggests that the absence of functional $GABA_AR$ on nociceptor leads to the reduction in inflammatory allodynia and contemporary to the insurgence of light hyperalgesia (fig 37.d; statistic 37.e).

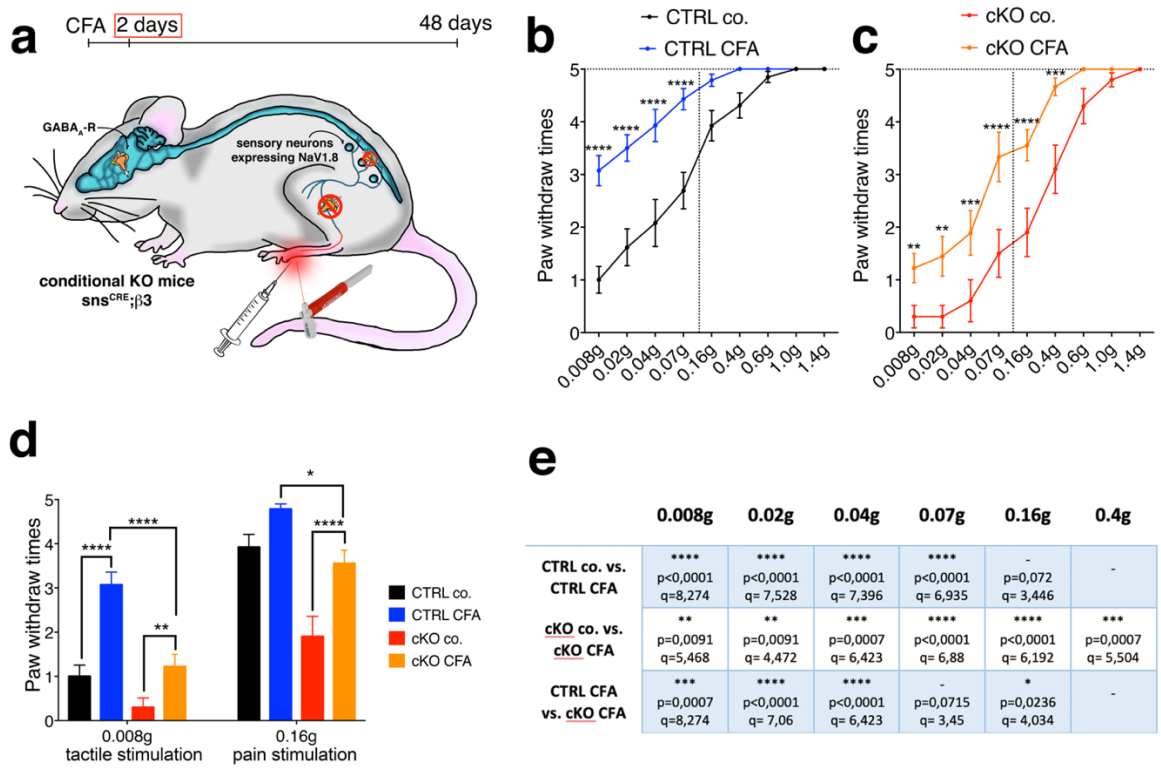

	0.008g	0.02g	0.04g	0.07g	0.16g	0.4g
CTRL co. vs. CTRL CFA	**** p<0,0001 q=8,274	**** p<0,0001 q= 7,528	**** p<0,0001 q= 7,396	**** p<0,0001 q= 6,935	- p=0,072 q= 3,446	-
cKO co. vs. cKO CFA	** p=0,0091 q=5,468	** p=0,0091 q= 4,472	*** p=0,0007 q= 6,423	**** p<0,0001 q= 6,88	**** p<0,0001 q= 6,192	*** p=0,0007 q= 5,504
CTRL CFA vs. cKO CFA	*** p=0,0007 q=8,274	**** p<0,0001 q= 7,06	**** p<0,0001 q= 6,423	- p=0,0715 q= 3,45	* p=0,0236 q= 4,034	-

Figure 37. (a) *Von-Frey test on sns^{CRE};β3 line, 2 days post CFA unilateral injection. We tested mechanical sensitivity by multiple measurement with different forces applied on the lower limbs. Forces from 0.008g to0.07g are canonically described as pure mechanical/not painful stimulation; forces above 0.16g are classified as painful stimulation.* ***(b)*** *control mice (sns^{CRE};β3$^{fl/fl}$) showed a typical hypersensitization to mechanical stimuli characterized by a lower pain threshold. CFA-induced sensitization is strong and restricted to tactile stimulation (from 0.008g to 0.07g applied).* ***(c)*** *cKO mice (sns^{CRE};β$^{-/-}$) showed a less intense sensitization after CFA and characterized by a different evolution related to intensity of forces applied. Indeed, cKO after CFA presented a constant sensitization to painful stimulation (above 0.16g).* ***(d)*** *cKO mice showed a stronger sensitization to pain stimuli (hyperalgesia) and CFA condition resulted statistically different in both experimental paradigms.* ***(e)*** *Statistical analysis.*

To investigate the possible contribution of axonal $GABA_AR$ in the pathogenesis of hyperalgesia, we tested axonal C-fibers conduction in the same mice treated unilaterally with CFA injections. Moreover, to corroborate *in vivo* observations, we evaluated axonal threshold in addition to conductance speed during high frequency stimulation (2.5 Hz stimulation for 3 min, as previously studied). This treatment mimic firing that occur during pain perception. C-fibers are in fact characterized by a typical desensitization process during high frequency, represented by the decrease of conduction speed (expressed as

increased latency, as previously reported in Figure 32) and the concomitant increase of electrical threshold (expresses as decrease in excitability index).

We demonstrated, indeed, that cKO mice reached a lower threshold plateau during 2.5Hz stimulation, compared with control littermates (Figure 38.a in red; unpaired t test p=0.0165, t=2.785; n=7).This effect was simultaneous with the decrease in conductance speed, already observed (Figure 38.e in red). Two days after CFA injection to control mice (blue line and bar in Figure 38 a, c), we observed a significant reduction in C-fibers threshold plateau, compared with the contralateral limb (black line and bar in Figure 38.a, c; paired t test p=0.0275 t=3.392; pair n=5;) and contemporary a tendency to increase conduction speed (blue line and bar in Figure 38 e, g; paired t test *p=0.0743*). Conversely, CFA injection do not cause modulation in threshold and latency of nerves lacking functional $GABA_AR$ in nociceptors axons, that is sns^{CRE};β3 (orange vs. red, lines and bars in Figure 38 a,b,d,e,f,h).

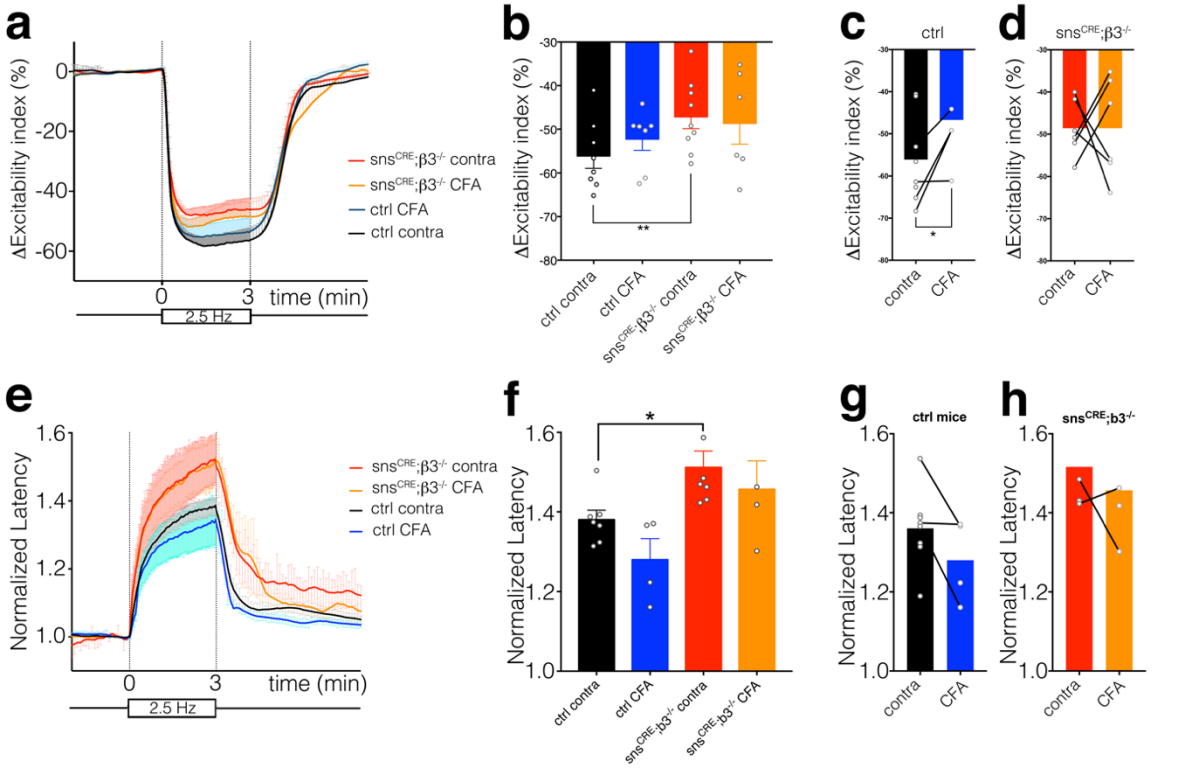

Figure 38. *Activity dependent desensitization of sural nerve from $sns^{CRE};\beta3^{fl\text{-}fl\text{-}}$ (ctrl) and $sns^{CRE};\beta3^{-/-}$ mice 2 days after unilateral CFA injection has been studied measuring excitability index and latency profile.* ***(a)*** *C-fibers quickly hyperpolarize during high frequency stimulation reaching a stable plateau and recovering completely when the stimulation slows down to 0.5 Hz.* ***(b)*** *we analyzed excitability values during the last 30*

second of 2.5 Hz stimulation and we observed that cKO ($sns^{CRE};\beta3^{-/-}$) are characterized by statistically significant higher excitability index indicating lower threshold. ***(c)*** *C-fibers of inflamed nerves (ctrl CFA in blue) were characterized by increase in excitability index wheatear* ***(d)*** *cKO mice seems not affected by CFA injections.* ***(e)*** *C-fibers decrease conduction speed during high frequency stimulation, reaching a maximum level at the end of 2.5Hz application, the conduction speed recovers completely when the stimulation slows down to 0.5Hz.* ***(f)*** *We confirmed the decrease in conduction speed observed in cKO mice* ***(g,h)****, although we observed just a trend in latency reduction after CFA injection in both controls and cKO mice.*

Based on our previous data on inflammatory mediators' sensitization of GABA currents, we tested whether CFA was able to sensitize C-fibers to exogenous GABA treatments. As already demonstrated, GABA induced enhancement in conductance speed during 2.5Hz stimulation (Figure 39.e,f,g), while it was not able to modulate excitability curves (Figure 39.a,b,c). In the acute phase of nerve inflammation, 2 days after CFA injection, It Is not possible to detect a sensitization to GABA treatment (Figure 39.d,h).

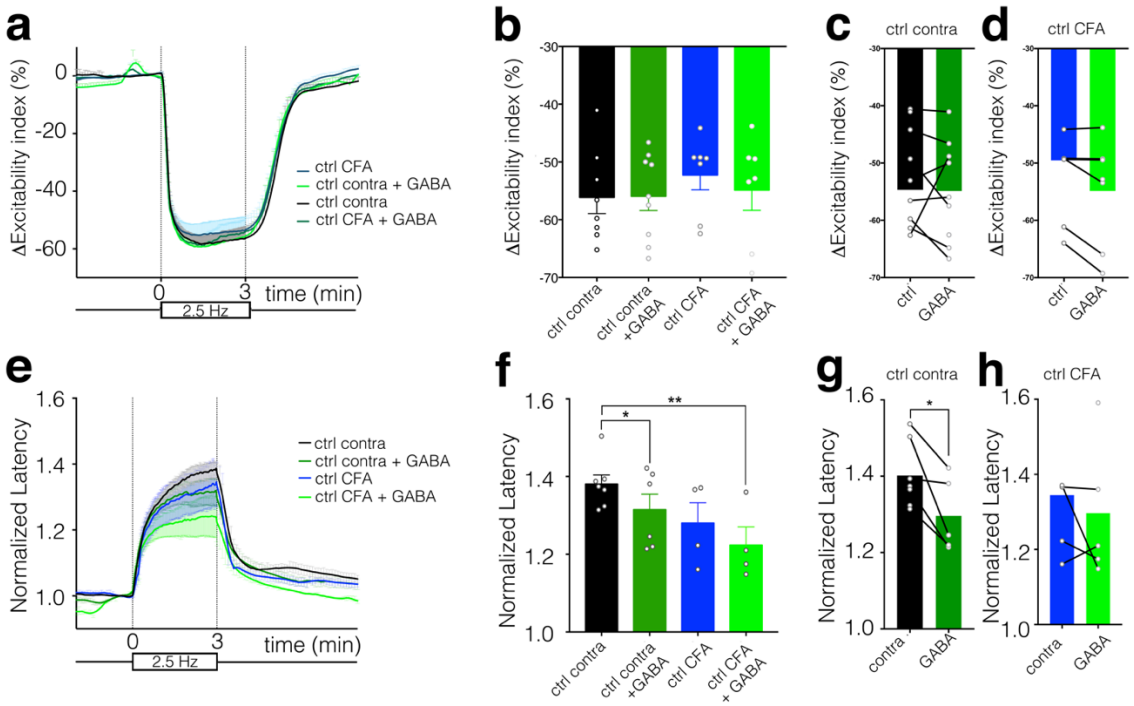

Figure 39. *In control mice (2 days after CFA injection) we applied GABA 1mM to the recording bath during 2.5Hz stimulation to evaluate modulation in Excitability index and conductance speed.* ***(a) (b) (c) (d)*** *Hyperpolarizing profile subsequent to high frequency stimulation do not appear modulated by GABA treatment in both contralateral and CFA conditions.* ***(e) (f) (g)*** *Conductance speed increase during GABA treatment* ***(h)*** *but It is not further increased in CFA condition.*

Effect of inflammation in *in-vivo* models – priming process after inflammation

We then tested mechanical pain threshold 4 weeks after CFA injection to test any long-lasting peripheral adjustment to inflammation that might indicate a chronicization process (Figure 40.a). We observed that 28 days after CFA injections, control mice showed a slight recovery in the phenotype but they presented the persistency of hypersensitivity to pain, in particular at low force intensity applied (Figure 40.b,c). On the contrary, cKO mice recovered completely from inflammation, coming back to the basal condition showing higher pain threshold at all forces applied (Figure 49.c; all statistics are reported in figure 40.e).

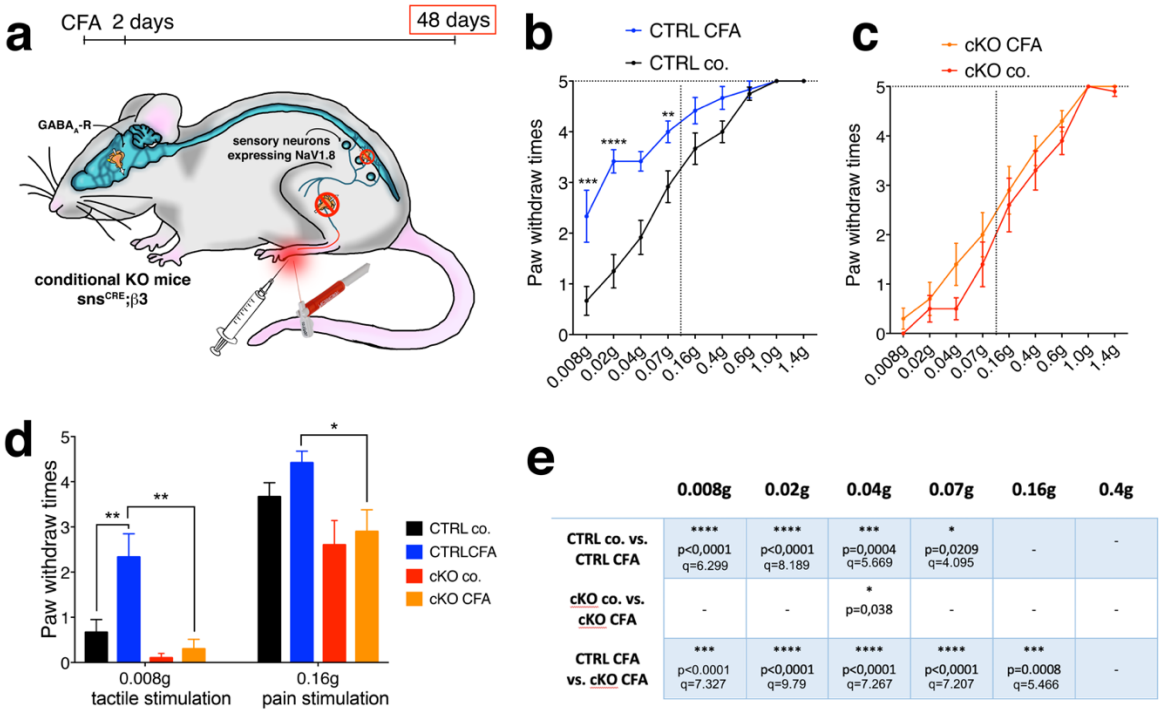

	0.008g	0.02g	0.04g	0.07g	0.16g	0.4g
CTRL co. vs. CTRL CFA	**** p<0,0001 q=6.299	**** p<0,0001 q=8.189	*** p=0,0004 q=5.669	* p=0,0209 q=4.095	-	-
cKO co. vs. cKO CFA	-	-	* p=0,038	-	-	-
CTRL CFA vs. cKO CFA	*** p<0.0001 q=7.327	**** p<0,0001 q=9.79	**** p<0,0001 q=7.267	**** p<0,0001 q=7.207	*** p=0.0008 q=5.466	-

Figure 40. (a) *Behavioral Von-Frey test on sns^{CRE};β3 line, 28 days post CFA unilateral injection. We tested mechanical sensitivity by multiple measurement with different forces applied on the lower limbs. Forces from 0.008g to0.07g are canonically described as pure mechanical/not painful stimulation; forces above 0.16g are classified as painful stimulation.* ***(b)*** *control mice showed a partial recovery in sensitization intensity compared with contralateral side but they still maintain a state of hypersensitivity to low intensity stimuli.* ***(c)*** *cKO mice, 28 days after inflammatory insult, completely recovered from inflammatory-mediated sensitization to mechanical stimuli at all range of forces studied.* ***(d)*** *CFA conditions are statistically different between controls and cKO mice.* ***(e)*** *statistical analysis.*

We then tested the possible long-lasting changes occurred in C-fibers, that might be responsible for the recovery from hypersensitive state. Interestingly, the effect of neuroinflammation on C-fiber conductance increased after a longer time point after injury. Twenty-eight days after a single injection of CFA we observed the same trend of modulation in threshold and conductance speed that we observed after 2 days, whereas that effects were stronger (Figure 41). We confirmed, indeed, that neuroinflammation causes a decrease in electrical threshold (Figure 41.a,c; n= 11, unpaired t test *p=0.0415, t=2.376*) and an increase in conduction velocity in control mice (Figure 41.e,g; n=13, unpaired t test *p=0.0472, t=2.234*). At this time point, also C-fibers lacking functional $GABA_AR$ presented differences between contralateral and CFA limbs. CFA induced an opposite modulation of electrical threshold (Figure 41b,d; n= 7, Unpaired t test *p=0.0868, t=2.127*), compared with control mice, but a comparable reduction in latency (Figure 41 f,h, n=9 Unpaired t test *p=0.00312, t=2.688*). The opposite modulation in excitability index during high frequency (between controls and cKO mice), observed in CFA condition, might be one of the mechanism responsible for the recovery observed with the behavioural tests. In fact, cKO C-fibers appeared to be more hyperpolarized after 28 days of inflammatory condition, compared with control CFA, indicating a higher threshold of activation. These observations demonstrated that $GABA_AR$ play a role in the adaptation process occurring in C-fiber after an inflammatory insult and modulating the recovery process.

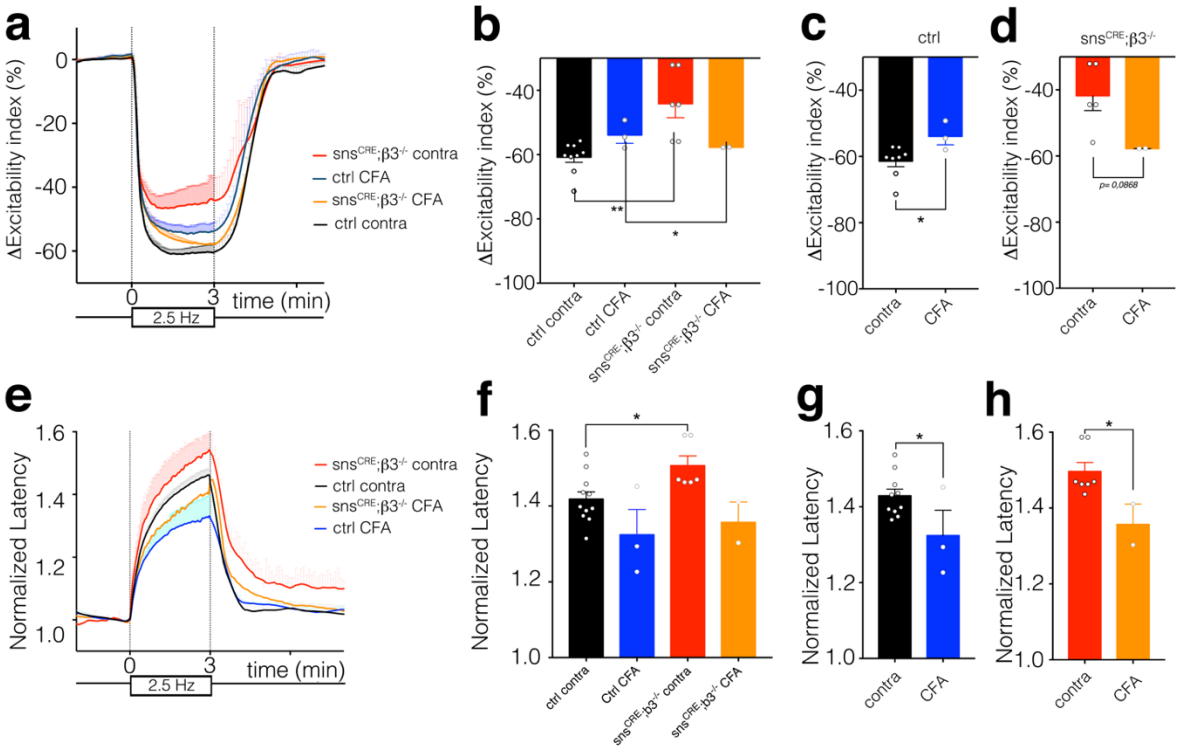

Figure 41. *activity dependent desensitization of sural nerve from* $sns^{CRE};\beta3^{fl\text{-}fl\text{-}}$ *(ctrl) and* $sns^{CRE};\beta3^{-/-}$ *mice 28 days after unilateral CFA injection has been studied measuring excitability index and latency profile.* ***(a)*** *all trends on C-fibers excitability modulation observed 2 days after CFA (Figure 12) were confirmed and even intensified 28 days after inflammation.* ***(b)*** *at this time-point CFA conditions between controls and cKO are statistically significant. cKO after CFA appear more hyperpolarized.* ***(c)*** *CFA induced reduction in excitability index in control mice,* ***(d)*** *while it induced an increase in cKO mice.* ***(e)*** *Also the modulation of C-fibers conductance speed appeared intensified after 28 days post CFA.* ***(f) (g) (h)*** *Inflammation induced increase in conductance speed in both controls and cKO mice.*

In addition, we observed that, at this time point, nociceptors were sensitized to GABA application, showing a strong increase in electrical threshold during 2.5Hz stimuli (Figure 42.a,c). This result suggests that, subsequently to an inflammatory insult, C-fibers slowly changes their capability to respond to GABA, increasing the magnitude of the current induced by $GABA_AR$.

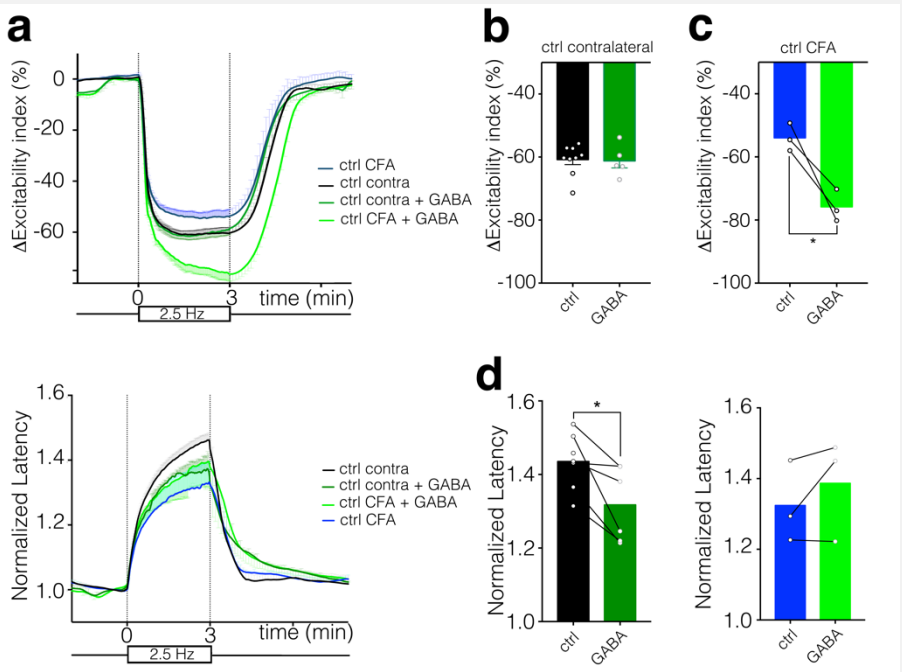

Figure 42. *We applied GABA 1mM to the recording bath during 2.5Hz stimulation to evaluate modulation in Excitability index and conductance speed in control mice 28 days after CFA injections.* ***(a) (b) The*** *hyperpolarizing profile subsequent to high frequency stimulation appears modulated by exogenous GABA application only in post-CFA condition.* ***(c)*** *GABA induced a strong hyperpolarization during 2.5Hz stimulation, representing a higher C-fibers excitability threshold.* ***(e) (f) (g)*** *Conductance speed increases during GABA treatment in control condition.*

CHAPTER 2 DISCUSSION

The observation regarding $GABA_AR$ localization at the extra-synaptic site along peripheral unmyelinated axons raises the question about its physiological and pathophysiological role. In the second chapter of this thesis we used a combination of *in vivo* and *ex vivo* experiments on inflammatory pain models, in order to answer these questions. We observed that $GABA_AR$ endogenous activation is relevant in the physiological perception of pain and in the maintenance of C-fiber conduction velocity during firing, restricting the excessive activity-dependent slowing of nociceptors. Interestingly, $GABA_AR$ modulates pain threshold in inflammatory pain condition, promoting allodynia and protecting from hyperalgesia in the acute phase of the disease. Moreover, $GABA_AR$ seems to be involved in the recovery phase and in the possible pain chronicization. Indeed, $GABA_AR$ potentiation in nociceptor fibers caused the prolongation up to 4 weeks of pain oversensitivity (allodynia), after a single inflammatory injury.

The characterization of mechanical pain sensitivity in $sns^{CRE};\beta3$ null mice, by using Von-Frey assay, demonstrated that cKO mice are characterized by a higher pain threshold, either at weak non-painful stimulation or at stronger painful stimulation. These observations were confirmed by the electrophysiological *ex vivo* analysis of C-fibers conductance, demonstrating that cKO mice were characterized by a stronger loss of conductance speed during firing, associated to a simultaneous maintenance of lower excitability threshold. The modulations observed in excitability, suggested that a higher number of unmyelinated fibers are able to follow 2.5Hz frequency stimulation. Consequently, these fibers are characterized by a more pronounced slowing profile. Therefore, the increased desensitization of cKO nerves, causes the onset of instable signalling in nociceptor. These observations suggest that $GABA_AR$ is able to stabilize nociceptor action potential

conductance, maintaining the frequency and temporal coding of action potential trains; these results in a stable and physiological perception of pain. The reduced pain perception of cKO mice might arise, indeed, from an unstable conductance of action potential along axons, causing the modulation of action potential encoding.

As previously described in the introduction, the process of encoding is crucial in the quali-quantitative interpretation of signals. The absence of $GABA_AR$ currents causes action potential conductance slowing, resulting in a drop of action potential rate, reaching the distal synapses. This phenomenon, theoretically, causes the transmission weaker signals to the spinal cord and subsequently a weaker central perception of pain.

As already observed in spinal cord and DRG neurons, the NKCC1 transporter can be upregulated (Cramer SW at al., 2008) and phosphorylated (Delpire E et al., 2010; Kahle KT et al., 2005; Darman RB et al., 2002) during injury, causing its strong activation and enhancing intracellular chloride concentration. On this regard, we evaluated the effect of inflammatory mediators on axonal chloride gradient, by the study of $GABA_AR$ mediated currents. We demonstrated that inflammation potentiate GABA currents also in C-fibers. Furthermore, these findings were evaluated also *in vivo*, studying the inflammatory pain model induced by CFA injections in mice limb. Two days after CFA injection, when inflammatory-induced hypersensitivity in control mice was assessed, $GABA_AR$ stimulation increased mechanical allodynia and prevented mechanical hyperalgesia onset. cKO mice, indeed, were characterized by weaker increase in tactile sensitivity while showed a significant increase in the response to painful stimuli. Chronically, 4 weeks after CFA injections, control mice were characterized by a partial recovery from hypersensitization, while cKO mice completely recovered. cKO mice showed the same responsivity to all forces

applied (bot tactile and painful stimuli). This observation demonstrates that $GABA_AR$ play a role in the chronicization of inflammatory pain, prolonging the symptomatology.

To elucidate the mechanism underneath this phenomenon, we also tested nociceptive fibers conductance *ex vivo,* in all conditions previously studied *in vivo*. We observed that C-fibers are characterized by a slow adaptative process, that emerged in the acute phase, while became pronounced after 4 weeks from the inflammatory injury. At the chronic time point, control C-fibers showed a different slowing profile during firing, characterized by maintenance of lower threshold and increase in conductance velocity. This capability of C-fiber to follow high frequency could be the reason for the maintenance of high sensitivity to pain stimuli. In addition, those nerves were hypersensitive to GABA treatments. On the other hand, cKO mice showed an opposite modulation in C-fibers threshold during firing; such an effect was characterized by higher electrical threshold. This modulation might be responsible for the effective fast recovery from inflammatory injury observed in sns^{CRE}; β3 null mice.

Overall, our findings about $GABA_AR$ involvement in peripheral inflammatory pain modulation are in accordance with Prof. Jing Hu observations, that attributed to the presynaptic inhibition a crucial role for the behavioural pain outcomes. However, it should be underlined that in sns^{CRE}; β3 null mice the contribution of $GABA_AR$ along nociceptor axons or in primary afferent presynaptic site in spinal cord is barely discernible. We hypothesize that peripheral pain chronicization, following inflammatory injury, might be also attributed to the chloride modulation and $GABA_AR$ activity along axons, likely playing a complementary role in this complex process.

In conclusion, we hypothesized that $GABA_AR$ play a role not only in the physiological perception of pain, but also in allodynia as well as in hyperalgesia onset and chronicization.

Although, further experiments are needed to support this hypotesize, we believed that $GABA_AR$ regulates basal pain threshold, and participate in the phenomena of peripheral priming of nociceptor fibers and chronicization.

CHAPTER D.3

Pathological involvement of axonal $GABA_AR$ in sensory C-fibers axons:

2. Neuroactive steroid modulation of pain markers and $GABA_A$ activity

GABA-evoked axonal depolarization is reduced by activation of PKCε

As demonstrated in chapter 1 GABA mediated depolarization in C-fibers is enhanced by treatments with the neuroactive steroid ALLO. It should be underlined that $GABA_AR$ γ subunit (Moss SJ & Smart TG, 1996) may be phosphorylated by the ε isoform of Protein kinase C (PKCε), causing its desensitization. Importantly PKCε, in CNS, is modulated by inflammatory mediators. In this light, we evaluated the possible effect of PKCε activation on axonal $GABA_AR$ activity along unmyelinated C-fibers.

Exposure to activators of the PKCε isoform, resulted in a protracted reduction in the phasic component of axonal GABA responses, whereas the tonic component was not affected. In fact, axons were exposed to GABA 100μM for 2 min repeatedly at 7 min intervals, and under control conditions both phasic and tonic GABA responses did not desensitize over time (Figure 43.a). In presence of the selective PKCε activator DCP-LA 200μM we observed a gradual desensitization of the phasic axonal response to GABA (Figure 43.b; second exposure 22.82 % decrease, C.I. 95% 5.68-39.96, $p<0.01$; third 30.26 % decrease, C.I. 95% 13.12-47.40, $p<0.0001$; fourth 27.63 % decrease, C.I. 95% 9.56-45.70, $p<0.001$) suggesting either a time or activity-dependent mechanism of PKCε-mediated $GABA_A$-R phosphorylation. Wash-out of DCP-LA for 15 min allowed the partial recovery of the phasic GABA response (Figure 43.b & c). In contrast, the tonic axonal response to GABA was not affected by PKCε activation (Figure 43.d)

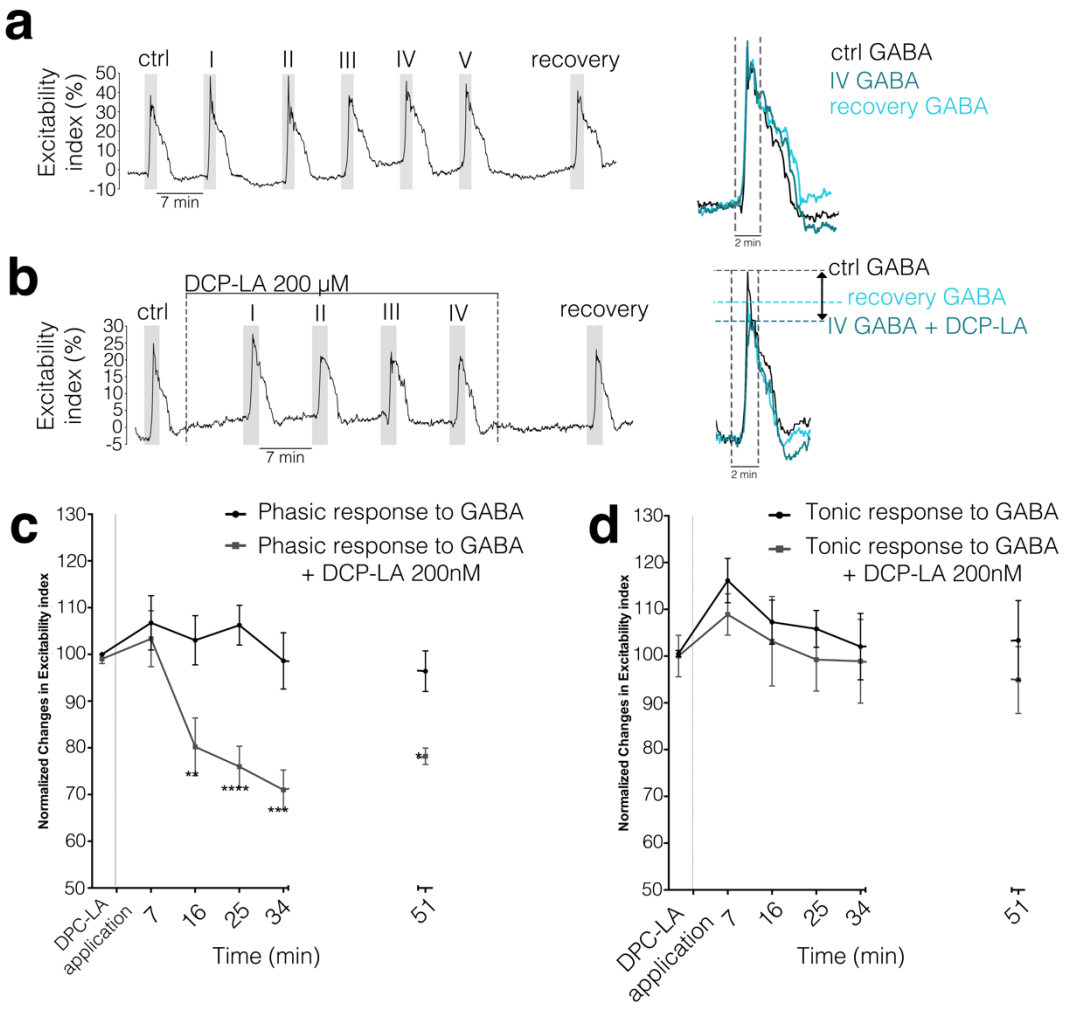

Figure 43. (a) *GABA treatments for 2 min, repeated every 7 min, evoked currents that remain stable; the recorded traces of these currents overlapped (see* ***a,*** *right panel).* ***(b)*** *The same repetition protocol was performed in presence of the specific PKCε activator DCP-LA, causing the inhibition of GABA-evoked depolarization and a partial recovery after 15min washout.* ***(c)*** *DPC-LA 200 nM caused specific phasic GABA response inhibition (two-way ANOVA test control vs. DCP-LA interaction p=0.0053, F (5.41)= 3.933; control vs DCP-LA factor p<0.0001, F (1.41)= 45.11), reducing 22.82% (C.I. 95% 5.68-39.96, p<0.01) following a second exposure; the reduction was of 30.26 % (C.I. 95% 13.12-47.40, p<0.0001) following a third exposure and a reduction of 27.63 % (C.I. 95% 9.56-45.70, p<0.001) following a fourth exposure (Sidak's multiple comparison test; data are mean ± s.e.m.).* ***(d)*** *The tonic response was not affected by this exposure (control vs DCP-LA interaction p=0.9857, F (5.73)= 0.1275; control vs DCL-LA factor p=0.1625, F (1.73)= 1.1991). Data are mean ± s.e.m.*

Peripheral neuronal PKCε is regulated by glial activity

Having established PKCε's ability to modulate GABA-evoked axonal depolarization in unmyelinated C-fibers, we further characterized its *in vitro* expression, in isolated DRG neurons and peripheral glia. We found high PKCε gene expression in DRG neurons,

compared to levels detected in SCs (Figure 44.a). IFL images confirmed that PKCε is located both in DRG neurons and SCs, and is evenly distributed throughout cytoplasm (Figure 44.b). Moreover, IFL showed prevalent activated PKCε localization in unmyelinated axons and surrounding non-myelinating SCs (Figure 44.b Double-labelling of PKCε with SMI32 (marker of high-density NF) confirmed the presence of phosphorylated and non-phosphorylated PKCε in unmyelinated axons, but also in SCs surrounding the myelinated fibers (Figure 44.c). These observations were confirmed in coronal section of sciatic nerve (Figure 44 c; magnification in right panels).

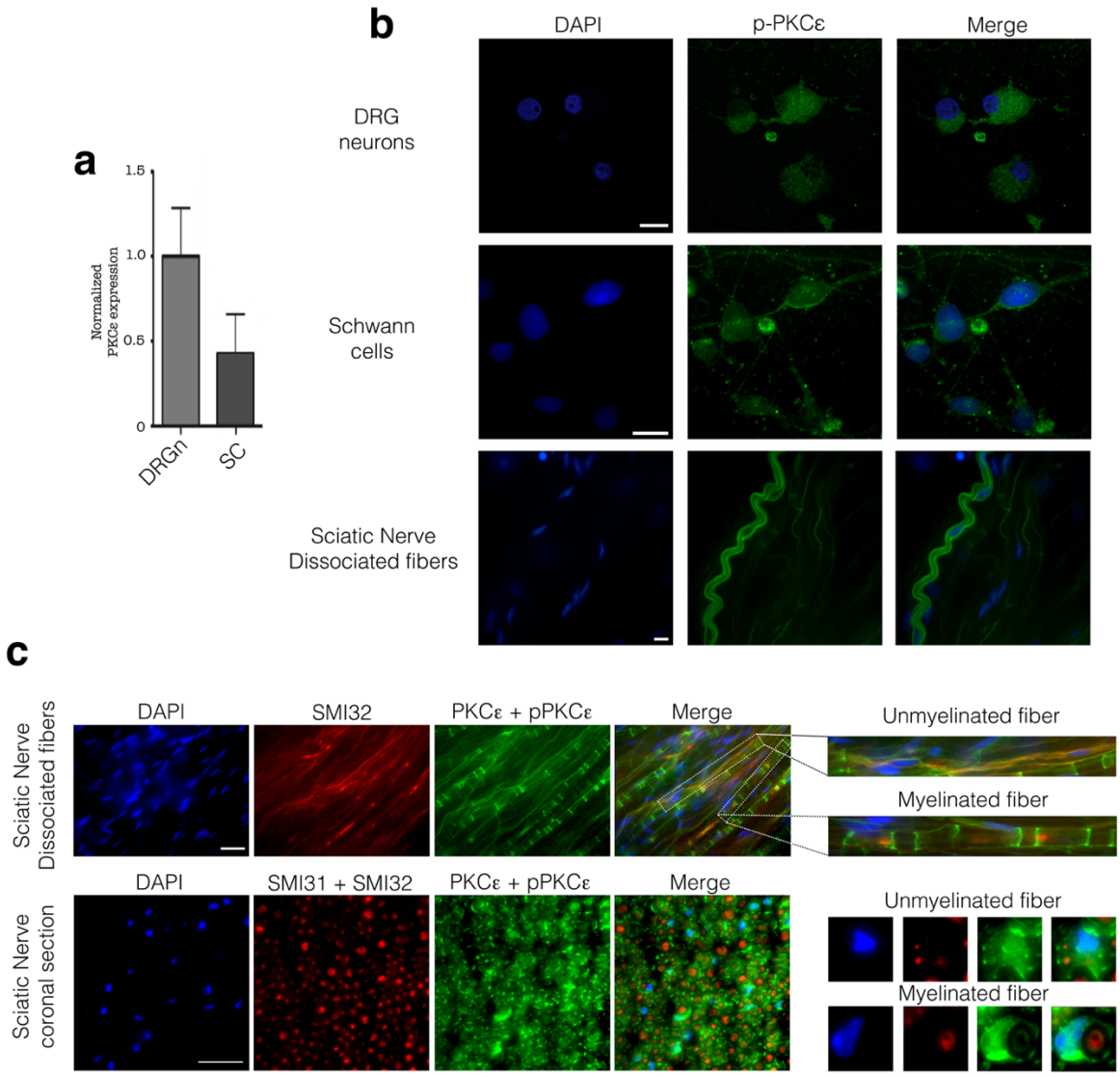

Figure 44. ***(a)*** *qRT-PCR analysis confirmed the presence of PKCε in DRG neurons and SC primary cultures,* ***(b)*** *IFL images demonstrated the presence of the active/phosphorylated form of PKCε in DRG neurons, SCs primary cultures and sciatic nerves dissociated fibers. p-PKCε immunopositivity was in green and dapi in blue. Bar 10 µm.* ***(c)*** *Co-labeling of PKCε (green) and neurofilament marker SMI32 (red), coupled with morphological analysis of myelinated and unmyelinated fibers, demonstrated the prevalence of immunopositive fibers in unmyelinated axons (yellow signal and absence of myelin structure), and confirmed the presence of PKCε in SCs (green signal and typical myelin structure). These observations were confirmed in coronal section of sciatic nerve (see also magnifications in right panels). Dapi in blue. Bar 20µm.*

To examine the possibility that ALLO might modulate neuronal PKCε, its expression was determined in DRG neurons following 24-h treatment with ALLO 1µM and found to be unaltered (Figure 45.a). However, when the conditioned medium (CM) from 24-h ALLO 1µM-treated SCs was applied to DRG neuron cultures for 24 h, PKCε gene expression was significantly ($p<0.01$) elevated (Figure 45.b), suggesting that a humoral mediator of glia-neuron cross-talk was able to regulate PKCε. IFL analysis showed that PKCε protein was increased in DRG neurons exposed to the ALLO CM from SCs (Figure 45.c).

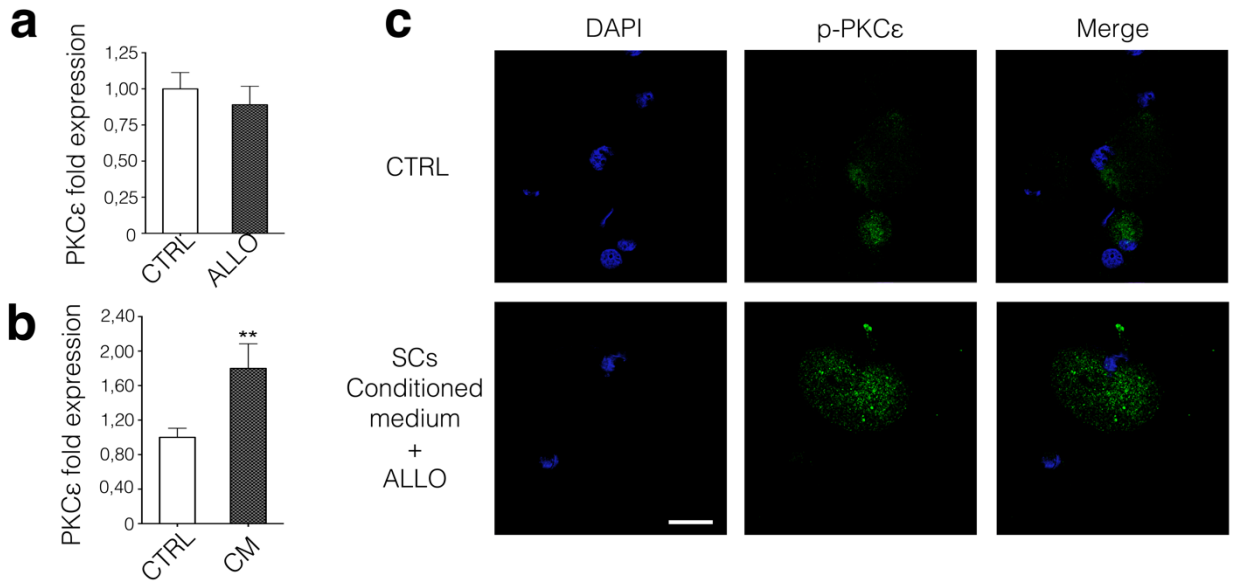

Figure 45. ***(a)*** *DRG neurons directly treated with ALLO (1µM) did not show PKCε expression modulation (CTRL n= 15, ALLO n=8; p=0,6284. The experiment was repeated 4 times. Data are mean ± s.e.m.)* ***(b)*** *but PKCε mRNA levels were upregulated by ALLO-treated SC's conditioned medium (p= 0,0040, t= 3,248, CTRL n=15, CM n =7 unpaired Student t-test. The experiment was repeated 3 times Data are mean ± s.e.m.).* ***(c)*** *IFL analysis confirmed the increase in PKCε signal intensity in DRG neurons treated with CM. p-PKCε immunopositivity was in green and dapi in blue. Bar 10 µm.*

BDNF released by SCs regulates neuronal PKCε activity

To identify the mediator responsible for the CM-induced effect, we focused our attention on the neurotrophin BDNF, previously shown to be released by activated SCs (Hanack C*, et al.,* 2015; Nguyen QA & Nicoll RA, 2018). Exposure of SC cultures to ALLO 1 µM showed a significant elevation of BDNF expression after 24h but not 2h of exposure (Figure 46.a; $p<0.05$). Accordingly, both pro-BDNF and mature BDNF protein levels increased significantly (Figure 46.b; $p<0.05$). Moreover, 24h CM treatment up-regulated the high affinity BDNF receptor trkB in cultured DRG neurons, corroborating the hypothesis of a BDNF-related mechanism (Figure 46.c).

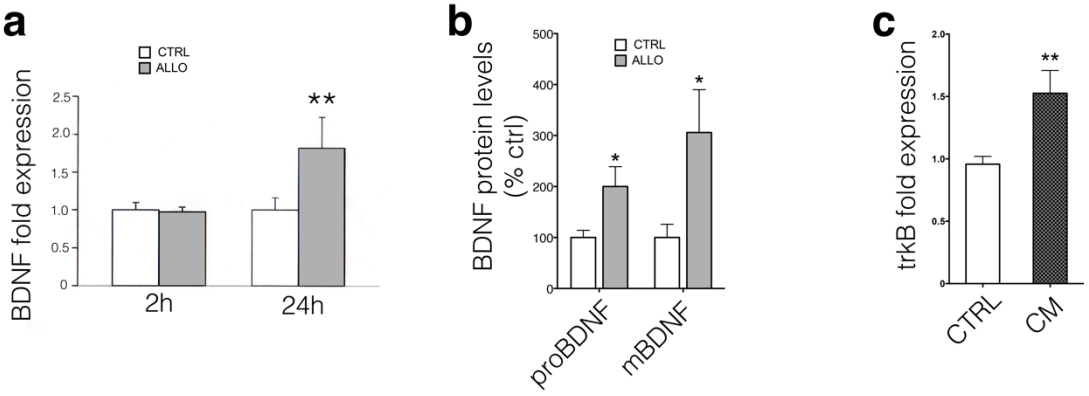

***Figure 46*. (a)** SCs treated with ALLO 1µM for 24h showed BDNF expression upregulation ($p=0.0034$, $t_)=3.52$, n=14 unpaired Student t-test. The experiment was repeated 4 times. Data are mean ± s.e.m.) **(b)** The western blot analysis confirmed the upregulation of proBDNF ($p=0.033$, $t=2.42$, n=12, unpaired Student t-test) and mature BDNF levels ($p=0.046$, $t=2.20$, n=13, unpaired Student t-test; The experiment was repeated 3 times. Data are mean ± s.e.m.) protein levels. (**c**) DRG neurons treated with SCs conditioned medium (CM) showed an up regulation of trkB receptor ($p=0.0012$, $t=3.556$, unpaired t test; CTRL n=21, CM n=12. The experiment was repeated 4 times. Data are mean ± s.e.m.)

IFL confirmed trkB activation in DRG neurons, with evidence of receptor translocation to the membrane (Fig. 47.b). To replicate the CM effects on PKCε levels in DRG neurons, we treated neurons directly with human recombinant BDNF, at 1pM and 1nM respectively.

BDNF 1nM significantly up-regulated PKCε gene expression ($p<0.05$) after 24-h exposure (Fig. 47.a).

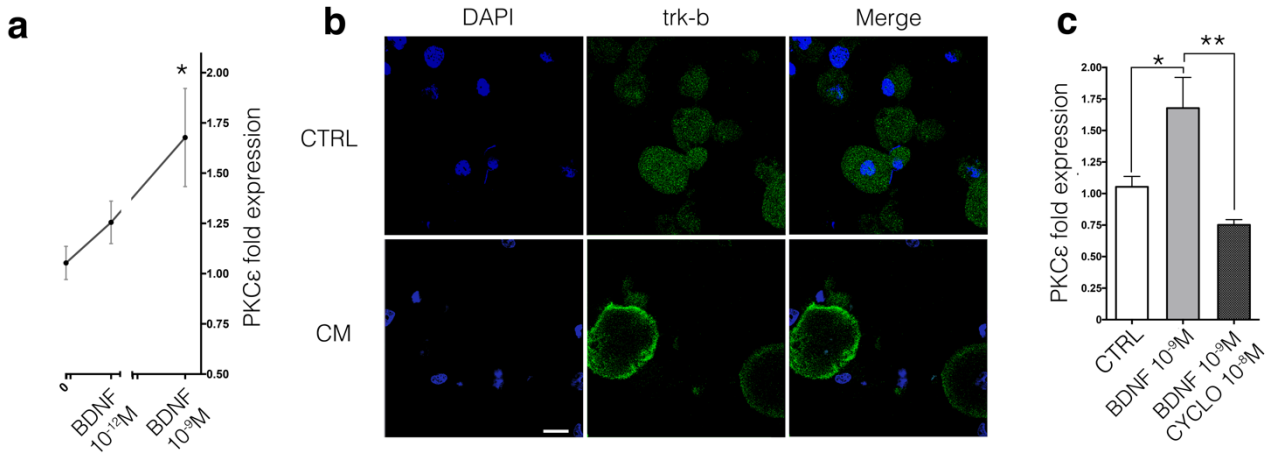

Figure 47. *(**a**) CM effect has been mimicked by exogenous human recombinant BDNF treatment (one-way ANOVA p=0.0144, F=4.762; Brown-Forsythe test p=0.0047, F (2.37) = 6.204; n=40; Tukey's multiple comparison test CTRL vs BDNF 10^{-9} M, p= 0.0108, q= 4.344. The experiment was repeated 4 times. Data are mean ± s.e.m.). **(b)** Furthermore CM induces translocation in the membrane of the specific BDNF receptor trk-b (trk-b labelled in green and DAPI in blue). **(c)** PKCε modulation mediated by exogenous BDNF was blocked by specific trkB antagonist CYCLO (one-way ANOVA p= 0.0016, F=7.972; Brown-Forsthe test p= 0.0017, F (2.31)= 7.909; n=34; Tukey's multiple comparison test CTRL vs BDNF 10^{-9} M p= 0.0115, q=4.362; BDNF 10^{-9} M vs BDNF 10^{-9} M+CYCLO p=0.0023, q= 5.240. The experiment was repeated 3 times. Data are mean ± s.e.m.).*

Data were strengthened by the IFL images. In DRG neurons treated transiently (30s) with BDNF 1nM, the phosphorylated form of PKCε was translocated to the membrane (Figure 48.a). Moreover, in support of a specific role of the trkB receptor, DRG neurons were co-treated with BDNF 1nM in presence of the specific trkB antagonist cyclotraxin-B (CYCLO) (Verheij M.M. et al., 2016). Qrt-PCR analysis showed that CYCLO 10nM was able to completely block the PKCε up-regulation induced by BDNF (Figure 48.c). Equally, CYCLO 10nM completely blocked the effect of CM on PKCε expression (Figure 48.a). As a control, the inactive form of CYCLO (TE) did not reverse the CM effect, confirming the specificity of the trkB antagonist (Figure 48.a). Overall, ALLO increased BDNF expression in SCs, which release leads to a trkB-mediated upregulation of PKCε in DRG neurons.

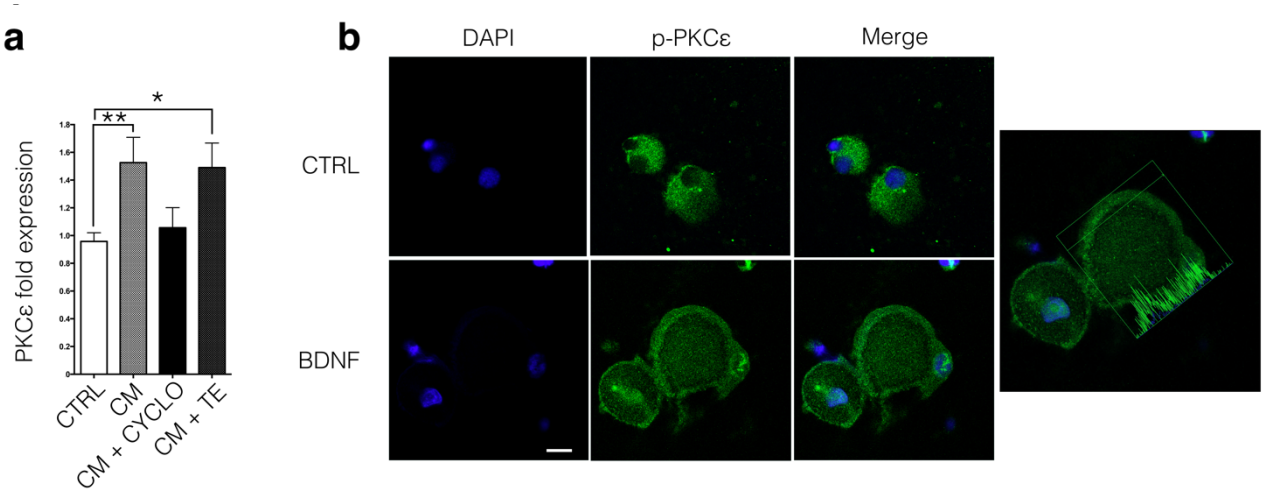

Figure 48. *(**a**) CYCLO treatment is also able to block CM action on DRG neurons (one-way ANOVA p=0.0024, Bartlett's test p=0.0252; n=49; Tukey's multiple comparison test CTRL vs CM p=0.0054; CTRL vs CM + CYCLO p=0.9507; CTRL vs CM + TE p=0.0307. The experiment was repeated 3 times. Data are mean ± s.e.m.). (**b**) Additionally, exogenous BDNF treatment caused a fast PKCε reorganization in DRG neurons, moving active-p-PKCε in the membrane. p-PKCε immunopositivity was in green and dapi in blue. Bar 10µm. Bar 10µm.*

In conclusion, we propose a new peripheral neuron-glial interaction pathway triggered by the neuroactive steroid ALLO. We demonstrated that ALLO is able to induce the synthesis of BDNF from SCs, targeting neuronal trkB receptor, then activating and upregulating PKCε. PKCε activation caused the inhibition of axonal $GABA_AR$ activity on C-fibers, modulating pain action potential propagation.

CHAPTER D.3 DISCUSSION

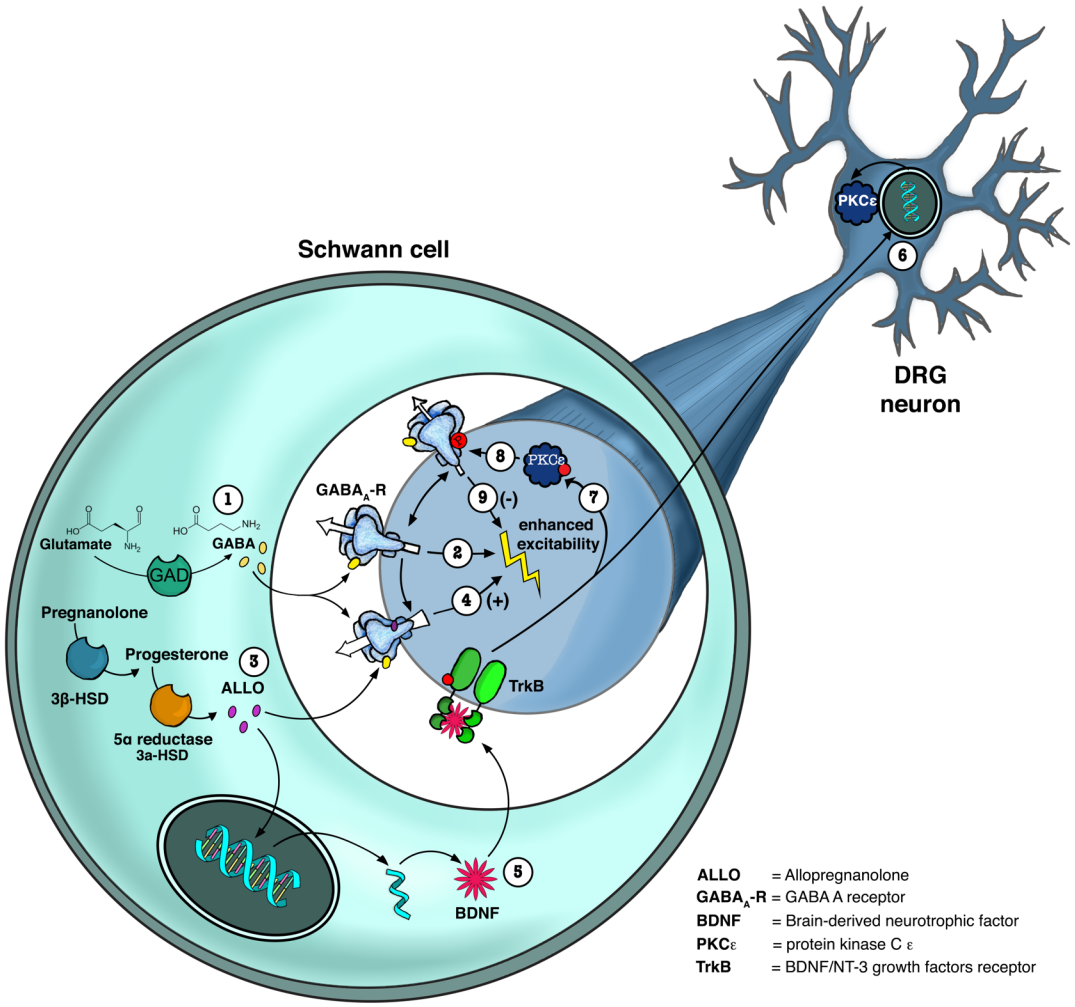

Figure 49. Schematic representation of neuron-glia cross-talk in peripheral afferent C-fibers via $GABA_A$-R. *In conclusion, we propose a cohesive picture illustrating SC-neuron interaction with C fibers involving autocrine/intracrine as well as paracrine mechanisms: SC-derived ALLO acutely sensitizes $GABA_A$-R increasing axonal excitability, while SC-derived BDNF leads to a paracrine effect that regulates GABA-evoked hyperactivity.* ***1****) SCs are able to synthesize GABA[14];* ***2****) GABA induces C-fibers depolarization, altering nociceptors threshold and conduction velocity through $GABA_A$ receptor;* ***3****) SCs synthesize ALLO;* ***4****) ALLO directly potentiates GABA effect on C-fibers;* ***5****) ALLO indirectly modulates BDNF expression and synthesis;* ***6****) BDNF induces enhancement in PKCε expression through trk-B mechanism;* ***7****) BDNF causes a fast activation of PKCε by phosphorylation and translocation in membrane;* ***8****) PKCε desensitizes $GABA_A$-R;* ***9****) PKCε activation causes selective desensitization of synaptic-like $GABA_A$R.*

A set of findings collected in the last decade demonstrated that glial GABA receptors, $GABA_A$R and $GABA_B$R, are involved in neuron glia interaction, maturation and myelination process of PNS (Faroni at al., 2010). In this last chapter we evaluate whether, other way

round, axonal $GABA_AR$ could be modulated by SC activity. In our laboratory we demonstrated that SCs are able to synthetize $GABA_AR$ agonists, such as GABA itself and the neuroactive steroid ALLO. Given the involvement of $GABA_AR$ in peripheral inflammatory pain, we focused the attention on the possible capability of SCs, via ALLO, to modulate a neuronal target involved in neuropathic pain, such as the protein kinase PKCε. We demonstrated that SC-derived ALLO acutely sensitizes $GABA_A$-R increasing axonal excitability, and autocrinally induces BDNF upregulation. SC-derived BDNF then leads to a paracrine effect, regulating GABA-evoked hyperexcitability.

We found that the allosteric $GABA_A$-R agonist ALLO directly potentiated axonal GABA currents, even at with inefficient GABA concentrations, which turn to be depolarizing in presence of ALLO. These data indicate that local allosteric action of ALLO is crucial to boost $GABA_A$-R mediated depolarization in axons. In this regard, we hypothesized that extracellular GABA concentration in nerves are comparable to the extracellular level found in the brain, whereas the ambient GABA was generally estimated in the range nanomolar to few micromolar (Lerma J. et al., 1986; Tossman U. et al., 1986; Kennedy R.T. et al., 2002). Notably, GABA synthesized by SCs may attain efficient concentration in the narrow space between SC membrane and axons, both in myelinated (i.e. in the periaxonal/adaxonal space) and/or unmyelinated fibers (i.e. Remak bundles).

The possible cellular pathways activated by ALLO in neuron-SC interaction were then investigated. We found that ALLO action is dependent by SCs signaling pathway activation, involving BDNF release, neuronal PKCε up-regulation and phosphorylation. In accordance, ALLO-induced BDNF synthesis and release has been previously demonstrated in CNS areas (Naert G. et al., 2007; reviewed in Nin M.S. et al., 2011).

The cross-talk regulating SC and DRG neurons might affect a subset of C fibers expressing trkB (Wetmore C and Olson L. , 1995; Salio C. et al., 2005; Matsumoto I. et al., 2001; Kashiba H. et al., 2003 ; Farbman Al. et al., 2004; Ichikawa H. et al., 2006, 2007). PKCε is generally known to be involved in $GABA_A$-R desensitization. Namely, PKCε phosphorylates the γ2 subunit of $GABA_A$-R (frequently present in synaptic isoforms and that we demonstrate to be mainly expressed along C-fibers axons) reducing its response to specific ligands (Hodge C.W. et al., 2002). Moreover, PKCε regulates also $GABA_A$R trafficking, decreasing its cell surface localization and GABA currents (Chou W.H. et al., 2010). Interestingly, the observed phasic response associated to $GABA_A$R currents, triggered by initial chloride gradient, was selectively inhibited by PKCε activation in C-fibers, corroborating our previous observation performed on cortical neurons (Puia G. et al., 2015). Furthermore, PKCε induced an activity-dependent desensitization of $GABA_A$R, providing evidences for the dynamical regulation of C-fiber excitability.

In conclusion, we propose a cohesive picture illustrating SC-neuron interaction in sensory C fibers (Figure 49), involving autocrine/intracrine as well as paracrine mechanisms. $GABA_A$R, expressed and active along axons, proved to be responsible for the modulation of C fibers conductance and targeted by glial humoral factors. SC-derived ALLO acutely sensitizes $GABA_A$-R, increasing axonal excitability, while SC-derived BDNF leads to a paracrine effect that regulates GABA-evoked hyperexcitability. Overall, $GABA_A$-R activity and its dynamic regulation in C-fiber highlight the contribution of peripheral exogenous challenges to the central interpretation of noxious signals.

CONCLUSIONS

The pathogenesis of neuropathic pain and the mechanisms regulating its chronicization are still not fully elucidated. Consequently, from a clinical point of view, the therapies currently applied to patients are more focused on the treatment of symptomatology, rather than to the identification of the molecular mechanisms for novel pharmacologic strategies. Therefore, current therapies are solely aimed to increase the quality of life and to reduce the sensitization process, normally occurring in the progression of the disease. Hence, the identification of novel and promising drugs represents a medical need in the field of chronic neuropathic pain.

In this light, in order to identify new pharmacological targets for the therapy of chronic pain, it was necessary to first investigate nociception under physiological condition, with the aim to identify new suitable molecular pathways for pharmacological approach. Furthermore, these findings established the basis to study the impact of these molecular pathways on the onset and evolution of chronic pain during pathological conditions.

In this PhD thesis, we focused our studies on the characterization of peripheral GABAergic system, primarily on $GABA_AR$, which is one of the most promising candidate target for the comprehension of the pathogenesis of chronic pain. GABAergic signalling, indeed, was studied along peripheral nociceptive axons, evaluating its putative role in the modulation of pain threshold and conduction velocity during different physio-pathological conditions.

We demonstrated that $GABA_AR$ is present and functional along unmyelinated peripheral axons and that mediates outward depolarizing Cl^- currents. Furthermore, we found that the prevalent axonal $GABA_AR$ subtype in peripheral DRG neurons is the synaptic form, composed by $\alpha2\beta3\gamma2$ subunits, characterized by fast kinetic and low sensitivity to GABA and benzodiazepines. Interestingly, GABA depolarizing currents were strongly modulated by the fiber activity state. Indeed, GABA responses were increased during and after firing of C-

fibers, modulating their conduction velocity and excitability level. Endogenous activation of $GABA_AR$ induced reduction in the conduction speed loss, that occur physiologically in unmyelinated fibers during sustained activity. Therefore, GABAergic transmission in axons increases conduction speed, stabilizing C-fiber conduction of action potential during firing. We demonstrated that the activity-dependent increase in GABAergic currents is mediated by the modulation of the NKCC1 transporter, that generate an increase in the intra-axonal Cl^- concentration and consequently in Cl^- gradient. We then hypothesized that $GABA_AR$ might be tonically activated by endogenous ligands and that, changes in C-fibers activity, dynamically modulates the intensity of Cl^- fluxes crossing through the receptor. Based on this hypothesis, we suggested that Cl^- fluxes through $GABA_AR$ might represent a kind of stabilizing currents, that ensure an efficient action potential conduction during sustained activity of nociceptors. In fact, nociceptors are formed by unmyelinated fibers, which poorly sustain high frequency stimulation during firing. Thereby, GABA currents might support fasted conduction of action potential.

The $GABA_AR$-mediated modulation of axonal conduction speed and excitability contributes to the behavioural decrease in pain threshold. In fact, mice lacking the $GABA_AR$ β3 subunit selectively in nociceptors, were characterized by higher threshold to mechanical pain stimuli. This *in vivo* modulation of pain sensitivity might results from the combination of two different changes of $GABA_AR$ receptors in DRG neurons. $GABA_AR$, in fact, can modulate the axonal conduction of action potential, but it is also present in primary afferent of the spinal cord, whereas it forms synaptic contact with inhibitory interneurons and mediates pre-synaptic inhibition.

To study selectively the peripheral contribution of GABAergic modulation on pain, we compared *in vivo* behavioural tests with *ex vivo* CAP recordings from peripheral nerves.

Based on this approach, we studied the role of GABAergic transmission also *in vivo,* in an inflammatory pain model. We demonstrated that $GABA_AR$ increases the intensity of allodynia and prevent the onset of hyperalgesia. Our observations suggest that during inflammation, an excessive activation of GABAergic system induces pain hypersensitivity and additional prolongation of recovery phase. This suggests the putative role $GABA_AR$ also in the chronicization process of inflammatory pain.

Lastly, our studies highlighted the concept that the axonal $GABA_ARs$ represent a target of local neuron-glia interaction. Peripheral unmyelinated axons, in fact, are in very close contact with the glial SCs, able to synthetize $GABA_AR$ agonist such as GABA itself and the NS ALLO. We then hypothesize that SCs might be the main sources of endogenous GABA, releasing the neurotrasmitter in the narrow space between the axon and the adaxonal membrane formed by SCs. In addition, we observed that SCs can modulate $GABA_AR$ activity state through a paracrine mechanism, releasing the neurotrophic factor BDNF. This alternative mechanism may activate the ε isoform of PKC, then able to desensitize $GABA_AR$ through phosphorylation. In detail, treating SCs with the NS ALLO, we observed the increase in BDNF synthesis, that in turn may increase the PKCε expression and activation in neurons, *via* trkB mediated mechanism. Then, neuronal PKCε could phosphorylate the $GABA_AR$, causing its desensitization and limiting its modulation on nociceptive axons.

Altogether, the results presented in this thesis point out the role of $GABA_AR$ in the regulation of the conduction of noxious stimuli from the periphery to the CNS, either in physiological or in pathological condition. Namely, $GABA_AR$-mediated currents proved able to stabilize peripheral nociceptive axons in physiological condition, promoting the efficient conduction of action potential. Similarly, $GABA_AR$-mediated currents, participate in promoting hypersensitivity and chronicization of pain in phatological conditions. Interestingly, SCs

capability to activate and modulate axonal $GABA_AR$ might represent a new and very promising pharmacological target, for future studies focused on the identification local therapeutic strategies for the peripheral neuropathies and associated chronic pain.

ABBREVIATION list

3α-HSD: 3a-hydroxysteroid oxidoreductase

ALLO: Allopregnanolone

Best1: Bestrophin 1 anion channel

BMP: bone morphogenic protein

CAP: compound action potential

CFA: complete Freund's adjuvant

cKO: conditional knock down

CM: conditioned medium

CNS: central nervous system

CYCLO: cyclotraxin-B

DAG: diacylglycerol

DHP: dihydroprogesterone

DRG: dorsal root ganglion

FGF: fibroblast growth factor

GABA-T: GABA transaminase

GABA: γ-amino butyric acid

$GABA_AR$: $GABA_A$ receptor

$GABA_BR$: $GABA_B$ receptor

GAD: glutamic acid decarboxylase

GAT: GABA transporter

GPCRs: G-protein coupled receptors

HDAC: histone deacetylases

NRG-1: neuregulin-1

PKC: Protein kinase C

PLC: phospholipase C

PNS: peripheral nervous system

PR: progesterone receptor

RACKs: receptors for activated C-kinase

SCs: Schwann cells

THDOC: allotetrahydrodeoxycorticosterone

THIP: gaboxadol

THP: 5a-pregnan-3a-ol-20-one

TRP: transient receptor potential

TRPV1: transient receptor potential Vanilloid 1

TSPO: translocator protein

$V_{eq.}$: equilibrium potential

V_m: Voltage membrane

WDR: wide dynamic ran

REFERENCES

- Abramian AM, Comenencia-Ortiz E, Vithlani M, Tretter EV, Sieghart W, Davies PA, and Moss SJ (2010) Protein kinase C phosphorylation regulates membrane insertion of GABAA receptor subtypes that mediate tonic inhibition. J Biol Chem 285:41795–41805.
- Adam MP, Ardinger HH, Pagon RA, et al., editors. Seattle (WA): University of Washington, Seattle; 1993-2019.Congenital Insensitivity to Pain Overview Copyright © 1993-2019, University of Washington, Seattle. GeneReviews is a registered trademark of the University of Washington, Seattle. All rights reserved.
- Adrian ED, Zotterman Y (1926). "The impulses produced by sensory nerve endings: Part II: The response of a single end organ". J Physiol. 61 (2): 151 171. doi:10.1113/jphysiol. (1926).

  sp002281. PMC 1514782. PMID 16993780.
- Agarwal N., S. Offermanns, R. Kuner, Conditional gene deletion in primary nociceptive neurons of trigeminal ganglia and dorsal root ganglia. Genesis 38, 122-129 (2004).
- Akaike N, Inomata N & Tokutomi N. (1987). Contribution of chloride shifts to the fade of gamma-aminobutyric acid-gated currents in frog dorsal root ganglion cells. J Physiol 391, 219-234.
- Al-Chaer ED, Lawand NB, Westlund KN, Willis WD. 1996. Visceral nociceptive input into the ventral posterolateral nucleus of the thalamus: a new function for the dorsal column pathway. J Neurophysiol 76:2661–2674.
- Aley KO, Martin A, McMahon T, Mok J, Levine JD, Messing RO. Nociceptor sensitization by extracellular signal-regulated kinases. J Neurosci 2001;21:6933–9.
- Amadesi S, Cottrell GS, Divino L, Chapman K, Grady EF, Bautista F, Karanjia R, Barajas-Lopez C, Vanner S, Vergnolle N, Bunnett NW. Protease-activated receptor 2 sensitizes TRPV1 by protein kinase Cepsilon- and A-dependent mechanisms in rats and mice. J Physiol. 2006; 575:555– 571. [PubMed: 16793902]
- Andersen P, Eccles JC, Loyning Y. Pathway of postsynaptic inhibition in the hippocampus. J Neurophysiol 27: 608–619, 1964.

- Aur D., Jog, MS., 2010 Neuroelectrodynamics: Understanding the brain language, IOS Press, 2010. doi:10.3233/978-1-60750-473-3-i
- Aur, D.; Connolly, C.I.; Jog, M.S. (2005). "Computing spike directivity with tetrodes". Journal of Neuroscience Methods. 149 (1): 57–63. doi:10.1016/j.jneumeth.2005.05.006. PMID 15978667.
- Bannai H, Lévi S, Schweizer C, Inoue T, Launey T, Racine V, Sibarita JB, Mikoshiba K, Triller A. Activity-dependent tuning of inhibitory neurotransmission based on GABAAR diffusion dynamics. Neuron. 2009 Jun 11;62(5):670-82. doi: 10.1016/j.neuron.2009.04.023.
- Barchi RL. Myotonia. An evaluation of the chloride hypothe- sis. Arch Neurol 32: 175–180, 1975. doi:10.1001/archneur.1975.00490450055007.
- Bardoni R. et al., Pre- and postsynaptic inhibitory control in the spinal cord dorsal horn. Ann N Y Acad Sci 1279, 90-96 (2013).
- Barker JL, Behar T, Li YX, Liu QY, Ma W, Maric D, Maric I, Schaffner AE, Serafini R, Smith SV, Somogyi R, Vautrin JY, Wen XL, Xian H. GABAergic cells and signals in CNS development. Perspect Dev Neurobiol 5: 305–322, 1998.
- Baulieu EE (1981) Steroid hormones in the brain: several mechanisms?, in Steroid Hormone Regulation of the Brain (Fuxe F, Gustafsson JA, and Wetterberg L eds) pp 3–14, Pergamon Press, Oxford.
- Belelli D, Lambert JJ (2005) Neurosteroids: endogenous regulators of the GABA(A) receptor Nat Rev Neurosci 6(7):565-75.
- Belelli, D., Pistis, M., Peters, J.A., Lambert, J.J., 1999. General anaesthetic action at transmitter-gated inhibitory amino acid receptors. Trends Pharmacol. Sci. 20, 496–502.
- Ben-Ari Y, Holmes GL. The multiple facets of gamma-aminobutyric acid dysfunction in epilepsy. Curr Opin Neurol 18: 141–145, 2005.
- Ben-Ari Y., Excitatory actions of gaba during development: the nature of the nurture. Nat Rev Neurosci 3, 728-739 (2002).
- Ben-Ari Y., Jean-Luc Gaiarsa, Roman Tyzio, And Rustem Khazipov. GABA: A Pioneer Transmitter That Excites Immature Neurons and Generates Primitive Oscillations. Physiol Rev 87: 1215–1284, 2007; doi:10.1152/physrev.00017.2006.
- Bhisitkul RB, Villa JE, & Kocsis JD (1987) Axonal GABA receptors are selectively present on normal and regenerated sensory fibers in rat peripheral nerve. Exp Brain Res 66(3):659-663.
- Bhisitkul RB., J. E. Villa, J. D. Kocsis, Axonal GABA receptors are selectively present on

normal and regenerated sensory fibers in rat peripheral nerve. Exp Brain Res 66, 659-663 (1987).

- Bianchi MT and Macdonald RL (2002) Slow phases of GABA(A) receptor desensitization: structural determinants and possible relevance for synaptic function. J Physiol 544:3–18.
- Bianchi, M.T., Haas, K.F., Macdonald, R.L., 2002.a1 anda6 subunits specifydistinct desensitization, deactivation and neurosteroid modulation of GABAAreceptors containing thedsubunit. Neuropharmacology 43,492–502.
- Bogdanov Y, Michels G, Armstrong-Gold C, Haydon PG, Lindstrom J, Pangalos M, Moss SJ. Synaptic GABAA receptors are directly recruited from their extrasynaptic counterparts. EMBO J. 2006 Sep 20;25(18):4381-9.
- Bogen, O., Alessandri-Haber, N., Chu, C., Gear, R.W., Levine, J.D. (2012). Generation of a pain memory in the primary afferent nociceptor triggered by PKCepsilon activation of CPEB. JNeurosci 32, 2018-2026.
- Bowery NG. et al., Indirect effects of amino-acids on sympathetic ganglion cells mediated through the release of gamma-aminobutyric acid from glial cells. Br J Pharmacol 57, 73-91 (1976).
- Boyd IA, Davey MR. 1968. Composition of Peripheral Nerves. Edinburgh: Livingston.
- Brain-derived neurotrophic factor-immunoreactive primary sensory neurons in the rat trigeminal ganglion and trigeminal sensory nuclei. Brain Res. 2006 Apr 7;1081(1):113-8. Epub 2006 Feb 28.
- Brandon NJ, Delmas P, Kittler JT, McDonald BJ, Sieghart W, Brown DA, Smart TG, and Moss SJ (2000) GABAA receptor phosphorylation and functional modulation in cortical neurons by a protein kinase C-dependent pathway. J Biol Chem 275: 38856–38862.
- Braz J, Solorzano C, Wang X, Basbaum AI. Transmitting pain and itch messages: a contemporary view of the spinal cord circuits that generate gate control. Neuron 2014, 82: 522–536.
- Brodsky MC (2016). Pediatric Neuro-Ophthalmology. Springer. p. 741. ISBN 978-1493933846. Retrieved April 13, 2017.
- Brown DA & Marsh S (1978) Axonal GABA-receptors in mammalian peripheral nerve trunks. Brain Res 156(1):187-191.
- Brumback AC & Staley KJ (2008) Thermodynamic regulation of NKCC1-mediated Cl- cotransport underlies plasticity of GABA(A) signaling in neonatal neurons. J Neurosci 28(6):1301-1312.

- Bryant SH, Conte-Camerino D. Chloride channel regulation in the skeletal muscle of normal and myotonic goats. Pflugers Arch 417: 605–610, 1991. doi:10.1007/BF00372958.
- Bullock, TH; Orkand, R; Grinnell, A (1977). Introduction to Nervous Systems. A series of books in biology. San Francisco: W. H. Freeman. ISBN 978-0-7167-00302. LCCN 76003735. OCLC 2048177.
- Butts DA, Weng C, Jin J, et al. (September 2007). "Temporal precision in the neural code and the timescales of natural vision". Nature. 449 (7158): 92 5. Bibcode:2007Natur.449...92B. doi:10.1038/ nature06105. PMID 17805296.
- Cairns SP, Ruzhynsky V, Renaud JM. Protective role of extra- cellular chloride in fatigue of isolated mammalian skeletal muscle. Am J Physiol Cell Physiol 287: C762–C770, 2004. doi:10.1152/ajpcell.00589.2003.
- Callachan H, Cottrell GA, Hather NY, Lambert JJ, Nooney JM, Peters JA (1987) Modulation of the GABAA receptor by progesterone metabolites Proc R Soc Lond B Biol Sci 231(1264):359-69.
- Cameron HA, Hazel TG, McKay RD. Regulation of neurogenesis by growth factors and neurotransmitters. J Neurobiol 36: 287–306, 1998.
- Cang CL, Zhang H, Zhang YQ, Zhao ZQ. PKCepsilon-dependent potentiation of TTX-resistant Nav1.8 current by neurokinin-1 receptor activation in rat dorsal root ganglion neurons. Mol Pain 2009;5:33.
- Carlton SM, Zhou S, Coggeshall RE. Peripheral GABA(A) receptors: evidence for peripheral primary afferent depolarization. Neuroscience. 1999;93(2):713 –722. doi: 10.1016/S0306-4522(99)00101-3.
- Carr RW, Sittl R, Fleckenstein J, & Grafe P (2010) GABA increases electrical excitability in a subset of human unmyelinated peripheral axons. PLoS One 5(1):e8780.
- Carver CM, Reddy DS (2013) Neurosteroid interactions with synaptic and extrasynaptic GABA(A) receptors: regulation of subunit plasticity, phasic and tonic inhibition, and neuronal network excitability Psychopharmacology (Berl) 230(2):151-88.
- Carver CM, Wu X, Gangisetty O, and Reddy DS. (2014) Perimenstrual-like hormonal regulation of extrasynaptic δ-containing GABAA receptors mediating tonic inhibition and neurosteroid sensitivity. J Neurosci 34:14181–14197.
- Caterina MJ, Leffler A, Malmberg AB, Martin WJ, Trafton J, Petersen-Zeitz KR, Koltzenburg M, Basbaum AI, Julius D. Impaired nociception and pain sensation

- Chen JT, Guo D, Campanelli D, Frattini F, Mayer F, Zhou L, Kuner R, Heppenstall PA, Knipper M & Hu J. (2014). Presynaptic GABAergic inhibition regulated by BDNF contributes to neuropathic pain induction. Nat Commun 5, 5331.
- Chou WH., D. Wang, T. McMahon, Z. H. Qi, M. Song, C. Zhang, K. M. Shokat, R. O. Messing, GABAA receptor trafficking is regulated by protein kinase C(epsilon) and the N-ethylmaleimide-sensitive factor. J Neurosci 30, 13955-13965 (2010).
- Clausen T, Nielsen OB. Potassium, Na^+ ,K^+ - pumps and fa- tigue in rat muscle. J Physiol 584: 295–304, 2007. doi:10. 1113/jphysiol.2007.136044.
- Coonan JR, Lamb GD. Effect of transverse-tubular chloride conductance on excitability in skinned skeletal muscle fibres of rat and toad. J Physiol 509: 551–564, 1998. doi:10.1111/ j.1469-7793.1998.551bn.x.
- Corell M. et al., GABA and its B-receptor are present at the node of Ranvier in a small population of sensory fibers, implicating a role in myelination. Journal of Neuroscience Research 93, 285-295 (2015).
- Coulter DA and Carlson GC (2007) Functional regulation of the dentate gyrus by GABA-mediated inhibition. Prog Brain Res 163:235–243.
- Craig AD. 2002. How do you feel? Interoception: the sense of the physiological condition of the body. Nat Rev Neurosci 3:655–666.
- Craig AD. 2004. Lamina I, but not lamina V, spinothalamic neurons exhibit responses that correspond with burning pain. J Neurophysiol 92:2604–2609.
- Cramer SW, Baggot C, Cain J et al. The role of cation-dependent chloride transporters in NP following spinal cord injury. Mol Pain. 2008;4:36–44.
- Crandall M, Kwash J, Yu W, White G. Activation of protein kinase C sensitizes human VR1 to capsaicin and to moderate decreases in pH at physiological temperatures in Xenopus oocytes. Pain. 2002; 98:109–117. [PubMed: 12098622]
- Curtis DR, Lodge D, Brand SJ. GABA and spinal afferent terminal excitability in the cat. Brain Res. 1977;130(2):360–363. doi: 10.1016/0006-8993(77)90283-9.
- Darman RB, Forbush B. A regulatory locus of phosphorylation in the N terminus of the Na-K-Cl cotransporter, NKCC1. J Biol Chem. 2002;277:37542–37550.
- Davis JB, Gray J, Gunthorpe MJ, Hatcher JP,

Davey PT, Overend P, Harries MH, Latcham J, Clapham C, Atkinson K, Hughes SA, Rance K, Grau E, Harper AJ, Pugh PL, Rogers DC, Bingham S, Randall A, Sheardown SA. Vanilloid receptor-1 is essential for inflammatory thermal hyperalgesia. Nature. 2000; 405:183–187. [PubMed: 10821274]

- Dayan, Peter; Abbott, L. F. (2001). Theoretical Neuroscience: Computational and Mathematical Modeling of Neural Systems. Massachusetts Institute of Technology Press. ISBN 978-0-262-04199-7.
- De Col R, Messlinger K, & Carr RW (2008) Conduction velocity is regulated by sodium channel inactivation in unmyelinated axons innervating the rat cranial meninges. J Physiol 586(4):1089-1103.
- De Col R, Messlinger K, & Carr RW (2012) Repetitive activity slows axonal conduction velocity and concomitantly increases mechanical activation threshold in single axons of the rat cranial dura. J Physiol 590(4):725-736.
- de Paoli FV, Broch-Lips M, Pedersen TH, Nielsen OB. Rela- tionship between membrane $Cl^{?}$ conductance and contrac- tile endurance in isolated rat muscles. J Physiol 591: 531–545, 2013. doi:10.1113/jphysiol.2012.243246.
- Deisz RA, Lux HD. The role of intracellular chloride in hyperpolarizing post-synaptic inhibition of crayfish stretch receptor neurones. J Physiol 326: 123–138, 1982.
- Delpire E, Austin TM. Kinase regulation of the Na-K-2Cl cotransporter in primary afferent neurons. J Physiol. 2010;588:3365–3373.
- Delpire E. Cation-chloride cotransporters in neuronal communication. News Physiol Sci 15: 309–312, 2000.
- Deschenes M, Feltz P, Lamour Y. A model for an estimate in vivo of the ionic basis of presynaptic inhibition: an intracellular analysis of the GABA-induced depolarization in rat dorsal root ganglia. Brain Res 118: 486–493, 1976. DOI: 10.1126/science.1184334originally published online September 23, (2010)
- Drasbek KR and Jensen K (2006) THIP, a hypnotic and antinociceptive drug, enhances an extrasynaptic GABAA receptor-mediated conductance in mouse neocortex. Cereb Cortex 16:1134–1141.
- Du X. et al., Local GABAergic signaling within sensory ganglia controls peripheral nociceptive transmission. J Clin Invest 127, 1741-1756 (2017).
- Dutka TL, Murphy RM, Stephenson DG, Lamb GD. Chloride conductance in the transverse tubular system of rat skeletal muscle fibres:

importance in excitation-contraction coupling and fatigue. J Physiol 586: 875–887, 2008. doi:10.1113/ jphysiol.2007.144667.

- Dzhala VI, Talos DM, Sdrulla DA, Brumback AC, Mathews GC, Benke TA, Delpire E, Jensen FE, Staley KJ. NKCC1 transporter facilitates seizures in the developing brain. Nat Med 11: 1205–1213, 2005.
- Eccles JC, Llinas R, Sasaki K. The inhibitory interneurones within the cerebellar cortex. Exp Brain Res 1: 1–16, 1966.
- Eccles JC. The development of the cerebellum of vertebrates in relation to the control of movement. Naturwissenschaften 56: 525–534, 1969.
- Eccles JC. The ionic mechanisms of excitatory and inhibitory synaptic action. Ann NY Acad Sci 137: 473–494, 1966.
- Edlund T, Jessell TM. Progression from extrinsic to intrinsic signaling in cell fate specification: a view from the nervous system. Cell 96: 211–224, 1999.
- Kandel ER, James H. Schwartz, Thomas M. Jessell, Steven A. Siegelbaum, A. J. Hudspeth- Principles of Neural Science, Fifth Edition- McGraw-Hill Professional (2013)
- Erlander MG, Tillakaratne NJ, Feldblum S, Patel N, Tobin AJ (1991) Two genes encode distinct glutamate decarboxylases Neuron 7(1):91-100.
- Essrich C., M. Lorez, J.A. Benson, J.M. Fritschy and B. Luscher. Postsynaptic clustering of major GABAA receptor subtypes requires the gamma 2 subunit and gephyrin. Nat. Neurosci., 1 (1998), pp. 563-571
- Fagan, Tom (2003). "Glial Cells Critical for Peripheral Nervous System Health". News from Harvard Medical, Dental and Public Health Schools.
- Farbman AI[1], Brann JH, Rozenblat A, Rochlin MW, Weiler E, Bhattacharyya M. Developmental expression of neurotrophin receptor genes in rat geniculate ganglion neurons. J Neurocytol. 2004 May;33(3):331-43.
- Faroni A, et al. (2019) GABA-B1 Receptor-Null Schwann Cells Exhibit Compromised In Vitro Myelination. Mol Neurobiol 56(2):1461-1474.
- Faroni A., Magnaghi V., The neurosteroid allopregnanolone modulates specific functions in central and peripheral glial cells. Front Endocrinol (Lausanne) 2, 103 (2011).
- Farrant, M., and Nusser,Z. (2005).Variations on an inhibitory theme: phasic and tonic activation of GABAA receptors. Nat.Rev.Neurosci. 6,215–229.
- Farrar,S.J., Whiting,P.J., Bonnert, T.P.,and Mc Kernan,R.M.(1999). Stoichiometry of aligand-

gate dion channel determined by fluorescence energy transfer. J. Biol.Chem. 274,10100–10104.

- Fein, A Nociceptors: the cells that sense pain
- Ferrari, L.F., Araldi, D., Levine, J.D. (2015). Distinct terminal and cell body mechanisms in the nociceptor mediate hyperalgesic priming. J Neurosci 35, 6107-6116.
- Fink R, Lüttgau HC. An evaluation of the membrane constants and the potassium conductance in metabolically exhausted muscle fibres. J Physiol 263: 215–238, 1976. doi:10.1113/jphysiol. 1976.sp011629.
- French CR, Sah P, Buckett KJ, Gage PW. A voltage-dependent persistent sodium current in mammalian hippocampal neurons. J Gen Physiol 95: 1139–1157, 1990.
- Fritschy JM. and I. Brunig. Formation and plasticity of GABA-ergic synapses: physiological mechanisms and pathophysiological implications. Pharmacol. Ther., 98 (2003), pp. 299-323
- Fukuda A, Muramatsu K, Okabe A, Shimano Y, Hida H, Fujimoto I, Nishino H. Changes in intracellular Ca2_ induced by GABAA receptor activation and reduction in Cl_ gradient in neonatal rat neocortex. J Neurophysiol 79: 439–446, 1998.
- Funk K, et al. (2008) Modulation of chloride homeostasis by inflammatory mediators in dorsal root ganglion neurons. Mol Pain 4:32.
- Gao XB, van den Pol AN. GABA release from mouse axonal growth cones. J Physiol 523: 629–637, 2000.
- Gold MS. Molecular biology of sensory transduction. In: McMahon SB, Koltzenburg M, Tracey I, Turk D, eds. Wall & Melzack's Textbook of Pain. Philadelphia, Pennsylvania, USA: Saunders; 2013:31–48.
- Haas, K.F., Macdonald, R.L., 1999. GABAAreceptor subunitg2 anddsubtypesconfer unique kinetic properties on recombinant GABAAreceptor currentsin mouse fibroblasts. J. Physiol. 514 (Pt 1), 27–45.
- Han ZS, Zhang ET, Craig AD. 1998. Nociceptive and thermoreceptive lamina I neurons are anatomically distinct. Nat Neurosci 1:218–225.
- Hanack C, Moroni M, Lima WC, Wende H, Kirchner M, Adelfinger L, Schrenk-Siemens K, Tappe-Theodor A, Wetzel C, Kuich PH, Gassmann M, Roggenkamp D, Bettler B, Lewin GR, Selbach M & Siemens J. (2015). GABA blocks pathological but not acute TRPV1 pain signals. Cell 160, 759-770.
- Hannan S[1], Minere M[2], Harris J[2], Izquierdo P[2], Thomas P[2], Tench B[2], Smart TG[3]. GABAAR isoform and subunit structural motifs

determine synaptic and extrasynaptic receptor localisation. Neuropharmacology. 2019 Feb 19. pii: S0028-3908(19)30056-5. doi: 10.1016/j.neuropharm.2019.02.022.

- Hartline DK, Colman DR (2007). "Rapid conduction and the evolution of giant axons and myelinated fibers". Curr. Biol. 17 (1): R29–R35. doi:10.1016/j.cub.2006.11.042. PMID 17208176.
- Hellier JL (2016). The Five Senses and Beyond: The Encyclopedia of Perception. ABC-CLIO. pp. 118–119. ISBN 978-1440834172. Retrieved April 13, 2017.
- Hodge CJ Jr, Apkarian AV. 1990. The spinothalamic tract. Crit Rev Neurobiol 5:363–397.
- Hodge CW, Mehmert KK, Kelley SP, McMahon T, Haywood A, Olive MF, Wang D, Sanchez-Perez AM, Messing RO. Supersensitivity to allosteric GABA(A) receptor modulators and alcohol in mice lacking PKCepsilon. Nat Neurosci. 1999; 2:997–1002. [PubMed: 10526339]
- Hodge CW., J. Raber, T. McMahon, H. Walter, A. M. Sanchez-Perez, M. F. Olive, K. Mehmert, A. L. Morrow, R. O. Messing, Decreased anxiety-like behavior, reduced stress hormones, and neurosteroid supersensitivity in mice lacking protein kinase Cepsilon. J Clin Invest 110, 1003-1010 (2002).
- Hodgkin AL, Huxley AF (1952). "A quantitative description of membrane current and its application to conduction and excitation in nerve". The Journal of Physiology. 117 (4): 500–544. doi:10.1113/jphysiol.1952.sp004764. PMC 1392413. PMID 12991237.
- Hubel DH, Wiesel TN (October 1959). "Receptive fields of single neurones in the cat's striate cortex". J. Physiol. 148 (3): 574–91. doi:10.1113/jphysiol.1959.sp006308. PMC 1363130. PMID 14403679.
- Hutter OF, Warner AE. Action of some foreign cations and anions on the chloride permeability of frog muscle. J Physiol 189: 445–460, 1967A. doi:10.1113/jphysiol.1967.sp008178.
- Huxley A (1949). "Direct determination of membrane resting potential and action potential in single myelinated nerve fibers". Journal of Physiology. 112 (3–4): 476–95. doi:10.1113/jphysiol.1951.sp004545. PMC 1393015. PMID 14825228.
- Huxley A (1949). "Evidence for saltatory conduction in peripheral myelinated nerve-fibers". Journal of Physiology. 108 (3): 315–

39. doi:10.1113/jphysiol.1949.sp004335. PMC 1392492. PMID 16991863.

- Ichikawa H[1], Terayama R, Yamaai T, Yan Z, Sugimoto T. Brain-derived neurotrophic factor-immunoreactive neurons in the rat vagal and glossopharyngeal sensory ganglia; co-expression with other neurochemical substances. Brain Res. 2007 Jun 25;1155:93-9. Epub 2007 May 21.
- Ichikawa H[1], Yabuuchi T, Jin HW, Terayama R, Yamaai T, Deguchi T, Kamioka H, Takano-Yamamoto T, Sugimoto T.
- Iggo A. 1960. Cutaneous mechanoreceptors with afferent C fibres. J Physiol (Lond) 152:337–353.
- Institute for Clinical Systems Improvement. Assessment and management of chronic pain. Bloomington (MN): Institute for Clinical Systems Improvement; 2008. 84 p. Disponibile all'indirizzo: www.guideline.gov/
- Ito M. The molecular organization of cerebellar long-term depression. Nat Rev Neurosci 3: 896–902, 2002.
- Jarolimek W, Lewen A, Misgeld U. A furosemide-sensitive K_- Cl_ cotransporter counteracts intracellular Cl_ accumulation and depletion in cultured rat midbrain neurons. J Neurosci 19: 4695– 4704, 1999.
- Jia F, Pignataro L,

and Harrison NL. (2007) GABAA receptors in the thalamus: alpha4 subunit expression and alcohol sensitivity. Alcohol 41:177–185.

- Junge, D (1981). Nerve and Muscle Excitation (2nd ed.). Sunderland, Mass.: Sinauer Associates. ISBN 978-0-87893-410-2. LCCN 80018158.
- Kaas JH. 2008. The somatosensory thalamus and associated pathways. In: JH Kaas, EP Gardner (eds). The Senses: A Comprehensive Reference, Vol. 6 Somatosensation, pp. 117–141. Oxford: Elsevier.
- Kahle KT, Rinehart J, de los Heros P et al. WNK3 modulates transport of Cl- in and out of cells: Implications for control of cell volume and neuronal excitability. Proc Natl Acad Sci. 2005;102:16783–16788.
- Kashiba H[1], Uchida Y, Senba E. Distribution and colocalization of NGF and GDNF family ligand receptor mRNAs in dorsal root and nodose ganglion neurons of adult rats. Brain Res Mol Brain Res. 2003 Jan 31;110(1):52-62.
- Kasugai Y[1], Swinny JD, Roberts JD, Dalezios Y, Fukazawa Y, Sieghart W, Shigemoto R, Somogyi P. Quantitative localisation of synaptic and extrasynaptic GABAA receptor subunits on hippocampal pyramidal cells by freeze-fracture replica immunolabelling. Eur J

Neurosci. 2010 Dec;32(11):1868-88. doi: 10.1111/j.1460-9568.2010.07473.x. Epub 2010 Nov 14.

- Kennedy RT., J. E. Thompson, T. W. Vickroy, In vivo monitoring of amino acids by direct sampling of brain extracellular fluid at ultralow flow rates and capillary electrophoresis. J Neurosci Methods 114, 39-49 (2002).
- Kessler W, Kirchhoff C, Reeh PW, & Handwerker HO (1992) Excitation of cutaneous afferent nerve endings in vitro by a combination of inflammatory mediators and conditioning effect of substance P. Exp Brain Res 91(3):467-476.
- Khasar SG, Lin Y-H, Martin A, Dadgar J, McMahon T, Wang D, Hundle B, Aley KO, Isenberg W, McCarter G, Green PG, Hodge CW, Levine JD, Messing RO. A novel nociceptor signaling pathway revealed in protein kinase C e mutant mice. Neuron. 1999; 24:253–260. [PubMed: 10677042]
- Khirug S, Huttu K, Ludwig A, Smirnov S, Voipio J, Rivera C, Kaila K, Khiroug L. Distinct properties of functional KCC2 expression in immature mouse hippocampal neurons in culture and in acute slices. Eur J Neurosci 21: 899–904, 2005.
- Kneussel M, Haverkamp S, Fuhrmann JC, Wang H, Wässle H, Olsen RW, Betz H. The gamma-aminobutyric acid type A receptor (GABAAR)-associated protein GABARAP interacts with gephyrin but is not involved in receptor anchoring at the synapse. Proc Natl Acad Sci U S A. 2000 Jul 18;97(15):8594-9.
- Koch MC, Steinmeyer K, Lorenz C, Ricker K, Wolf F, Otto M, Zoll B, Lehmann-Horn F, Grzeschik KH, Jentsch TJ. The skeletal muscle chloride channel in dominant and recessive human myo- tonia. Science 257: 797– 800, 1992. doi:10.1126/ science.1379744.
- Kriegstein AR. Constructing circuits: neurogenesis and migration in the developing neocortex. Epilepsia 46 Suppl 7: 15–21, 2005.
- Lagrange, A.H., Botzolakis, E.J., Macdonald, R.L., 2007. Enhanced macro-scopic desensitization shapes the response ofa4 subtype-containingGABAAreceptors to synaptic and extrasynaptic GABA. J. Physiol. 578,655–676.
- Landis SC. Target regulation of neurotransmitter phenotype. Trends Neurosci 13: 344–350, 1990.
- Lang EJ[1], Sugihara I, Llinás R. GABAergic modulation of complex spike activity by the cerebellar nucleoolivary pathway in rat. J Neurophysiol. 1996 Jul;76(1):255-75.
- Lauder JM. Neurotransmitters as growth regulatory signals: role of receptors and second

messengers. Trends Neurosci 16: 233–240, 1993.

- Lerma J., A. S. Herranz, O. Herreras, V. Abraira, R. Martin del Rio, In vivo determination of extracellular concentration of amino acids in the rat hippocampus. A method based on brain dialysis and computerized analysis. Brain Res 384, 145-155 (1986).
- Li H, Tornberg J, Kaila K, Airaksinen MS, Rivera C. Patterns of cation-chloride cotransporter expression during embryonic rodent CNS development. Eur J Neurosci 16: 2358–2370, 2002.
- Lillie RS (1925). "Factors affecting transmission and recovery in passive iron nerve model". J. Gen. Physiol. 7 (4): 473–507. doi:10.1085/jgp.7.4.473. PMC 2140733. PMID 19872151. See also Keynes and Aidley, p. 78.
- Linton S (2005). Understanding Pain for Better Clinical Practice: A Psychological Perspective. Elsevier Health Sciences. p. 14. ISBN 978-0444515919. Retrieved April 13, 2017.
- Lipicky RJ, Bryant SH, Salmon JH. Cable parameters, sodium, potassium, chloride, and water content, and potassium efflux in isolated external intercostal muscle of normal volunteers and pa- tients with myotonia congenita. J Clin Invest 50: 2091–2103, 1971. doi:10.1172/JCI106703.
- Llinás R[1], Sasaki K. The Functional Organization of the Olivo-Cerebellar System as Examined by Multiple Purkinje Cell Recordings. Eur J Neurosci. 1989 Jan;1(6):587-602.
- Lorenzo LE, Godin AG, Wang F, St-Louis M, Carbonetto S, Wiseman PW, Ribeiro-da-Silva A & De Koninck Y. (2014). Gephyrin clusters are absent from small diameter primary afferent terminals despite the presence of GABA(A) receptors. J Neurosci 34, 8300-8317.
- Lu J, Karadsheh M, Delpire E. Developmental regulation of the neuronal-specific isoform of K-Cl cotransporter KCC2 in postnatal rat brains. J Neurobiol 39: 558–568, 1999.
- Lueck JD, Mankodi A, Swanson MS, Thornton CA, Dirksen RT. Muscle chloride channel dysfunc- tion in two mouse models of myotonic dystro- phy. J Gen Physiol 129: 79–94, 2007. doi:10. 1085/jgp.200609635.
- Luhmann HJ, Prince DA. Postnatal maturation of the GABAergic system in rat neocortex. J Neurophysiol 247–263, 1991.
- Lumpkin EA, Caterina MJ. 2007. Mechanisms of sensory transduction in the skin. Nature 445:858–865.
- Ma W, Saunders PA, Somogyi R, Poulter MO & Barker JL. (1993). Ontogeny of GABAA receptor

subunit mRNAs in rat spinal cord and dorsal root ganglia. J Comp Neurol 338, 337-359.

- Maddox FN, Valeyev AY, Poth K, Holohean AM, Wood PM, Davidoff RA, Hackman JC & Luetje CW. (2004). GABAA receptor subunit mRNA expression in cultured embryonic and adult human dorsal root ganglion neurons. Brain Res Dev Brain Res 149, 143-151.
- Maduke M, Miller C, Mindell JA. A decade of CLC chloride channels: structure, mechanism, and many unsettled questions. Annu Rev Biophys Biomol Struct 29: 411– 438, 2000. doi:10.1146/ annurev.biophys.29.1.411.
- Magnaghi V, Ballabio M, Cavarretta IT, Froestl W, Lambert JJ, Zucchi I & Melcangi RC. (2004). GABAB receptors in Schwann cells influence proliferation and myelin protein expression. Eur J Neurosci 19, 2641-2649.
- Magnaghi V, Ballabio M, Consoli A, Lambert JJ, Roglio I & Melcangi RC. (2006). GABA receptor-mediated effects in the peripheral nervous system: A cross-interaction with neuroactive steroids. J Mol Neurosci 28, 89-102.
- Magnaghi V, Cavarretta I, Galbiati M, Martini L, Melcangi RC (2001) Neuroactive steroids and peripheral myelin proteins Brain Res Brain Res Rev 37(1-3):360-71.
- Magnaghi V, Parducz A, Frasca A, Ballabio M, Procacci P, Racagni G, Bonanno G & Fumagalli F. (2010). GABA synthesis in Schwann cells is induced by the neuroactive steroid allopregnanolone. J Neurochem 112, 980-990.
- Magnaghi V. (2007). GABA and neuroactive steroid interactions in glia: new roles for old players? Curr Neuropharmacol 5, 47-64.
- Mano T, Iwase S, Toma S. 2006. Microneurography as a tool in clinical neurophysiology to investigate peripheral neural traf1c in humans. Clin Neurophysiol 117:2357–2384.
- Marandi N, Konnerth A, Garaschuk O. Two-photon chloride imaging in neurons of brain slices. Pflu¨ gers Arch 445: 357–365, 2002.
- Matsumoto I, Emori Y, Ninomiya Y, Abe K. A comparative study of three cranial sensory ganglia projecting into the oral cavity: in situ hybridization analyses of neurotrophin receptors and thermosensitive cation channels. Brain Res Mol Brain Res. 2001 Sep 30;93(2):105-12.
- Meera P, Wallner M, & Otis TS (2011) Molecular basis for the high THIP/gaboxadol sensitivity of extrasynaptic GABA(A) receptors. J Neurophysiol 106(4):2057-2064.
- Mehrke G, Brinkmeier H, Jockusch H. The myo-tonic mouse mutant ADR: electrophysiology of the muscle fiber. Muscle Nerve 11: 440 – 446, 1988. doi:10.1002/mus.880110505.

- Melcangi RC, Magnaghi V, Cavarretta I, Zucchi I, Bovolin P, D'Urso D & Martini L. (1999). Progesterone derivatives are able to influence peripheral myelin protein 22 and P0 gene expression: Possible mechanisms of action. Journal of Neuroscience Research 56, 349-357.
- Melfi S, et al. (2017) Src and phospho-FAK kinases are activated by allopregnanolone promoting Schwann cell motility, morphology and myelination. J Neurochem 141(2):165-178.
- Mercado A, Mount DB, Gamba G. Electroneutral cation-chloride cotransporters in the central nervous system. Neurochem Res 29: 17–25, 2004.
- Mikawa S, Wang C, Shu F, Wang T, Fukuda A, Sato K. Developmental changes in KCC1, KCC2 and NKCC1 mRNAs in the rat cerebellum. Brain Res 136: 93–100, 2002.
- Milanese M, Tardito D, Musazzi L, Treccani G, Mallei A, Bonifacino T, Gabriel C, Mocaer E, Racagni G, Popoli M, Bonanno G. Chronic treatment with agomelatine or venlafaxine reduces depolarization-evoked glutamate release from hippocampal synaptosomes.BMC Neurosci. 2013 Jul 29;14:75. doi: 10.1186/1471-2202-14-75.
- Misgeld U, Deisz RA, Dodt HU, Lux HD. The role of chloride transport in postsynaptic inhibition of hippocampal neurons. Science 232: 1413–1415, 1986.
- Moalem-Taylor G., P. M. Lang, D. J. Tracey, P. Grafe, Post-spike excitability indicates changes in membrane potential of isolated C-fibers. Muscle Nerve 36, 172-182 (2007).
- Mortensen M, Patel B, and Smart TG (2012) GABA potency at GABA(A) receptors found in synaptic and extrasynaptic zones. Front Cell Neurosci 6:1–12.
- Moss SJ & Smart TG (1996) Modulation of amino acid-gated ion channels by protein phosphorylation. Int Rev Neurobiol 39:1-52.
- Mukherjee J, Kretschmannova K, Gouzer G, Maric HM, Ramsden S, Tretter V, Harvey K, Davies PA, Triller A, Schindelin H, Moss SJ. The residence time of GABA(A)Rs at inhibitory synapses is determined by direct binding of the receptor α1 subunit to gephyrin. J Neurosci. 2011 Oct 12;31(41):14677-87. doi: 10.1523/JNEUROSCI.2001-11.2011.
- Murinson, BB; JW Griffin (2004). "C-fiber structure varies with location in peripheral nerve". Journal of Neuropathology and Experimental Neurology. 63 (3): 246–254. doi:10.1093/jnen/63.3.246. PMID 15055448.
- Naert G., T. Maurice, L. Tapia-Arancibia, L. Givalois, Neuroactive steroids modulate HPA

axis activity and cerebral brain-derived neurotrophic factor (BDNF) protein levels in adult male rats. Psychoneuroendocrinology 32, 1062-1078 (2007).

- Neuroscience. Purves, Dale. (5th ed.). Sunderland, Mass.: Sinauer Associates. 2012. ISBN 9780878936953. OCLC 754389847 .
- Nguyen QA & Nicoll RA (2018) The GABAA Receptor beta Subunit Is Required for Inhibitory Transmission. Neuron 98(4):718-725 e713.
- Nielsen OB., Frank Vincenzo de Paoli, Anders Riisager, and Thomas Holm Pedersen. Chloride Channels Take Center Stage in Acute Regulation of Excitability in Skeletal Muscle: Implications for Fatigue. PHYSIOLOGY 32: 425–434, 2017. Published October 11, 2017; doi:10.1152/physiol.00006.2015
- Nin MS, Martinez LA, Pibiri F, Nelson M, & Pinna G (2011) Neurosteroids reduce social isolation-induced behavioral deficits: a proposed link with neurosteroid-mediated upregulation of BDNF expression. Front Endocrinol (Lausanne) 2:73.
- Nusser Z, Sieghart W, Benke D, Fritschy JM & Somogyi P. (1996). Differential synaptic localization of two major gamma-aminobutyric acid type A receptor alpha subunits on hippocampal pyramidal cells. Proc Natl Acad Sci U S A 93, 11939-11944.
- O'Neill N, Sylantyev S[1]. The Functional Role of Spontaneously Opening GABAA Receptors in Neural Transmission. Front Mol Neurosci. 2019 Mar 28;12:72. doi: 10.3389/fnmol.2019.00072. eCollection 2019.
- Olmos Serrano JL, Paluszkiewicz SM, Martin BS, Kaufmann WE, Corbin JG, and Huntsman M. (2010) Defective GABAergic neurotransmission and pharmacological rescue of neuronal hyperexcitability in the amygdala in a mouse model of fragile X syndrome. J Neurosci 30:9929–9938.
- Olsen RW1, Sieghart W. LXX. Subtypes of gamma-aminobutyricacid(A) receptors: classification on the basis of subunit composition, pharmacology, andf unction. Pharmacol. Rev. 60, 243–260.
- Ospina M, Harstall C. Multidisciplinary pain programs for chronic pain: evidence from systematic reviews. Edmonton: Alberta Heritage Foundation for Medical Research; 2003. 53 p.
- Owens DF, Kriegstein AR. Is there more to gaba than synaptic inhibition? Nat Rev Neurosci 3: 715–727, 2002.

- Palade PT, Barchi RL. Characteristics of the chloride conductance in muscle fibers of the rat dia- phragm. J Gen Physiol 69: 325–342, 1977A. doi: 10.1085/jgp.69.3.325.
- Park-Chung M, Malayev A, Purdy RH, Gibbs TT, Farb DH (1999) Sulfated and unsulfated steroids modulate gamma-aminobutyric acidA receptor function through distinct sites Brain Res 830(1):72-87.
- Parpura V1, Verkhratsky A. (2011) The astrocyte excitability brief: from receptors to gliotransmission. Neurochem Int. 2012 Sep;61(4):610-21. doi: 10.1016/j.neuint.2011.12.001. Epub 2011 Dec 9.
- Paul SM and Purdy RH (1992) Neuroactive steroids. FASEB J 6:2311–2322.
- Payne JA, Rivera C, Voipio J, Kaila K. Cation-chloride cotransporters in neuronal communication, development and trauma. Trends Neurosci 26: 199–206, 2003.
- Pedersen TH, de Paoli F, Nielsen OB. Increased excitability of acidified skeletal muscle: role of chloride conductance. J Gen Physiol 125: 237–246, (2005). doi:10.1085/jgp.200409173.
- Pedersen TH, Macdonald WA, de Paoli FV, Gu-rung IS, Nielsen OB. Comparison of regulated passive membrane conductance in action poten- tial-firing fast- and slow-twitch muscle. J Gen Physiol 134: 323–337, (2009). doi:10.1085/jgp. 200910291.
- Pedersen TH, Nielsen OB, Lamb GD, Stephenson DG. Intracellular acidosis enhances the excitabil- ity of working muscle. Science 305: 1144–1147, (2004). doi:10.1126/science.1101141.
- Perego C, Di Cairano ES, Ballabio M, Magnaghi V. (2012) Neurosteroid allopregnanolone regulates EAAC1-mediated glutamate uptake and triggers actin changes in Schwann cells. J Cell Physiol. 2012 Apr;227(4):1740-51. doi: 10.1002/jcp.22898.
- Pierno S, Desaphy JF, Liantonio A, De Luca A, Zarrilli A, Mastrofrancesco L, Procino G, Valenti G, Conte Camerino D. Disuse of rat muscle in vivo reduces protein kinase C activity controlling the sarcolemma chloride conductance. J Physiol 584: 983–995, 2007. doi:10.1113/jphysiol.2007. 141358.
- Pinal CS, Tobin AJ (1998) Uniqueness and redundancy in GABA production Perspect Dev Neurobiol 5(2-3):109-18
- Plotkin MD, Snyder EY, Hebert SC, Delpire E. Expression of the Na-K-2Cl cotransporter is developmentally regulated in postnatal rat brains: a possible mechanism underlying GABA's excitatory role in immature brain. J Neurobiol 33: 781–795, 1997.

- Poliak S.; E. Peles (2006). "The local differentiation of myelinated axons at nodes of Ranvier". Nature Reviews Neuroscience. 4 (12): 968–80. doi:10.1038/nrn1253. PMID 14682359.
- Prenosil GA, Schneider Gasser EM, Rudolph U, Keist R, Fritschy JM, Vogt KE. Specific subtypes of GABAA receptors mediate phasic and tonic forms of inhibition in hippocampal pyramidal neurons. J Neurophysiol. 2006 Aug;96(2):846-57.
- Price TJ, Cervero F, Gold MS, Hammond DL, & Prescott SA (2009) Chloride regulation in the pain pathway. Brain Res Rev 60(1):149-170.
- Procacci P, Ballabio M, Castelnovo LF, Mantovani C & Magnaghi V. (2012). GABA-B receptors in the PNS have a role in Schwann cells differentiation? Front Cell Neurosci 6, 68.
- Puia G, F. Ravazzini, L. F. Castelnovo, V. Magnaghi, PKCepsilon and allopregnanolone: functional cross-talk at the GABAA receptor level. Front Cell Neurosci 9, 83 (2015).
- Purves, D; Augustine, GJ; Fitzpatrick, D; Hall, WC; Lamantia, A-S; McNamara, JO; White, LE (2008). Neuroscience (4th ed.). Sunderland, MA: Sinauer Associates. ISBN 978-0-87893-697-7. LCCN 2007024950. OCLC 144771764.
- Purves, Dale; et al. (2004). Neuroscience. Massachusetts: Sinauer Associates, Inc. ISBN 978-0-87893-725-7.
- Pusch M. Myotonia caused by mutations in the muscle chloride channel gene CLCN1. Hum Mutat 19: 423– 434, 2002. doi:10.1002/humu.10063.
- Qi ZH, Song M, Wallace MJ, Wang D, Newton PM, McMahon T, Chou WH, Zhang C, Shokat KM, Messing RO. Protein kinase C epsilon regulates gamma-aminobutyrate type A receptor sensitivity to ethanol and benzodiazepines through phosphorylation of gamma2 subunits. J Biol Chem. 2007; 282:33052–33063. [PubMed: 17875639]
- Rang HP & Ritchie JM (1968) On the electrogenic sodium pump in mammalian non-myelinated nerve fibres and its activation by various external cations. J. Physiol 196(1):183-221.
- Reddy DS (2003a) Is there a physiological role for the neurosteroid THDOC in stresssensitive conditions? Trends Pharmacol Sci 24:103–106.
- Reddy DS (2003b) Pharmacology of endogenous neuroactive steroids. Crit Rev Neurobiol 15:197–234.
- Rivera C, Voipio J, Payne JA, Ruusuvuori E, Lahtinen H, Lamsa K, Pirvola U, Saarma M, Kaila

K. The K_/Cl_ co-transporter KCC2 renders GABA hyperpolarizing during neuronal maturation. Nature 397: 251–255, 1999.

- Robert F, Guennoun R, Desarnaud F, Do-Thi A, Benmessahel Y, Baulieu EE & Schumacher M. (2001). Synthesis of progesterone in Schwann cells: regulation by sensory neurons. Eur J Neurosci 13, 916-924.
- Roberts E, Frankel S (1950) gamma-Aminobutyric acid in brain: its formation from glutamic acid J Biol Chem 187(1):55-63.
- Roberts E. Disinhibition as an organizing principle in the nervous system. The role of gamma-aminobutyric acid. Adv Neurol 5: 127–143, (1974).
- Roberts E. Failure of GABAergic inhibition: a key to local and global seizures. Adv Neurol 44: 319–341, (1986). 527.
- Roberts E. What do GABA neurons really do? They make possible variability generation in relation to demand. Exp Neurol 93: 279– 290, 1986.
- Rohrbough J, Spitzer NC. Regulation of intracellular Cl_ levels by Na(_)-dependent Cl_ cotransport distinguishes depolarizing from hyperpolarizing GABAA receptor-mediated responses in spinal neurons. J Neurosci 16: 82–91, 1996.
- Rudolph, U., Mohler, H., 2006. GABA-based therapeutic approaches: $GABA_A$ receptor subtype functions. Curr. Opin. Pharmacol. 6, 18–23.
- Salio C, Lossi L, Ferrini F, Merighi A. Ultrastructural evidence for a pre- and postsynaptic localization of full-length trkB receptors in substantia gelatinosa (lamina II) of rat and mouse spinal cord. Eur J Neurosci. 2005 Oct;22(8):1951-66.
- Sasaki, T., Matsuki, N., Ikegaya, Y. 2011 Action-potential modulation during axonal conduction Science 331 (6017), pp. 599–601
- Saxena, N.C., Macdonald, R.L., 1994. Assembly of GABAAreceptor subunits:role of thedsubunit. J. Neurosci. 14, 7077–7086.
- Scascighini L, Toma V, Dober-Spielmann S, et al. Multidisciplinary treatment for chronic pain: a systematic review of interventions and outcomes. Rheumatology 2008;47(5):670-8.
- Schmidt-Nielsen, K (1997). Animal Physiology: Adaptation and Environment (5th ed.). Cambridge: Cambridge University Press. ISBN 978-0-521-57098-5.
- Schweizer C. , S. Balsiger, H. Bluethmann, I.M. Mansuy,J.M. Fritschy, H.Mohler and B. Lusche r. The γ2 subunit of GABAA receptors is required for maintenance of receptors at

mature synapses. Mol. Cell. Neurosci., 24 (2003), pp. 442-450

- Serra J, Campero M, Ochoa J, & Bostock H (1999) Activity-dependent slowing of conduction differentiates functional subtypes of C fibres innervating human skin. J. Physiol 515:799-811.
- Shimizu-Okabe C, Yokokura M, Okabe A, Ikeda M, Sato K, Kilb W, Luhmann HJ, Fukuda A. Layer-specific expression of Cl_ transporters and differential [Cl_]i in newborn rat cortex. Neuroreport 13: 2433–2437, 2002.
- Shu HJ, Eisenman LN, Jinadasa D, Covey DF, Zorumski CF, Mennerick S (2004) Slow actions of neuroactive steroids at GABAA receptors J Neurosci 24(30):6667-75.
- Shu-Hui Chuang and Doodipala Samba Reddy. Genetic and Molecular Regulation of Extrasynaptic GABA-A Receptors in the Brain: Therapeutic Insights for Epilepsy. Journal of Pharmacology and Experimental Therapeutics February 2018, 364 (2) 180-197; DOI: https://doi.org/10.1124/jpet.117.244673
- Sieghart W. and Sperk G. (2002). Sub- unit composition, distribution and function of GABAA receptorsub-types. Curr.Top.Med.Chem. 2, 795–816.
- Sieghart, W., 1995. Structure and pharmacology of g-aminobutyric $acid_A$ receptor subtypes. Pharmacol. Rev. 47, 181–234.
- Sigel, E., Buhr, A., 1997. The benzodiazepine binding site of $GABA_A$ receptors. Trends Pharmacol. Sci. 18, 425–429.
- Simons M, Trotter J (October 2007). "Wrapping it up: the cell biology of myelination". Curr. Opin. Neurobiol. 17 (5): 533–40. doi:10.1016/j.conb.2007.08.003. PMID 17 923405.
- Skljarevski, V.; Ramadan, N. M. "The nociceptive flexion reflex in humans – review article". Pain. 96 (1): 3–8. doi:10.1016/s0304-3959(02)00018-0.
- Soojung Lee, Bo-Eun Yoon, Ken Berglund, Soo-Jin Oh, Hyungju Park, Hee-Sup Shin, George J. Augustine and C. Justin Lee- Channel-Mediated Tonic GABA Release from Glia. Science 330 (6005), 790-796.
- Spitzer NC, Debaca RC, Allen KA, Holliday J. Calcium dependence of differentiation of GABA immunoreactivity in spinal neurons. J Comp Neurol 337: 168–175, 1993.
- Srinivasan R, Wolfe D, Goss J, Watkins S, de Groat WC, Sculptoreanu A, Glorioso JC. Protein kinase C epsilon contributes to basal and sensitizing responses of TRPV1 to capsaicin in rat dorsal root ganglion neurons. Eur J Neurosci 2008;28:1241–54.

- Stell BM, Brickley SG, Tang CY, Farrant M, and Mody I. (2003) Neuroactive steroids reduce neuronal excitability by selectively enhancing tonic inhibition mediated by delta subunit-containing GABAA receptors. Proc Natl Acad Sci USA 100:14439–14444.
- Striedter, Georg F. Neurobiology : a functional approach (Instructor's ed.). (1962) New York. ISBN 9780195396157. OCLC 919041751.
- Sugiura T, Tominaga M, Katsuya H, Mizumura K. Bradykinin lowers the threshold temperature for heat activation of vanilloid receptor 1. Journal of neurophysiology. 2002; 88:544–548. [PubMed: 12091579]
- Sung KW, Kirby M, McDonald MP, Lovinger DM, Delpire E. Abnormal GABAA receptor mediated currents in dorsal root ganglion neurons isolated from Na-K-2l cotransport null mice. J Neurosci 20: 7531–7508, 2000.
- Tasaki I (1939). "Electro-saltatory transmission of nerve impulse and effect of narcosis upon nerve fiber". Am. J. Physiol. 127: 211–27. doi:10.1152/ajplegacy.1939.127.2.211.
- Tasaki I, Takeuchi T (1941). "Der am Ranvierschen Knoten entstehende Aktionsstrom und seine Bedeutung für die Erregungsleitung". Pflügers Archiv für die gesamte Physiologie. 244 (6): 696–711. doi:10.1007/BF01755414.
- Tasaki I, Takeuchi T (1942). "Weitere Studien über den Aktionsstrom der markhaltigen Nervenfaser und über die elektrosaltatorische Übertragung des nervenimpulses". Pflügers Archiv für die gesamte Physiologie. 245 (5): 764–82. doi:10.1007/BF01755237.
- Thalhammer JG, Raymond SA, Popitz-Bergez FA, & Strichartz GR (1994) Modality-dependent modulation of conduction by impulse activity in functionally characterized single cutaneous afferents in the rat. Somatosens. Mot. Res 11(3):243-257.
- Theunissen, F; Miller, JP (1995). "Temporal Encoding in Nervous Systems: A Rigorous Definition". Journal of Computational Neuroscience. 2 (2): 149–162. doi:10.1007/bf00961885.
- Thomas P, Mortensen M, Hosie AM, Smart TG. Dynamic mobility of functional GABAA receptors at inhibitory synapses. Nat Neurosci. 2005 Jul;8(7):889-97.
- Thompson SM, Deisz RA, Prince DA. Outward chloride/cation co-transport in mammalian cortical neurons. Neurosci Lett 89: 49–54, 1988a.
- Thompson SM, Deisz RA, Prince DA. Relative contributions of passive equilibrium and active transport to the distribution of chloride in

mammalian cortical neurons. J Neurophysiol 60: 105– 124, 1988b.

- Thompson SM, Ga¨hwiller BH. Activity-dependent disinhibition. II. Effects of extracellular potassium, Furosemide, membrane potential on Ecl-in hippocampal CA3 neurons. J Neurophysiol 61: 512–523, 1989.
- Thorpe, S.J. (1990). "Spike arrival times: A highly efficient coding scheme for neural networks". In Eckmiller, R.; Hartmann, G.; Hauske, G. (eds.). Parallel processing in neural systems and computers (PDF). North-Holland. pp. 91–94. ISBN 978-0-444-88390-2.
- Todd AJ. Neuronal circuitry for pain processing in the dorsal horn. Nat Rev Neurosci. 2010, 11: 823–836.
- Tominaga M, Caterina MJ. Thermosensation and pain. Journal of neurobiology. 2004; 61:3–12. [PubMed: 15362149]
- Tominaga M, Tominaga T. Structure and function of TRPV1. Pflugers Arch. 2005; 451:143–150. [PubMed: 15971082]
- Tossman U., G. Jonsson, U. Ungerstedt, Regional distribution and extracellular levels of amino acids in rat central nervous system. Acta Physiol Scand 127, 533-545 (1986).
- Tretter V, Jacob TC, Mukherjee J, Fritschy JM, Pangalos MN, Moss SJ. The clustering of GABA(A) receptor subtypes at inhibitory synapses is facilitated via the direct binding of receptor alpha 2 subunits to gephyrin. J Neurosci. 2008 Feb 6;28(6):1356-65. doi: 10.1523/JNEUROSCI.5050-07.2008.
- Tretter V, Kerschner B, Milenkovic I, Ramsden SL, Ramerstorfer J, Saiepour L, Maric HM, Moss SJ, Schindelin H, Harvey RJ, Sieghart W, Harvey K. (2011) Molecular basis of the γ-aminobutyric acid A receptor α3 subunit interaction with the clustering protein gephyrin. J Biol Chem. 2011 Oct 28;286(43):37702-11. doi: 10.1074/jbc.M111.291336. Epub 2011 Aug 31.
- Tretter V[1], Jacob TC, Mukherjee J, Fritschy JM, Pangalos MN, Moss SJ. The clustering of GABA(A) receptor subtypes at inhibitory synapses is facilitated via the direct binding of receptor alpha 2 subunits to gephyrin. J Neurosci. 2008 Feb 6;28(6):1356-65. doi: 10.1523/JNEUROSCI.5050-07.2008.
- Vallbo ÅB, Hagbarth KE, Torebjörk HE, Wallin BG. 1979. Somatosensory, proprioceptive, and sympathetic activity in human peripheral nerves. Physiol Rev 59:919–957.
- Vellani V, Mapplebeck S, Moriondo A, Davis JB, McNaughton PA. Protein kinase C activation potentiates gating of the vanilloid receptor VR1 by capsaicin, protons, heat and anandamide. J Physiol. 2001; 534:813–825. [PubMed:

11483711]

- Verheij MM., L. F. Vendruscolo, L. Caffino, G. Giannotti, M. Cazorla, F. Fumagalli, M. A. Riva, J. R. Homberg, G. F. Koob, C. Contet, Systemic Delivery of a Brain-Penetrant TrkB Antagonist Reduces Cocaine Self-Administration and Normalizes TrkB Signaling in the Nucleus Accumbens and Prefrontal Cortex. J Neurosci 36, 8149-8159 (2016).
- Villarreal CF, Sachs D, Funez MI, Parada CA, de Queiroz Cunha F, Ferreira SH. The peripheral pro-nociceptive state induced by repetitive inflammatory stimuli involves continuous activation of protein kinase A and protein kinase C epsilon and its Na(V)1. 8 sodium channel functional regulation in the primary sensory neuron. Biochem Pharmacol 2009;77:867–77.
- Wang C, Shimizu-Okabe C, Watanabe K, Okabe A, Matsuzaki H, Ogawa T, Mori N, Fukuda A, Sato K. Developmental changes in KCC1, KCC2, NKCC1 mRNA expressions in the rat brain. Brain Res 139: 59–66, 2002.
- Wang H, Bedford FK, Brandon NJ, Moss SJ, Olsen RW. GABA(A)-receptor-associated protein links GABA(A) receptors and the cytoskeleton. Nature. 1999 Jan 7;397(6714):69-72.
- Wen-Hai Chou, Dan Wang, Thomas McMahon, Zhan-Heng Qi, Maengseok Song, Chao Zhang, Kevan M. Shokat and Robert O. Messing. GABAA Receptor Trafficking Is Regulated by Protein Kinase Cε and the N-Ethylmaleimide-Sensitive Factor. Journal of Neuroscience 20 October 2010, 30 (42) 13955-13965; DOI: https://doi.org/10.1523/JNEUROSCI.0270-10.2010
- Wetmore C, Olson L. Neuronal and nonneuronal expression of neurotrophins and their receptors in sensory and sympathetic ganglia suggest new intercellular trophic interactions. J Comp Neurol. 1995 Feb 27;353(1):143-59.
- WHO. WHO normative guidelines on pain management report of a Delphi Study to determine the need for guidelines and to identify the number and topics of guidelines that should be developed by WHO. Geneva: 2007. Disponibile all'indirizzo: www.who.int/.
- Wohlfarth KM, Bianchi MT, Macdonald RL. (2002) Enhanced neurosteroid potentiation of ternary GABA(A) receptors containing the delta subunit. J Neurosci 22:1541–1549.
- Woolf CJ, Ma Q (August 2007). "Nociceptors—noxious stimulus detectors". Neuron. 55 (3): 353–64. doi:10.1016/j.neuron.2007.07.016. PMID 17678850.

- Yamada J, Okabe A, Toyoda H, Kilb W, Luhmann HJ, Fukuda A. Cl_ uptake promoting depolarizing GABA actions in immature rat neocortical neurones is mediated by NKCC1. J Physiol 557: 829–841, 2004.
- Zalc B (2006). "The acquisition of myelin: a success story". Novartis Found. Symp. Novartis Foundation Symposia. 276: 15–21, discussion 21–5, 54–7, 275–81. doi:10.1002/9780470032244.ch3. ISBN 97 8-0-470-03224-4. PMID 16805421.
- Zhang L, Spigelman I, Carlen PL. Development of GABA-mediated chloride-dependent inhibition in CA1 pyramidal neurones of immature rat hippocampal slices. J Physiol 444: 25–49, 1991.
- Zhang XL, Lee KY, Priest BT, Belfer I & Gold MS. (2015). Inflammatory mediator-induced modulation of GABAA currents in human sensory neurons. Neuroscience 310, 401-409.
- Zhu W, Xu P, Cuascut FX, Hall AK, Oxford GS. Activin acutely sensitizes dorsal root ganglion neurons and induces hyperalgesia via PKC-mediated potentiation of transient receptor potential vanilloid I. J Neurosci 2007;27:13770
- Zurborg S. et al., Generation and characterization of an Advillin-Cre driver mouse line. Mol Pain 7, 66 (2011).